Overcoming Cisplatin Resistance in Pancreatic Cancer

Dissertation

for the award of the degree

"Doctor rerum naturalium"
of the Georg-August-Universität Göttingen

within the doctoral program Molecular Medicine
of the Georg-August University School of Science (GAUSS)
at the Georg-August-Universität-Göttingen

submitted by
Katharina Maria Annette Ewers
from Duderstadt

Göttingen 2021

Thesis Committee

1. Prof. Dr. Matthias Dobbelstein, Institute of Molecular Oncology, University Medical Center Goettingen (UMG)

2. Prof. Dr. Elisabeth Heßmann, Department of Gastroenterology, Gastrointestinal Oncology and Endocrinology, University Medical Center Goettingen (UMG)

3. Prof. Dr. Heidi Hahn, Department of Human Genetics, University Medical Center Goettingen (UMG)

Members of the Examination Board

1st reviewer: Prof. Dr. Matthias Dobbelstein, Institute of Molecular Oncology, University Medical Center Goettingen (UMG)
2nd reviewer: Prof. Dr. Elisabeth Heßmann, Department of Gastroenterology, Gastrointestinal Oncology and Endocrinology, University Medical Center Goettingen (UMG)

External members of the Examination Board

1. Prof. Dr. Heidi Hahn, Department of Human Genetics, University Medical Center Goettingen (UMG)
2. Prof. Dr. Peter Burfeind, Department of Human Genetics, University Medical Center Goettingen (UMG)

3. Prof. Dr. Dieter Kube, Department of Haematology and Medical Oncology, University Medical Center Goettingen (UMG)

4. Prof. Dr. Lutz Walter, Department of Primate Genetics, German Primate Center (DPZ) Goettingen

Date of oral examination: 12th of October 2021

Affidavit

Herewith I declare that the PhD Thesis entitled “Overcoming Cisplatin Resistance in Pancreatic Cancer” was written independently and with no other sources and aids than quoted.

Göttingen, 03rd September 2021_____

(Katharina Ewers)

Table of Contents

List of Figures

1 Abstract

Pancreatic ductal adenocarcinoma (PDAC) is the most common species of pancreatic cancer with high lethality. Despite intensive research, no major therapy improvements have been achieved due to late-stage diagnosis and aggressive tumour biology resulting in low therapy response and poor survival of patients. Thus, PDAC is predicted to be the second leading cause of cancer-related death within the next decade. We were thus aiming at new treatment strategies.

We analysed the response of a panel of seven PDAC cell lines against the chemotherapeutic agent cisplatin, determining two clearly separated response categories, cisplatin-sensitive and resistant cells. Interestingly, the sensitive cells correspond to the classical form of molecular PDAC subtypes, displaying a less aggressive biology and relatively good prognosis for the patients. The cisplatin-resistant cells can be linked to the basal-like subtype, which is characterised by even higher aggressiveness, lower survival rate and chemo-resistance. Interestingly, the basal-like cells had a lower degree of platinised DNA upon treatment, which was reversed by an inhibitor of platinum export from cells. This suggests a higher degree of platinum export in basal-like cells as a mechanism of their resistance. Besides the transcription factor GATA6, which was already identified as a marker for the classical subtype, we could show that the expression of the microRNAs 200a and 200b could be linked to cisplatin-sensitive cells, serving as potential biomarkers for cisplatin responsiveness.

Previous results suggested that a combination of HSP90 inhibitors and the cisplatin analogue carboplatin resulted in a strong antitumour synergy in ovarian cancer cells. Here we found that in basal-like PDAC cells, the combination of HSP90 inhibition and cisplatin treatment resulted in a synergistic reduction of cell viability, increased DNA damage and chromosome fragmentation. These effects are mediated by the degradation of the DNA repair pathway protein FANCA. Further, cisplatin efflux by export transporter seemed compromised upon HSP90 inhibition, as the platinum-DNA adduct formation was increased upon HSP90 inhibition.

Moving towards clinical application, we transferred our approach into a mouse model with orthotopically transplanted KPC cells (LSL-Kras$^{G12D/+}$; LSL-Trp53$^{R172H/+}$; Pdx-1-Cre; C57/BL6 genetic background). The combination treatment was highly efficient and resulted in a strong reduction of tumour size with increased apoptosis.

Our study suggests that PDAC cells show a distinct response towards cisplatin treatment and that combination of cisplatin with the HSP90 inhibitor onalespib is able to overcome cisplatin resistance in basal-like PDAC cells.

2 Introduction

2.1 Cancer

In over 50 % of the countries worldwide, the first or second leading cause of death before the age of 70 is related to cancer. (Nagai and Kim, 2017). Cancer describes a group of diseases with malignant neoplasms, characterised by the ability to invade other tissues (Hanahan and Weinberg, 2000). Over the past decades, both cancer incidence and mortality have risen (Sung et al., 2021), which is linked to the ageing of the population and the improved treatment of cardiovascular diseases. (Clegg et al., 2009; Wu et al., 2018).

2.2 Pancreatic Ductal Adenocarcinoma

The pancreas is a glandular organ consisting of the endocrinal and exocrine parts. The exocrine part, which is composed of acinar and ductal cells, is responsible for producing and releasing digestive enzymes. The endocrinal part is involved in the regulation of blood glucose levels by balancing glucagon and insulin release. Around 90 % of pancreatic cancers arise in the exocrine part of acinar cells and belong to the species called pancreatic ductal adenocarcinoma (PDAC) (Adamska et al., 2017; Xu et al., 2019).

PDAC is the fourth leading cause of cancer-related deaths worldwide (Siegel et al., 2015). The overall 5-year survival rate of PDAC patients is less than 5 %, with a median survival of 6-12 months after diagnosis, one of the shortest among all malignancies. PDAC presents with rising incidences due to age, obesity, smoking and metabolic syndromes (Bengtsson et al., 2020) and is predicted to become the second leading cause of cancer-related deaths within the next decade (Rawla et al., 2019; Tavakkoli et al., 2020). This high mortality rate is linked to different reasons: on the one hand, many patients show no symptoms at early stages, and no specific early detection methods are available. Additionally, PDAC has a high probability of developing metastasis at this stage, leaving around 80 % of patients with locally advanced unresectable and metastatic tumours at the time of first diagnosis (Ansari et al., 2019). On the other hand, pancreatic tumours are often resistant to chemo- and radiotherapy because of heterogeneity, dynamic cellular plasticity and insufficient treatment strategies (Orth et al., 2019).

In 1988, Smit et al. discovered that PDAC tumours often carry a point mutation of codon 12 in the Kirsten rat sarcoma (KRAS) gene (Smit et al., 1988). Later on, it was confirmed that this mutation is the earliest event in a cascade of mutations that drive PDAC formation and occurs in almost 90 % of PDAC patients (Hingorani et al., 2003; Olive and Tuveson, 2006). Mutations in this gene result

in constitutive activation of KRAS signalling by reducing its inherent Guanosine triphosphatase (GTPase) activity. This leads to activation of the RAS/mitogen-activated protein kinase (MAPK) and the phosphoinositide 3-kinases (PI3K)/Protein kinase B (AKT) signalling pathways, resulting in enhanced proliferation and cell survival with compromised differentiation (Ellis and Clark, 2000). A progression model has been proposed, where a cascade of mutations drive the oncogenic alteration from the normal pancreas to pancreatic intraepithelial neoplasia (PanINs) and then to PDAC (Hruban et al., 2000; Morris et al., 2010).

The PanINs, which are precursor lesions, are classified into three stages (PanIN I, PanIN II, PanIN III), depending on their cytological abnormalities and genetic alterations (Hruban et al., 2001). The initiator of the progress is the KRAS mutation, accompanied by additional mutations or deletions in genes such as cyclin-dependent kinase inhibitor 2 (CDKN2A), inactivated in 90 % of PanIN II (Caldas et al., 1994), tumour protein p53 (TP53), mutated in 50-70 % (Barton and Staddon, 1991; Rozenblum et al., 1997) and mothers against decapentaplegic homolog 4 (SMAD4) (Hahn et al., 1996) inactivated in 55 % of PanIN III (Figure 1).

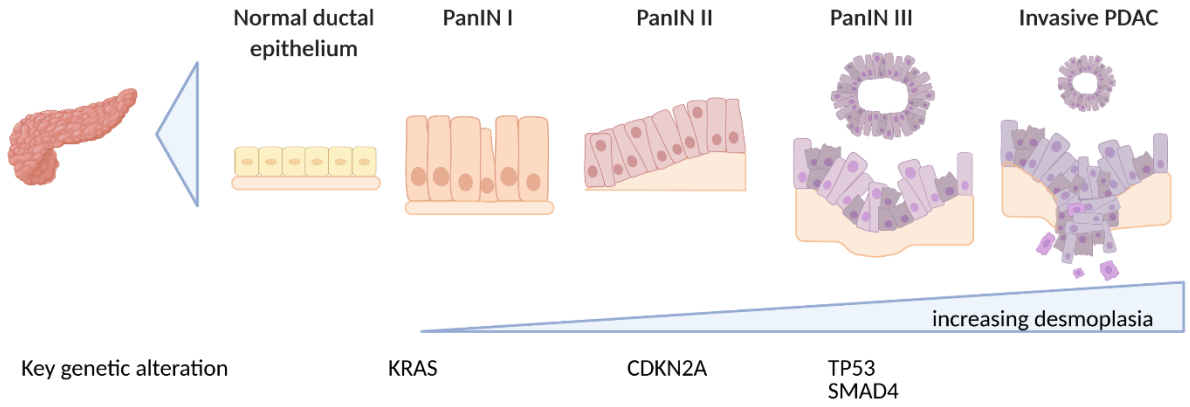

Figure 1: Progression Model for PDAC. Development of high-grade PDAC from normal ductal epithelium via low-grade PanIN. This development is associated with the accumulation of mutations and an increase in desmoplasia. Transformation of normal ductal epithelium starts with KRAS mutation. Mutations of CDKN2A, TP53 and SMAD4 further progress the PanIN towards invasive PDAC. Adapted from (Guo et al., 2016). Created with BioRender.com.

2.2.1 Molecular Subtypes of PDAC

A severe challenge for the treatment of PDAC tumours is the therapeutic resistance and aggressive tumour biology, which is reflected by the high molecular heterogeneity of this tumour entity. The decoding of the molecular signatures enables an insight into the complexity of PDAC. Whole-exome sequencing approaches uncovered various mutational and copy

number variations of oncogenes and tumour suppressor genes in PDAC (Adamo et al., 2017; Bailey et al., 2016; Jones et al., 2008). This method verified not only the somatic driver mutations of KRAS, TP53, SMAD4 and CDKN2A but also genetic changes with lower prevalence, such as breast cancer 1/2 (BRCA1/2) or AT-rich interactive domain-containing protein 1A (ARID1A) (Bailey et al., 2016; Biankin et al., 2012; Du et al., 2017).

Gene expression profiling for identifying new molecular taxonomy is an emerging approach in the field of PDAC. In other tumour entities such as lung, melanoma, colon or breast cancer, molecular characteristics can vary widely in microscopically indistinguishable cancers (Dai et al., 2015b; Rabbie et al., 2019; Rudin et al., 2019; Singh et al., 2021). Molecular subtyping is considered a helpful tool to predict the response to chemotherapy and therefore personalise the therapy options to improve patient prognosis. Since the first subtyping approach in 2011, many different classifications have been performed (Collisson et al., 2011). However, in the section below, only the major PDAC classifications are mentioned.

In 2011, Collisson et al. performed the first subtyping approach with microarray-based transcriptome analysis in mouse and human PDAC cell lines and microdissected PDAC samples (Collisson et al., 2011). Based on the analysis of 62 genes, three different subtypes were identified: classical, quasi-mesenchymal (QM) and exocrine-like(Figure 2). The classical subtype is characterised by an increased expression of epithelial genes, whereas the QM subtype reveals an increased expression of mesenchymal genes. An enhanced expression of genes coding for digestive enzymes could be shown for the exocrine subtype. The different subtypes could further be linked to clinical outcome and therapy response. The classical subtype exhibits the highest survival, the exocrine-like intermediate and the QM subtype a poor survival.

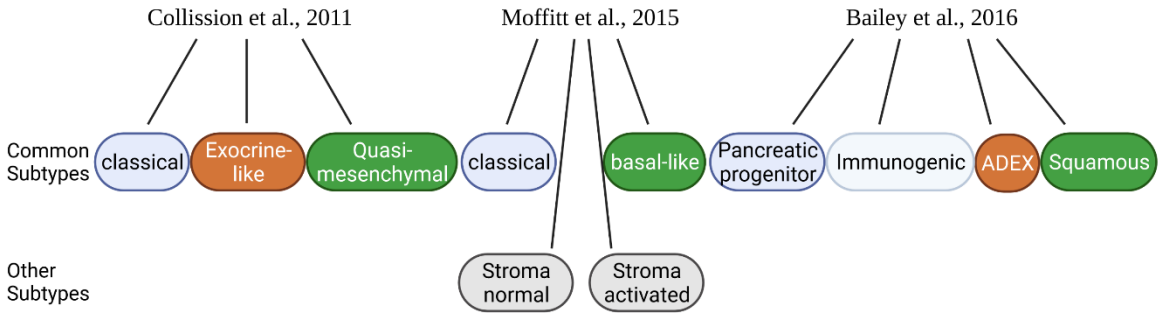

Figure 2: Schematic classification model for PDAC. Overview of some transcription-based subtypes in PDAC. Correlated common subtypes were grouped in columns. The other subtypes could not be correlated and grouped. ADEX: aberrantly differentiated endocrine exocrine (Bailey et al., 2016; Collisson et al., 2011; Moffitt et al., 2015). Created with BioRender.com.

Another subtyping approach was performed by Moffitt et al. in 2015 (Moffitt et al., 2015). They separated stroma from epithelial tumours by virtual microdissection and analysed the gene expression in both groups. After an initial microarray analysis, the samples of both compartments were validated by RNA sequencing (RNA-seq). For the stromal compartment, two distinct subtypes were described: normal and activated stroma. Also, two subtypes for the tumour group were discovered: the classical subtype, which show similarities with the Collisson classical subtype and the basal-like subtype, which overlaps with the Collisson QM subtype (Moffitt et al., 2015).

In 2016, Bailey et al. published a list of 32 significantly mutated genes involved in 10 molecular pathways, identified by deep-exome sequencing and RNA-seq analysis. With this analysis, four subtypes were discovered: the squamous and progenitor subtype, similar to Collisson's QM and classical subtype, whereas the aberrantly differentiated endocrine exocrine (ADEX) and immunogenic subtypes were classified by The Cancer Genome Atlas (TCGA) as less pure subtypes and likely derived from non-transformed stroma cells. (Bailey et al., 2016).

Rashid et al. investigated the robustness and overall clinical relevance of the subtypes described by Collisson et al., Moffitt et al. and Bailey et al. They could prove that the basal-like and classical subtypes by Moffitt et al. were the most replicable and robust classification which is associated with patient prognosis and treatment response. They further introduced a single-sample classifier based on the two subtypes, which allows the classification across different gene expression platforms (Rashid et al., 2020).

Even though these studies identified distinct subtypes, all transcription-based studies determined a classical and basal-like subtype. The classical subtype is characterized by lower aggressiveness, relatively good prognosis, and gene signature expression for epithelial differentiation. However, the basal-like subtype describes poorly differentiated, highly aggressive tumours associated with reduced survival and chemoresistance (Bailey et al., 2016; Collisson et al., 2011; Moffitt et al., 2015; O'Kane et al., 2020). These studies highlight the importance of classifying the molecular PDAC subtypes to improve patient-orientated therapy.

2.2.1.1 Epithelial to Mesenchymal Transition in PDAC

Transcriptional subtyping analysis revealed an enrichment of the epithelial to mesenchymal transition (EMT) pathway for the basal-like subtype (Dijk et al., 2020). EMT is a developmental process that naturally occurs during embryonic development, tissue regeneration, wound

healing and organ fibrosis (Micalizzi and Ford, 2009). Biochemical changes, as invasiveness, increased migratory capacity, enhanced resistance to apoptosis and upregulated production of ECM components allow the transformation of epithelial cells into mesenchymal cells in a dynamic process (Kalluri and Weinberg, 2009; Roche, 2018). By cytoskeletal remodelling and gain of mobility, the epithelial cells lose their intracellular contacts and apico-basal polarisation (Larue and Bellacosa, 2005). EMT plays a crucial role in tumour development and progression, as the cells gain the ability to leave the primary tumour site, enter the bloodstream and metastasise to a distant site (Guo et al., 2016). The cellular transition to a more mesenchymal state is mediated by different factors, including transcription factors such as Zeb1, Snail, Twist and microRNAs (miRNA), e.g. microRNA-200 (miRNA-200) (Kalluri and Weinberg, 2009). The activation of various signalling pathways, such as hypoxia, Notch, Wnt, and Transforming Growth Factor beta (TGF-beta), can also induce EMT (Liao and Yang, 2017). Typical epithelial markers, such as the cell adhesion proteins epithelial cadherin (E-cadherin), epithelial cell adhesion molecule (Epcam) and occludin, a protein for tight junctions, are lost upon the EMT process. Mesenchymal markers such as the intermediate filament vimentin, fibronectin, a glycoprotein of the extracellular matrix, and neural cadherin (N-cadherin) are expressed upon activation of EMT (Figure 3) (Dongre and Weinberg, 2019).

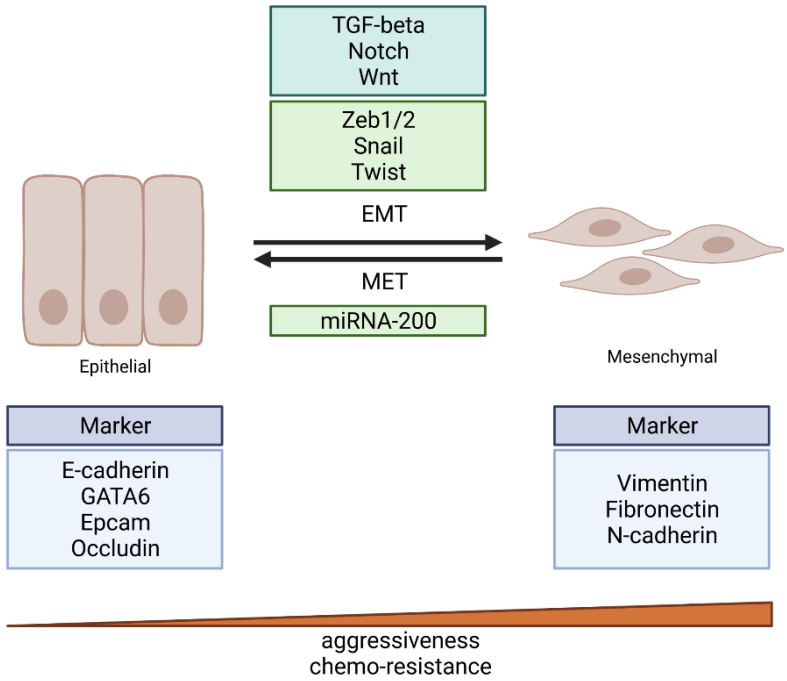

Figure 3: Schematic model for epithelial to mesenchymal transition. Epithelial cells are characterised by the expression of E-cadherin, GATA6, epithelial cell adhesion molecule (Epcam) and occluding. The transcription factors Zeb1/2, Snai or Twist, as well as the TGF-beta, Notch or Wnt pathways, can induce the epithelial to mesenchymal transition (EMT). Mesenchymal cells express vimentin, fibronectin, and N-cadherin. The expression of miRNA-200 can initiate the mesenchymal to epithelial transition (MET). Aggressiveness and chemoresistance increase from epithelial to mesenchymal state. Created with BioRender.com.

The major hallmark of EMT is the loss of E-cadherin. The transcription factor Zeb1/2 can directly bind to the E-cadherin promoter, repressing its transcription and keeping the cell in a mesenchymal state (Vandewalle et al., 2009). This process can also be reversed by downregulation of Zeb1/2, leading to mesenchymal to epithelial transition mediated, for example through miRNA-200 (Park et al., 2008). The transcription factor GATA6 is also a regulator of the EMT process. The binding of GATA6 to the E-cadherin and Zeb1 promotor inhibits the dedifferentiation and EMT, stabilising the epithelial state (Martinelli et al., 2017).

The EMT marker expression could strongly be linked to the basal-like (Moffitt et al., 2015), squamous (Bailey et al., 2016) and quasi-mesenchymal (Collisson et al., 2011) PDAC subtypes, which share common features as dedifferentiation, expression of mesenchymal genes, metabolism, low survival and poor prognosis (Aiello et al., 2018; Bailey et al., 2016; Collisson et al., 2011; Georgakopoulos-Soares et al., 2020; Moffitt et al., 2015). Further, Arumugam et al. revealed that the absence of E-cadherin and expression of Zeb1 could be correlated to chemoresistance in PDAC cell lines which has also been shown for the basal-like subtypes, making these cells challenging to treat (Arumugam et al., 2009; Aung et al., 2019; Bailey et al., 2016; O'Kane et al., 2020).

2.2.2 PDAC Therapy

The only potentially curative treatment strategy for pancreatic cancer is the resection of the tumour (Beger et al., 2002; Oettle et al., 2013). However, less than 20 % of patients are eligible for the surgery at the time of diagnosis (Kleeff et al., 2016). For patients with advanced pancreatic cancer, the gold standard since 1997 is the treatment with the nucleoside analogue gemcitabine (Burris et al., 1997). Depending on the age and health status, a combination of gemcitabine together with the taxane nab-paclitaxel or a combination of folinic acid, 5-fluorouracil (5-FU), which is a thymidylate synthase inhibitor, the topoisomerase I inhibitor irinotecan and the alkylating-like agent oxaliplatin, summarised as FOLFIRINOX, can be administered to patients with good performance due to severe toxicity associated with this therapy (Conroy et al., 2011; Von Hoff et al., 2013). Despite the adverse effects of FOLFIRINOX, this therapy leads to increased disease-free survival, median overall survival and response rate compared to gemcitabine (Conroy et al., 2011).

Nevertheless, advanced pancreatic cancer therapy options are palliative and only lead to a slightly improved outcome (Perone et al., 2016). An enhanced understanding of PDAC is

crucial for improved therapy options as it has been found that therapy response is highly dependent on the mutational status of patients. While, for example, the alkylating-like agent cisplatin together with gemcitabine leads to no improved effect in advanced pancreatic cancer patients in general, the treatment in a subgroup with germline BRCA1/2 or Partner and localizer of BRCA2 (PALB2) mutations, which accounts for 5-9 %, was effective. The results were so profound that this combination was introduced as a standard-care option for patients with this mutational status (Heinemann et al., 2006; O'Reilly et al., 2020). Besides the mutations of BRCA1/2 or PALB2, patients with other defects in the homologous recombination DNA damage response pathway may profit from the combination of cisplatin-based chemotherapy (Perkhofer et al., 2021).

2.2.3 Platinum Compounds

In 1844, Michele Peyrone first synthesised cisplatin (*cis*-diammine-dichloro-platinum); however, it took till the late 1960s until the anti-proliferative property of cisplatin was discovered in *E.coli* bacteria and confirmed in a sarcoma mouse model by Barnett Rosenberg (Peyrone, 1844; Rosenberg et al., 1965). A few years later, in 1971, the first patient with testicular cancer was treated with cisplatin, which led to Food and Drug Administration (FDA) approval in 1978 to treat testicular, advanced ovarian and bladder cancer (Alderden et al., 2006; Hambley, 1997; Higby et al., 1974). By now, cisplatin has become the mainstay for various cancer treatments, including advanced pancreatic, breast, cervix, head and neck, esophageal and non-small cell lung cancer, and some paediatric malignancies (Dasari and Tchounwou, 2014; Ruggiero et al., 2013). Driven by the high organ toxicity, the cisplatin analogue carboplatin was discovered to reduce the side effects like nephrotoxicity, myelosuppression, emesis, neurotoxicity, and ototoxicity (McKeage, 1995) (Figure 4A).

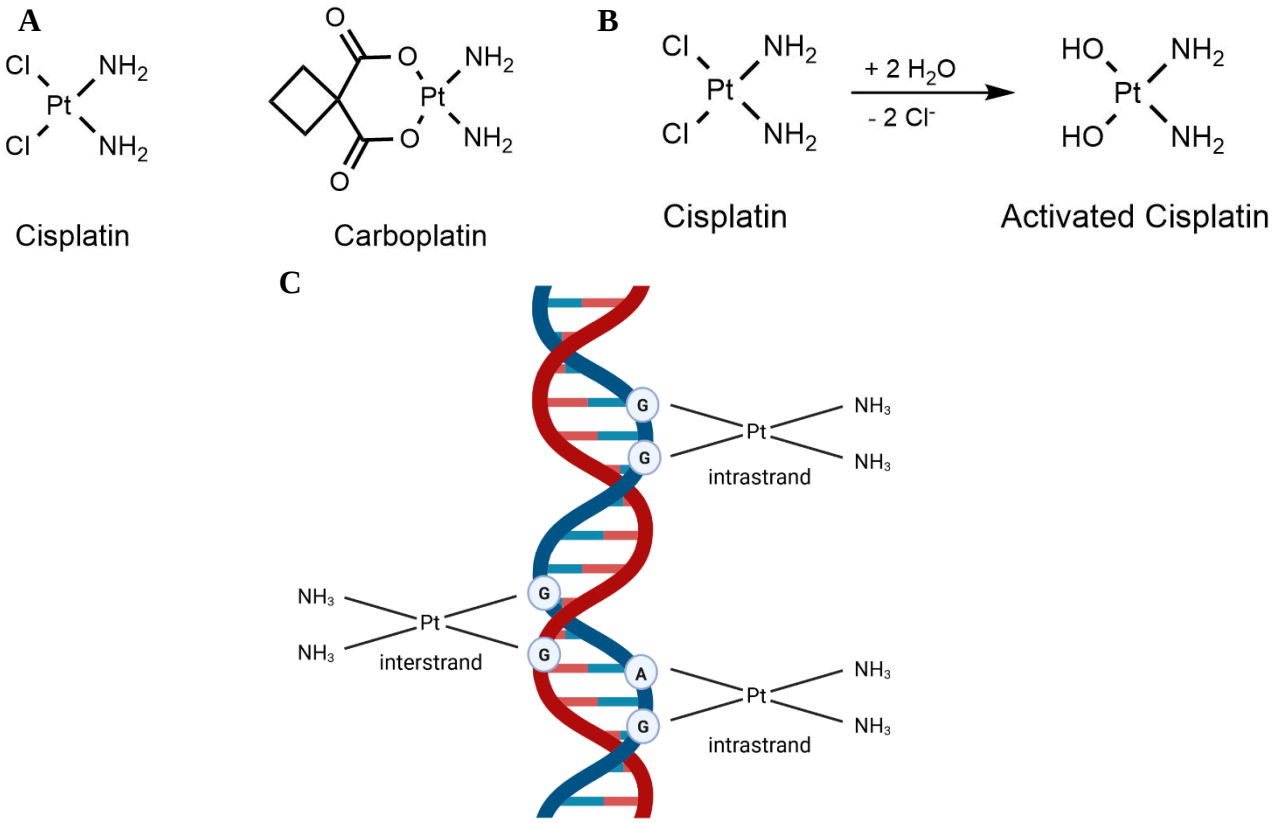

Figure 4: Platinum analogues and formation of cisplatin adducts. **A** Structure of platinum analogue cisplatin and carboplatin. **B** Activation mechanism of cisplatin by aquation. **C** Formation of cisplatin-DNA adducts preferably at N7 position of the guanosine but also to adenosine leading to intra- and inter-strand crosslinks. Adapted from (Rocha et al., 2018). Created with BioRender.com.

Cisplatin is a neutral inorganic compound with two inert ammine ligands and two labile chloride ions. Upon aquation in the cell, both chloro-groups are substituted with water molecules leading to the activation of cisplatin (Figure 4B) (Davies et al., 2000). In this form, cisplatin composed of nucleophilic propensity reacting with cysteine-rich, cytosolic peptides or proteins, such as glutathione (GSH) and metallothionein (MT) (Eastman, 1987; El-Khateeb et al., 1999). Furthermore, the activated cisplatin can interfere with the DNA, preferably at the nucleophilic N7-site on guanosine, which leads to the generation of platinum-DNA complexes and DNA crosslinks (Eastman, 1987). These crosslinks can occur within one DNA strand forming an intra-strand crosslink (85-90 % of total lesions) or between both DNA strands leading to inter-strand crosslinks (ICL) in around 1-3 % of all lesions (Dai et al., 2015a) (Figure 4C). After entering the cell, the formation of platinum-DNA adducts is the central cytotoxic mechanism, whereby the ICL intensely contributes to the toxicity despite the low formation rate as they have severe effects on the cell by suppressing replication and transcription and involve complex repair mechanisms (Wang and Lippard, 2005). Small amounts of cisplatin-induced DNA

damage lesions can be removed by the DNA repair system of the cell. While intra-strand crosslinks are most prominently recognized and repaired by nucleotide excision repair (NER), the ICLs are especially repaired by the Fanconi anemia (FA) pathway (Kee and D'Andrea, 2010).

This pathway mainly involves 22 Fanc proteins, among others BRCA1 and BRCA2, along with FA associated factors, which recognize ICL primarily during S phase of the cell cycle. These proteins are assumed to cooperate in a common signalling pathway to repair the DNA damage lesions (Niraj et al., 2019). After recognizing the DNA damage, the FA core complex consisting of FANCA, FANCB, FANCC, FANCE, FANCF, FANCG, FANCL and FANCM, acts as an E3 ubiquitin ligase and activates the pathway by FANCI-FANCD2 monoubiquitination (Figure 5) (Walden and Deans, 2014). The activated FANCI-FANCD2 is translocated to the chromatin damage, where it recruits and activates additional repair proteins, including BRCA1, BRCA2 and PALB. The monoubiquitination and nuclear foci formation of FANCI-FancD2 are thereby the essential steps (Duan et al., 2013). This pathway coordinates the different double-strand break (DSB) repair sub-pathways, preferably the homologous recombination (HR) pathway, as many FA proteins are well-established HR factors (Liu et al., 2020). FA pathway deficiency results in enhancement of the error-prone non-homologous end joining, while the HR efficiency is reduced (Nakanishi et al., 2005).

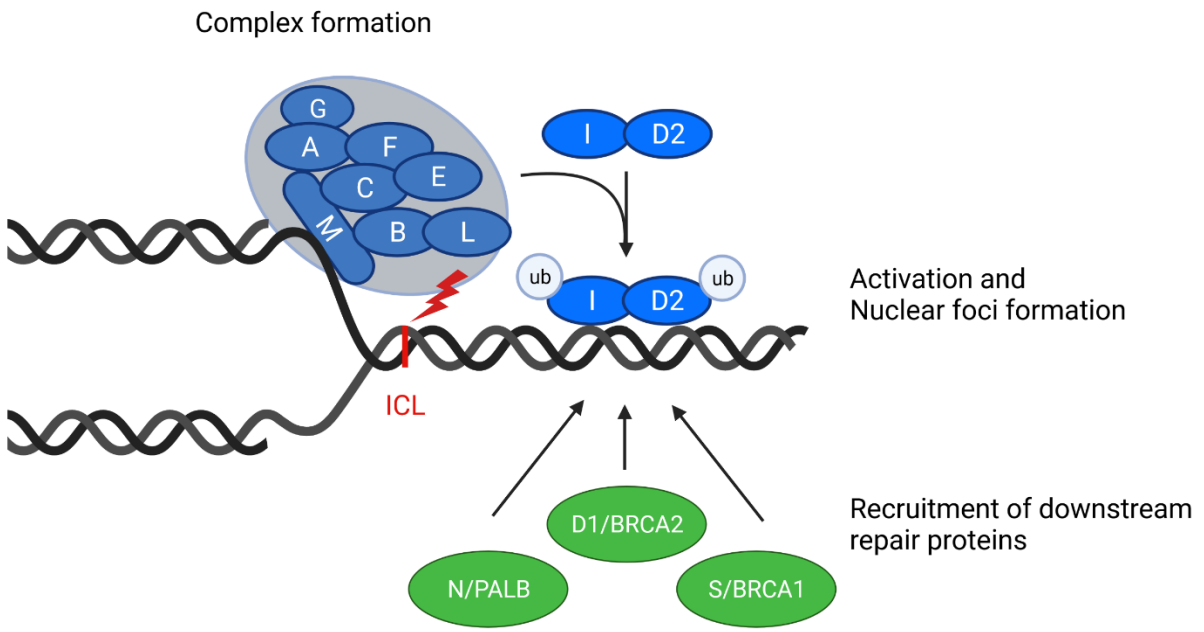

Figure 5: Schematic overview of Fanconi anemia pathway. The FA core complex consisting of FANCA, B, C, E, F, G, L and M. activate FANCI/FANCD2 by monoubiquitination. After nuclear foci formation, other repair proteins as BRCA1/2 and PALB are recruited. Adapted from (Walden and Deans, 2014). Created with BioRender.com.

Depending on the severity of the damage, the cell either arrests in the cell cycle to repair the DNA damage and prevent the cell from abnormal mitosis, or it activates the apoptosis pathway (McCabe et al., 2009). Although cisplatin displays a potent induction of apoptosis and anti-proliferative effects and is one of the most effective broad-spectrum anti-neoplastic drugs, resistance is a significant drawback (Siddik, 2003).

2.2.4 Cellular Resistance Mechanisms towards Platinum Compounds

Although the primary mechanism of platinum cytotoxicity is the formation of platinum-DNA adducts, four significant mechanisms have been described by which the adduct formation can be reduced, leading to resistance development. 1. Reduced cellular adduct accumulation by decreasing the drug influx and increasing the efflux. 2. Increased detoxification activity by protein binding. 3. Increased DNA damage response, and 4. Inactivation of apoptosis induction (Figure 6) (Chen and Chang, 2019).

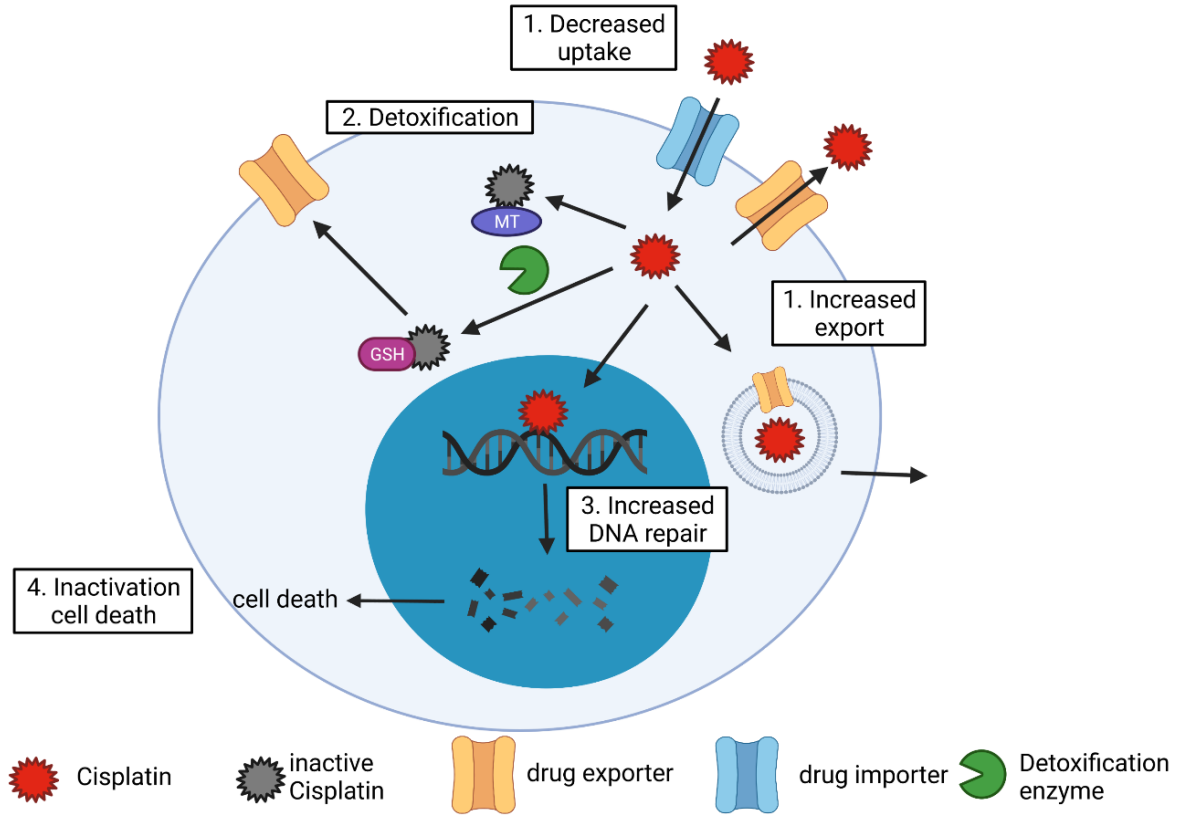

Figure 6: Schematic overview of cisplatin resistance mechanisms. Resistance mechanisms include **1**. decreased drug import mediated by copper transporter and increased drug export by copper-transporting ATPase 1 and 2 (ATP7A/B) or multidrug resistance protein 2 (MRP2). **2**. Enhanced detoxification by binding of cisplatin to glutathione (GSH) and metallothionein (MT). **3**. Increased DNA damage repair process to remove the cisplatin-DNA adducts. **4**. Failure of the DNA repair system induced apoptosis, which can be neutralized by upregulation of anti-apoptotic or downregulation of pro-apoptotic signals. Adapted from (Chen and Chang, 2019). Created with BioRender.com.

2.2.4.1 Decreased uptake or increased efflux

The accumulation of platinum compounds in the cell is an essential requirement for cytotoxicity. Changes in influx and efflux mediated by various transporters can affect platinum efficacy.

The influx of cisplatin is mediated by passive diffusion and transmembrane transportation systems. Members of the solute carrier superfamily (SCL) family, such as SCL22A1, SCL22A2 and SCL47A1, are involved in cisplatin uptake (Yonezawa et al., 2006). Mislocation, downregulation or inhibited activity of these carriers are linked to reduced intracellular concentrations of cisplatin (Zhou et al., 2020). Another transporter involved in the uptake of platinum drugs is the copper transporter 1 (CTR1) (Holzer et al., 2006). Song et al. could show that overexpression of the transporter resulted in enhanced sensitivity of small cell lung cancer cells towards platinum compounds (Song et al., 2004).

Besides the decreased influx of platinum compounds, increased efflux can also contribute to resistance. The export is mediated by the copper-transporting ATPase 1 and 2 (ATP7A/B) (Safaei et al., 2012). Upon binding platinum drugs, the ATP7A/B, located in the trans-Golgi network, translocate to cytoplasmic vesicle in an ATP-dependent manner and release the platinum out of the cell upon fusion with the plasma membrane (Safaei et al., 2008). Overexpression of ATP7A revealed decreased cellular cisplatin intensity and exclusion from the nucleus, as ATP7A acts as an insulator, preventing the access of cisplatin to the nucleus (Chisholm et al., 2016). The high expression of ATP7B might be used as a prognostic factor in colorectal cancer, revealing prolonged progression time (Martinez-Balibrea et al., 2009). In patients with ovarian cancer, the increased expression of ATP7A/B was associated with shorter survival (Lukanović et al., 2020).

Another exporter involved in platinum resistance is the multidrug resistance protein 2 (MRP2), which belongs to the ATP-binding cassette transporters (Borst et al., 2000). This transporter is a unidirectional efflux pump that removes cisplatin-bound glutathione from the cells. Intrinsic resistance and poor clinical outcome in ovarian and small cell lung cancer patients could be linked to high levels of MRP2 (Surowiak et al., 2006; Ushijima et al., 2007).

2.2.4.2 Detoxification

The initially inert cisplatin gains a high affinity for cytoplasmic nucleophilic species in the aquated state. Thereby, platinum forms strong bonds to cysteine-rich proteins and peptides, as

glutathione (GSH) or metallothionein (MT) (Eastman, 1987; El-Khateeb et al., 1999). The glutathione-S-transferase catalyses the binding of platinum to GSH. Platinum-bound GSH is removed from the cell in cooperation with the MRP transporter (Kuo and Chen, 2010). Overexpression of GSH or glutathione-S-transferase are linked to resistance by inactivation and export of platinum compounds in bladder and ovarian cancer (Byun et al., 2005; Surowiak et al., 2005). Another detoxification mechanism involves the metal-binding protein MT which can form a chelating complex with platinum resulting in the inactivation of platinum drugs (Kimura and Kambe, 2016). Platinum agents might also induce the biosynthesis of MT proteins by binding the metal transcription inhibitor, further contributing to the resistance (Krizkova et al., 2010). Overexpression of MT could be linked to chemoresistance to cisplatin in neuroblastoma and oesophageal cancer (Hishikawa et al., 1997; Rodrigo et al., 2021).

2.2.4.3 Enhanced DNA repair

The formation of ICL and intra-strand crosslinks inhibits replication and transcription (Wang and Lippard, 2005). Intra-strand crosslinks activate the NER mechanism, in which DNA excision repair protein (ERCC-1) and ERCC1-DNA repair endonuclease XPF dimerize and function as a nuclease (Hashimoto et al., 2016). Upregulation of this complex results in increased excision of cisplatin adducts and repair of DNA lesions (Ferry et al., 2000). For the repair of DSB and DNA crosslinks, BRCA plays a crucial role through the FA and HR pathway. Mutation of BRCA1, BRCA2 and other FA components lead to the impaired detection and repair of DNA damage caused by cross-linking agents (Fang et al., 2020; Sy et al., 2009). Short-term treatment of ovarian cancer cells revealed the same levels of platinum-DNA adduct formation after acquired resistance, suggesting that the upregulation of the DNA repair machinery is considered to be the most effective mechanism in platinum-resistant cells (Dijt et al., 1988; Wynne et al., 2007).

2.2.4.4 Evading apoptosis

Pro-apoptotic and anti-apoptotic proteins tightly regulate the intrinsic apoptosis pathway (O'Brien and Kirby, 2008). An imbalance of this homeostasis by overexpression of anti-apoptotic or repression of pro-apoptotic proteins prevents the induction of apoptosis (Kim et al., 2002). For example, the anti-apoptotic myeloid cell leukemia-1 (Mcl-1) protein was found to be overexpressed in many tumours, preventing apoptosis by sequestering pro-apoptotic factors (Wang et al., 2021). Upregulation of the anti-apoptotic proteins Bcl-2 (B-cell lymphoma

protein 2) or Bcl-XL (B-cell lymphoma protein extra-large) are linked to enhanced cisplatin resistance (Keitel et al., 2014). Also, small non-coding RNAs can regulate pro- and anti-apoptotic proteins, and dysregulation can interfere with the platinum response (Zhou et al., 2020).

The tumour suppressor p53 plays a crucial role in the cytotoxic effects of cisplatin since some of the target genes induce apoptosis. Mutation or loss of p53 occur in over 50 % of tumours (Hollstein, 1994). Despite cisplatin treatment, the regulation of checkpoint response, cell cycle arrest, and induction of apoptosis fail, leading to the survival of the cells and resistance to oxaliplatin and 5-FU. A clear link between p53 status and cisplatin has not been shown (Arango et al., 2004; Martinez-Rivera and Siddik, 2012).

2.3 microRNA

Various cellular processes involved in cancer biology, as proliferation, differentiation, invasion and metastasis, apoptosis and drug resistance, are mediated by microRNAs (miRNA) (Chen et al., 2012). miRNA are small non-coding RNAs, which post-transcriptionally regulate protein-coding gene expression. Interaction of the miRNA seed sequence with target mRNAs leads to translational repression and mRNA degradation. The seed sequence is a 6 to 8 long nucleotide sequence at the 5’ end of the mature miRNA (Bhayani et al., 2012). This sequence characterizes the specificity of the miRNA to their targets, whereby one miRNA can bind several mRNAs, and different miRNAs can regulate multiple mRNAs (Hashimoto et al., 2013). A mature miRNA consists of 20-25 nucleotides and is generated by a multi-step process (Figure 7) (Bartel, 2004).

The miRNA gene is transcribed by RNA polymerase II within the nucleus (Borchert et al., 2006). The post-transcriptional structure of this primary miRNA (pri-miRNA) forms a hairpin. The pri-miRNA is spliced into a 70 nucleotide long precursor miRNA (pre-miRNA) by the Drosha- DiGeorge syndrome critical region 8 (DGCR8) complex. After nuclear exportation by Ran-GTP dependent transport receptor Exportin-5, the pre-miRNA is cleaved into the mature miRNA by the type III RNase Dicer. Following the processing step, one strand of the duplex miRNA is degraded, leaving one strand which forms a multimeric protein-RNA complex, called RNA induced silencing complex (RISC). This complex comprises of Argonaute family proteins, enabling the cleavage and repression of target mRNA (MacFarlane and R. Murphy,

2010). miRNAs mostly form the interaction between their seed sequence and the 3' untranslated region (3'-UTR) or the open reading frame of their target mRNA (Grimson et al., 2007).

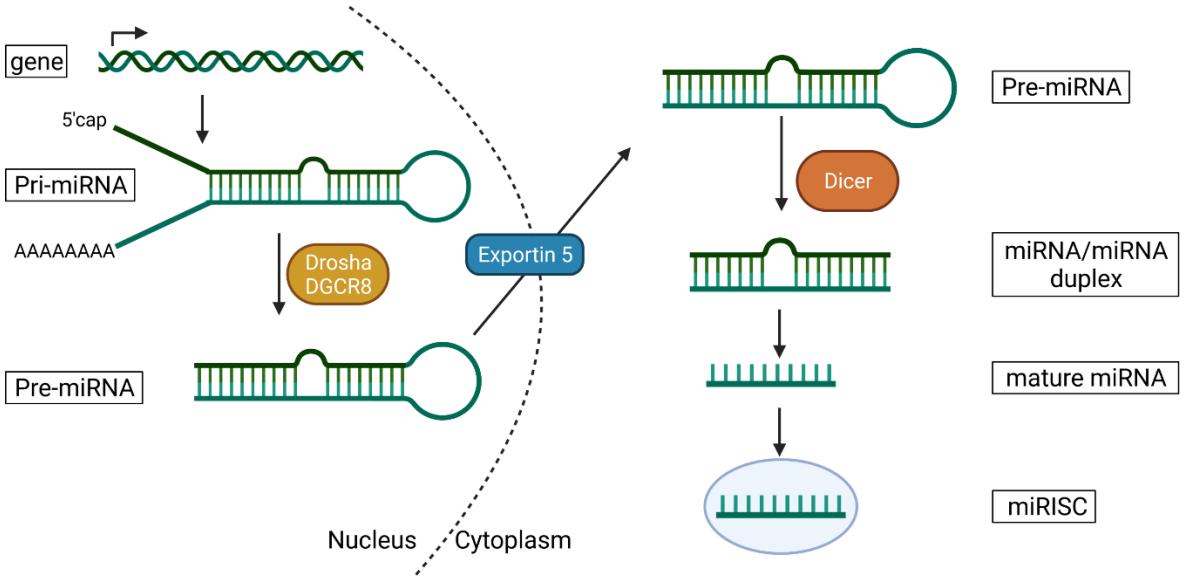

Figure 7:Simplified scheme for the biogenesis of miRNAs. RNA Polymerase II transcribes the miRNA genes into pri-miRNA. The pre-miRNA is produced by processing the pri-miRNA mediated by the Drosha-DGCR-8 complex. After the nuclear exportation by Exportin-5, the mature miRNA is produced by type III RNase Dicer. One miRNA strand gets degraded, and the remaining strand is part of the RISC complex, a multimeric protein-RNA complex. The RISC complex composes of Argonaut proteins which mediate the targeting and repression of target mRNA. Adapted from (Winter et al., 2009). Created with BioRender.com.

Depending on the seed and target sequence consensus, the mRNA transcript is repressed by two different mechanisms. The standard mechanism involves imperfect binding of the miRNA and the target mRNA leading to the repression of target gene translation (Martin et al., 2014). The perfect binding of miRNA and mRNA occurs at a lower rate, resulting in endonucleolytic cleavage catalysed by the Argonaute complex (Park and Shin, 2014). Around two-thirds of all protein-coding genes are regulated by miRNAs, therefore being involved in nearly all cellular processes (Hammond, 2015). With this high impact on regulating signalling pathways and cellular processes, miRNAs can also act as tumour suppressors or oncogenes, assigning them an essential role in the development, progression, and treatment of cancer (Zhang et al., 2007).

2.3.1 microRNA-200 Family

One of the most thoroughly investigated functional miRNA clusters, also involved in cancer development, is the miRNA-200 family. It consists of five members, which can be divided into two clusters. miRNA-200b/200a/429 are located on chromosome 1 and miRNA-200c/141 on chromosome 12 (Altuvia et al., 2005). The miRNA-200 family can also be separated into two

functional groups based on their seed sequences: cluster 1 consisting of miRNA-200b/200c/429 and cluster 2 with miRNA-200a/141 (Figure 8) (Humphries and Yang, 2015).

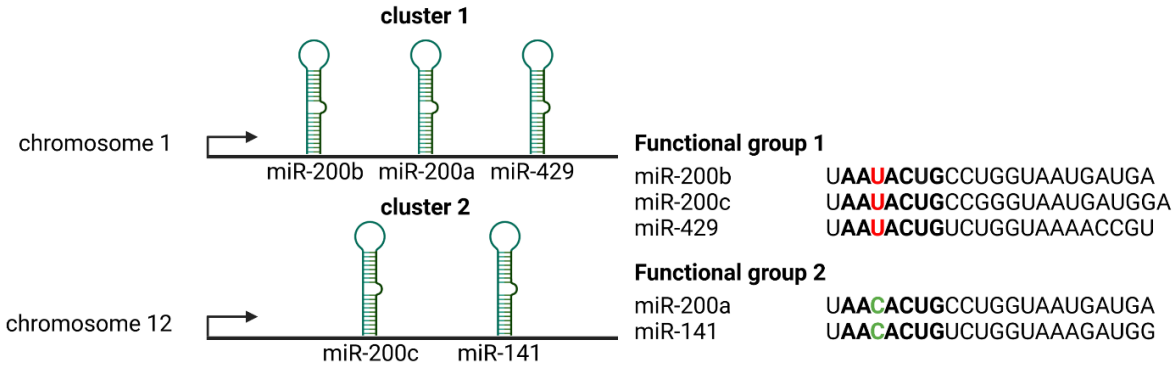

Figure 8: Genomic location and seed sequence of miRNA-200 family members. miRNA-200 family members can be separated into two clusters as they are located on chromosomes 1 and 12. Based on the seed sequence, two functional groups can be distinguished. Adapted from (Humphries and Yang, 2015). Created with BioRender.com.

miRNA-200 is highly expressed in epithelial cells and conserved among vertebrates (Humphries and Yang, 2015). It is mainly regulated by DNA methylation or silencing of the promotor region by polycomb group-mediated histone modifications. These modifications can lead to the loss of miRNA-200 expression (Neves et al., 2010) and decreased miRNA-200 level can significantly impact epithelial to mesenchymal transition, tumour metastasis, cancer cell renewal, and chemoresistance (Brozovic et al., 2015; Park et al., 2008). The process of EMT is believed to be an important step in metastasis formation of tumours that originated from epithelial cells. miRNA-200 is involved in regulating CHD1 by inhibiting Zeb1/2 and, therefore, stabilizing the epithelial phenotype. Mesenchymal cells mostly lack the expression of miRNA-200 (Mongroo and Rustgi, 2010). It is also enhanced in angiogenesis, inducing the vascular endothelial growth factor A (VEGFA) (Choi et al., 2011). The expression level of miRNA-200 could also be associated with the sensitivity towards chemotherapy. In ovarian cancer cells, the downregulation of miRNA-200 was linked to the resistance of paclitaxel and carboplatin (Brozovic et al., 2015). Similar effects could be shown in colorectal cancer, where the downregulation of miRNA-200 and reversal of EMT contribute to the resistance towards 5-FU and oxaliplatin (Senfter et al., 2016; Tanaka et al., 2015).

2.4 The Molecular Chaperone HSP90

Protein structures are vulnerable to stressful stimuli as hypoxia, increased oxygen species and heat. The unfolding of the proteins may result in the loss of function, and the aggregation of

misfolded proteins disturbs the proteostasis. The coping mechanism of the cell involves the upregulation of stress proteins as molecular chaperones (Hartl et al., 2011). Molecular chaperones assist the folding and assembly of their client structures but are not part of the active protein complex (Miyata et al., 2013). One of the central chaperones are heat shock protein 90 (HSP90) and heat shock protein 70 (HSP70), which also assist the folding, maintenance, and degradation of proteins under non-stressful conditions (Buchner, 1999).

HSP90 is mainly located in the cytoplasm, but the HSP90 family members TRAP1 (Altieri et al., 2012) and GRP94 (Marzec et al., 2012) can also be found in mitochondria or the endoplasmic reticulum, respectively. Under a non-stress situation, HSP90 is one of the most abundant proteins, compromising 1-2 % of total proteins (Hoter et al., 2018). Upon stressful conditions, the master regulator heat shock factor 1 (HSF-1), which is repressed in the absence of stress, induces the expression of even higher levels of HSP90, HSP70 and other pro-survival components of the heat shock response pathway (Do et al., 2015; McMillan et al., 1998; Sistonen et al., 1994).

The primary function of HSP90 is the binding of client proteins at a late stage to mediate correct folding of the native structure or stabilization of the clients. Missing HSP90 function leads to ubiquitination of clients, followed by proteasomal degradation (Blacklock and Verkhivker, 2014). The importance of HSP90 in eukaryotes is also reflected by the highly conserved sequence, which shares 60 % identity between the human and yeast HSP90 sequence (Chen et al., 2006). HSP90 is expressed in two different isoforms: the heat shock inducible form HSP90α and the constitutively expressed form HSP90β (Johnson, 2012). Both isoforms share 85 % of sequence identity. However, it could be shown that both isoforms have distinctive roles, although their diverse function is poorly understood (Millson et al., 2007). HSP90 acts as a homodimer, whereas dimerization, mediated by the C-terminal dimerization domains, is essential for its function (Harris et al., 2004; Mayer and Le Breton, 2015). The middle domain is responsible for client binding, whereas the N-terminal region harbours the ATP binding pocket (Hainzl et al., 2009; Prodromou et al., 1997). HSP90 molecular chaperones display structural similarities to histidine kinase, MutL DNA-mismatch-repair and DNA remodelling DNA gyrase to the GHKL superfamily (Dutta and Inouye, 2000). The shared similar characteristics are the Bergerat fold, an ATP-binging domain crucial for ATP binding and hydrolysis (Prodromou et al., 1997). HSP90 function is therefore characterized by ATPase activity and cycling between the open and closed form. On the one hand, ATP binding promotes the closer and more compact complex of HSP90 by a lid segment that twists the HSP90 complex and, on the other hand, the association of the N-terminal region to form a catalytically active

state. This state enables most clients to interact with the dimer. After ATP hydrolysis, the folded client protein, as well as ADP and Pi, are released, restoring HSP90 to the open state again (Figure 9) (Prodromou, 2000).

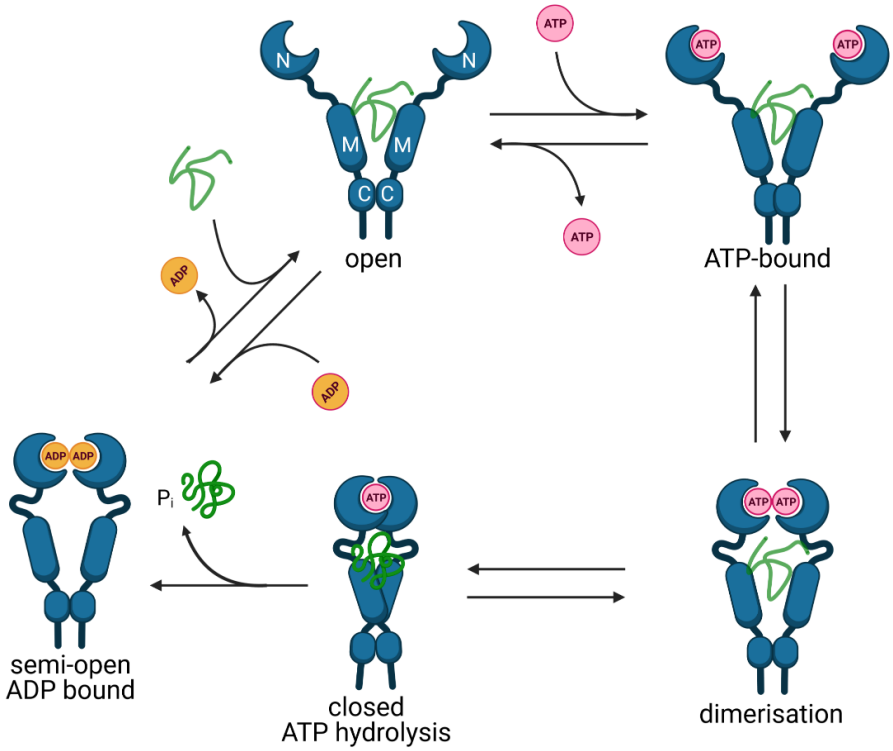

Figure 9: Scheme of the ATPase cycle of HSP90. HSP90 homodimer in the open V-shaped conformation can bind the client (green bundle) and ATP at the M- and N-terminal domain, respectively. The binding of ATP induces the dimerization of the N-terminal domain and a conformational change to the closed state. After ATP hydrolysis, the dimers dissociate into a semi-open conformation with ADP bound, releasing the client. Release of ADP recycle the dimers into the open conformation allowing a new ATPase cycle. Adapted from (Lackie et al., 2017). Created with BioRender.com.

An extensive network of co-chaperones further regulates the activity of HSP90. Many co-chaperones contain a tetratricopeptide repeat (TRP), a motif of anti-parallel alpha-helices enabling the binding to the chaperone (Kenneth Allan and Ratajczak, 2011; Lamb et al., 1995). HSP70, assisted by heat shock protein 40 (HSP40), recruits client proteins (Cintron and Toft, 2006). The TRP-co-chaperone Hop/Stip1 binds to the open conformation of HSP90 and mediates the client protein transfer between HSP70 and HSP90 (Wegele et al., 2006). Immunophils also interact with HSP90 to facilitate client protein maturation (Mazaira et al., 2016). The non-TPR co-chaperones p23/Sba1 binds to the closed formation and helps with the maturation of client proteins by partially inhibiting the ATP hydrolysis (McLaughlin et al., 2006; Richter et al., 2004). Cdc37 is a kinase-specific co-chaperone involved in around 60 %

of human kinase maturation and oncogenic kinases (Citri et al., 2006). The most important activator of Hsp90 ATPase activity is Aha1 (Panaretou et al., 2002).

2.4.1 HSP90 and its Role in Cancer

HSP90 was found to be constitutively expressed in cancer cells with a 2-to-10-fold higher expression than normal cells, which is why the disruption of the HSP90 folding machinery might result in a higher impact on cancer cells (Ferrarini et al., 1992). Around 800 proteins are described as HSP90 clients, including transcription factors like protein kinases and hormone receptors, but also oncogenic proteins covering all cancer hallmarks (Figure 10) (Echeverría et al., 2011; Miyata et al., 2013; Picard, 2021). By also stabilizing mutated and conformationally unstable proteins, HSP90 is a key factor for cell survival, growth control and developmental processes, all needed to maintain tumour formation (Mahalingam et al., 2009). Active HSP90 preserves the function of mutated client proteins and further protects them from proteasomal degradation (Theodoraki and Caplan, 2012). Thereby, they interfere with processes as angiogenesis (e.g. Hypoxia-inducible factor 1-alpha HIF1α), immortalization (e.g. telomerase), genome instability (e.g. FancA), apoptosis evasion (protein kinase B (AKT)) and proliferation (e.g. Receptor tyrosine-protein kinase ErbB2/Her2) (Shibbiru, 2016). The most prominent tumour suppressor p53, which is mutated in around 50 % of tumours, is also described as an HSP90 client (Peng et al., 2001). Interestingly, the mutant variant forms a more stable complex than the wildtype that underlies a high turnover by proteasomal degradation. Thus the stabilization leads to an accumulation of mutant p53 protein (Müller et al., 2005).

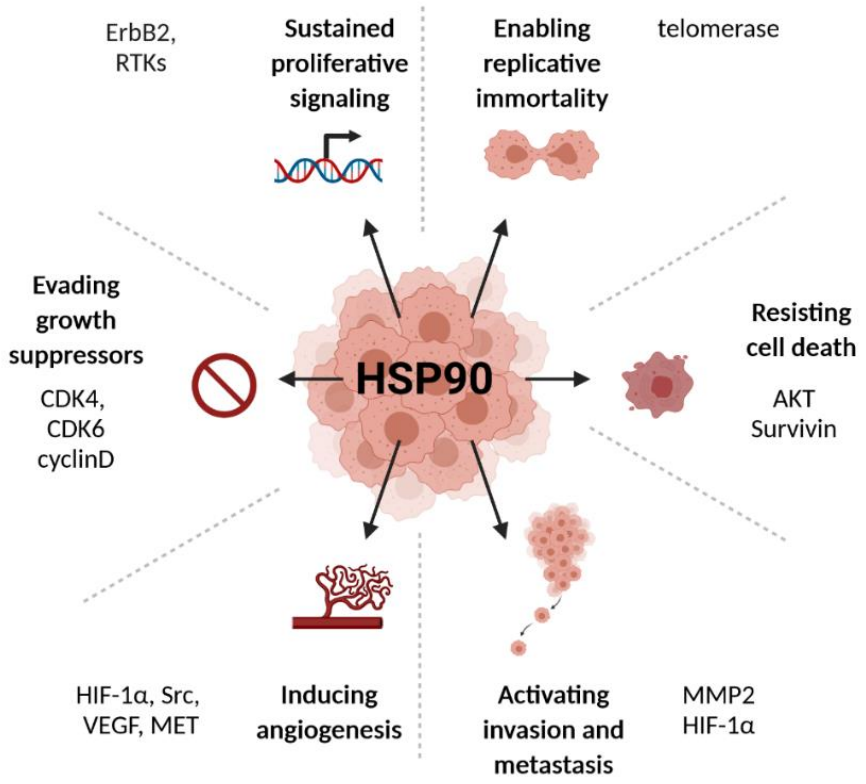

Figure 10: The central role of HSP90 client stabilization for the hallmarks of cancer. HSP90 plays a crucial role in supporting all six hallmarks of cancer, published by Hanahan and Weinberg, by stabilizing a subset of clients, as depicted. ErbB2 receptor tyrosine-protein kinase erbB-2, RTKs receptor tyrosine kinases, AKT protein kinase B, MMP2 matrix metalloproteinase-2, HIF-1α hypoxia-inducible factor 1-alpha, Src proto-oncogene tyrosine-protein kinase Src, VEGF vascular endothelial growth factor, MET tyrosine-protein kinase Met, CDK4,6 cyclin-dependent kinase 4, 6. Adapted from (Shibbiru, 2016). Created with BioRender.com.

Cancer cells are strongly dependent on HSP90 to ensure proteostasis, as in these cells high amounts of misfolded and mutated proteins are present. Upregulation of HSP90 leads to an increased protein folding and degradation, preventing proteotoxic stress (Park et al., 2020). To fulfil this task, HSP90 assembles with co-chaperones to a stable, highly active complex called the super-chaperone complex (Figure 11) (Seo, 2015). It displays a higher ATPase activity and higher affinity to ATP compared to normal cells. This enhanced affinity to ATP allows the specific, up to 100-fold increased, inhibition of HSP90 in cancer cells by inhibitors targeting the ATP binding site (Kamal et al., 2003). Besides the specificity, the simultaneous targeting of different transforming signalling pathways makes HSP90 inhibitors a promising target for cancer therapy (Powers and Workman, 2006).

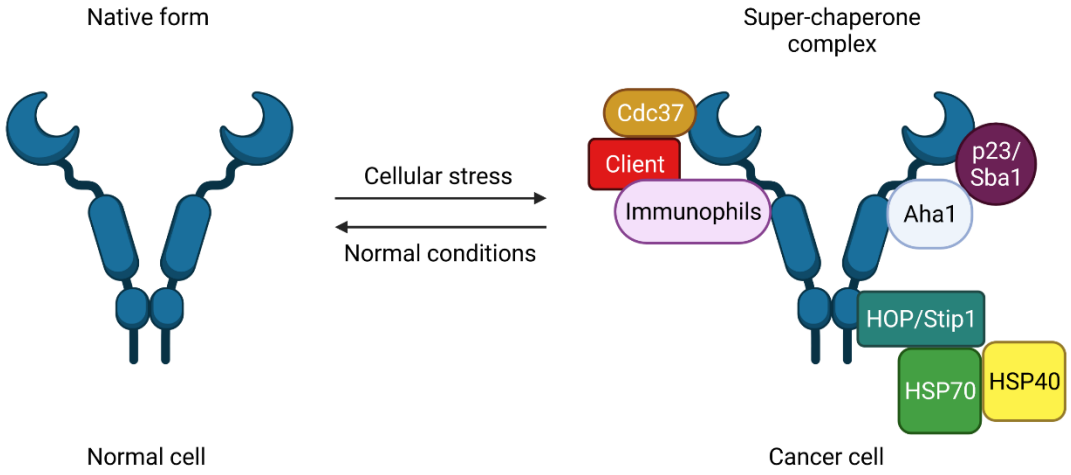

Figure 11: The HSP90 super-chaperone complex. In normal cells, the native form of HSP90 is present. A multi-chaperone complex is formed upon cellular stress, consisting of HSP90 and its overexpressed co-chaperones leading to increased client stabilization. Adapted from (Seo, 2015). Created with BioRender.com.

2.4.2 Inhibition of HSP90 as Cancer Treatment

Geldanamycin (GA), found in 1970, was the first discovered HSP90 inhibitor isolated from *Streptomyces hygroscopicus* (DeBoer et al., 1970). It was initially investigated for the weak antibiotic effects; however, the HSP90 inhibitory effect was displayed when an oncoprotein v-Src driven transformation could be reversed (Whitesell et al., 1992). The second natural compound inhibiting HSP90 was radicol (RD), originally isolated from the root of *Dictamnus radicis* and the most potent natural inhibitor of HSP90 (Delmotte and Delmotte-Plaquee, 1953). Both compounds inhibit the HSP90 activity by selectively binding to the N-terminal domain, preventing ATP binding and hydrolysis (Roe et al., 1999). However, GA and its analogue 17-AAG (tanespymicin) failed clinical trials because of high hepatotoxicity induced by the quinone moiety (Figure 12A). Furthermore, they revealed a low bioavailability, poor solubility, and weak target potency (Solit and Chiosis, 2008). These significant drawbacks resulted in the development of the second generation of ATP competing HSP90 inhibitors, which are mainly developed on the base of RD to reduce hepatotoxicity (Butler et al., 2015).

Until now, 18 pharmacological HSP90 inhibitors have been under clinical development, however, none of them has been approved by the FDA so far (Park et al., 2020). Two of these inhibitors are ganetespib and onalespib, which are second generation inhibitors developed based on the structure of radicol (Figure 12B) (Lin et al., 2008b; Woodhead et al., 2010). They are under investigation against various cancer types as monotherapy or combined with cytostatic compounds (e.g. carboplatin (NCT03783949), docetaxel (NCT01798485), capecitabine (NCT01554969)) or small molecule inhibitors (crizotinib (NCT01579994), olaparib (NCT02898207)). Second generation inhibitors are more potent than those of the first generation, based on the ability to bind the ATP binding pocket of HSP90 in the open and closed conformation, in contrast to the first generation, which is limited to the open conformation due to their larger size (Ying et al., 2012). The main advantage of HSP90 inhibitors is the ability to target multiple oncogenic proteins and pathways, including targets that are difficult to drug or evade therapy resistance of well-established drugs. Pharmacological HSP90 inhibition particularly interferes with the proliferation and survival of cancer cells, which is associated with the degradation of oncogenic HSP90 clients (Rong and Yang, 2018). The inhibitors also reveal tumour selectivity based on the higher binding affinity to HSP90 in tumours than normal tissue.

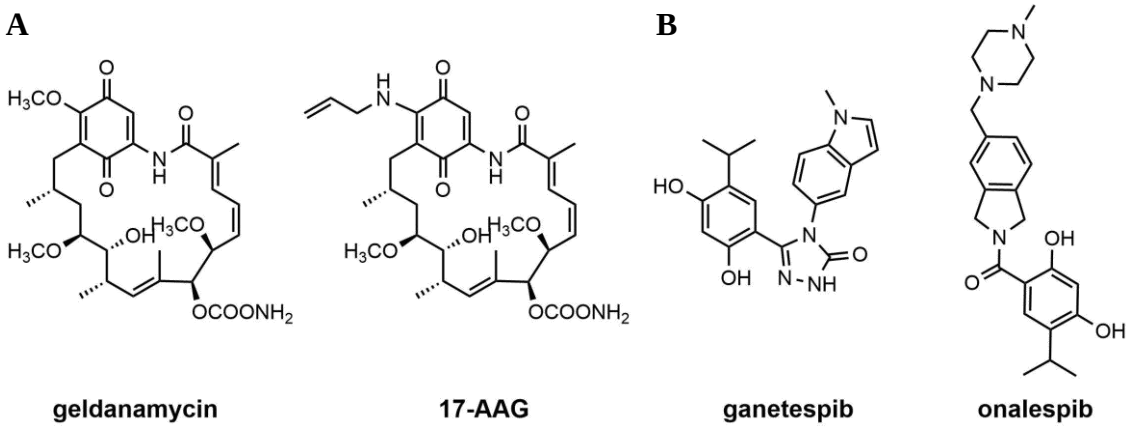

Figure 12 HSP90 inhibitors. A Structures of geldanamycin and its derivate 17-AAG. **B** Structures of the radicol based second generation HSP90 inhibitors ganetespib and onalespib.

However, the use of HSP90 as a single agent in clinical trials only showed limited clinical efficacy, leading to the investigation as combined therapy (Hong et al., 2013). As HSP90 protects the cell under stress conditions, such as chemotherapy or targeted therapy, the inhibition of the protective HSP90 can potentiate the anti-neoplastic effect. In, for example, pancreatic, cervical, breast cancer and adenocarcinoma, HSP90 inhibitors were able to sensitise the cells towards radiotherapy (Bisht et al., 2003; Nagaraju et al., 2019; Spiegelberg et al.,

2020). Proia et al. could show that a combination of ganetespib and taxanes improved the treatment of non-small cell lung cancer cells (Proia et al., 2012). Colorectal cancer cells could be successfully treated with a combination of chemotherapeutic 5-FU and ganetespib (Nagaraju et al., 2014). The combination of platinum-based chemotherapy, like cisplatin or carboplatin with HSP90 inhibitors, displayed a prominent response and synergy in head and neck, gastric and ovarian cancer (Klameth et al., 2017; Kramer et al., 2017; McLaughlin et al., 2017). In ovarian cancer cells, the inhibition of HSP90 by ganetespib upon carboplatin treatment leads to the degradation of Fa components and consequently a failure of ICL repair, resulting in increased double-strand breaks (Kramer et al., 2017). In addition, the effect of targeted therapy such as Jak2 or MEK inhibitors could also be improved by adding HSP90 inhibitors (Acquaviva et al., 2014; Hobbs et al., 2018).

2.5 Scope of the study

In this study, we aim to investigate the response of PDAC cells to cisplatin chemotherapy. Despite intensive research, the overall survival of PDAC patients remains very low. Cisplatin is the most widely used cytotoxic agent against cancer, with a broad efficacy in various cancer types; however, many tumours display resistance. It is vital to understand which PDAC patients benefit from the cisplatin treatment, allowing the treatment of only those patients who benefit. To address this problem, markers correlating with the response to therapy can help to improve the personalised treatment. On top of finding potential biomarkers, we are also aiming at combining cisplatin with sensitising drugs for treating resistant cells.

To gain further insights into the treatment options for PDAC with cisplatin, we addressed the following questions.

1. How do PDAC cells of different lines and subtypes respond to cisplatin treatment?

Gemcitabine and FOLFIRINOX could only slightly improve the clinical outcome for metastatic PDAC patients. Treatment with cisplatin leads to no improvement of clinical outcomes in PDAC patients. However, the subgroup of patients with BRCA1/2 or PALB mutations showed a favourable outcome. To elucidate the cisplatin response in PDAC cells from different subtypes, we used a panel of seven PDAC cell lines and measured the cell viability with an ATP based viability assay. We then quantified the DNA damage and cisplatin-DNA adduct formation by immunoblot analysis and immune-cytological assay, respectively. To assess

potential causality between the response and marker expression, silencing and overexpression studies of the markers were performed.

2. Are there markers that predict cisplatin sensitivity?

Pancreatic cancer reveals a high molecular heterogeneity. It is essential to understand which patients benefit from a treatment to avoid unnecessary side effects. For FOLFIRINOX, Rashid et al. could already show that the basal-like subtype revealed reduced treatment response compared to the classical subtype. For personalised therapy, there is the need for a set of markers that predict the response. To identify marker genes, we correlated their expression with the response of PDAC cells to cisplatin. In search for candidates, we analysed RNA-seq data and verified our findings by RT-PCR and immunoblot analysis.

3. Is there a way to sensitise resistant cells to cisplatin?

In ovarian cancer, Kramer et al. could show that the combination of platinum-based chemotherapy and HSP90 inhibitors resulted in a strong synergism. The inhibition of HSP90 leads to the degradation of Fanconi anemia pathway components, removing the central repair mechanism of cisplatin-DNA crosslinks. Without the repair mechanism, the cells are left with double-strand breaks resulting in chromosome fragmentation and induction of cell death. We asked the question whether this successful combination might also be active in PDAC, especially in the cisplatin-resistant cells. We investigated the response by assessing cell viability after combination treatment, using an ATP-based viability assay, immunofluorescence of the DNA damage marker phospho H2A histone family member X (phospho-H2Ax), immunoblot analysis against FANCA, and metaphase chromosome spreads. Finally, we tested our hypothesis in an orthotopic and syngeneic PDAC transplant model.

3 Manuscript

HSP90 inhibition synergizes with cisplatin treatment of basal pancreatic ductal adenocarcinoma cells

Katharina M. Ewers [1], Shilpa Patil [2], Waltraut Kopp [2], Jürgen Thomale[3], Tabea Quilitz[1], Anna Magerhans[1], Xin Wang [4], Elisabeth Hessmann [2], Matthias Dobbelstein [1,5]

1) *Institute of Molecular Oncology, Goettingen Center of Molecular Biosciences (GZMB), University Medical Center Goettingen, D-37077 Goettingen, Germany*
2) *Department of Gastroenterology, Gastrointestinal Oncology and Endocrinology, University Medical Center Goettingen, Goettingen, Germany.*
3) *Institute of Cell Biology (Cancer Research), University of Duisburg - Essen Medical School, Germany*
4) *Department of General, Visceral and Pediatric Surgery, University Medical Center Goettingen, Goettingen, Germany.*
5) *Lead Contact. Correspondence and requests for materials should be addressed to M. D. (e-mail: mdobbel@uni-goettingen.de)*

Running Title: Overcoming cisplatin resistance in PDAC

Keywords: PDAC, cisplatin, HSP90 inhibition, synergism, basal-like subtype

Contribution to manuscript:

Conducted experiments and data analyses for all figures except Manuscript Fig. 1 D-F (analysis, T.H.), Manuscript Fig. 2 H (A.M.), Manuscript Fig. 3 J (analysis, T.H.), Supplemental. Fig. 2 A (analysis, X.W.) and Supplemental Fig. 2 H-L (A.M.). Involved in the conception of the project, figure arrangement, writing and revising of the manuscript.

***Figures and corresponding figure legends are located at the end of the manuscript*

3.1 Abstract

To improve the treatment of pancreatic ductal adenocarcinoma (PDAC), a promising strategy consists in personalised chemotherapy based on gene expression profiles. Investigating a panel of PDAC-derived human cell lines, we found that their sensitivities towards cisplatin fall in two distinct classes. The platinum-sensitive class is characterised by the classical subtype and the expression of GATA6, miRNA-200a and miRNA-200b, which might be developable as predictive biomarkers. In the case of resistant, basal-like PDAC cells, we identified a synergism of cisplatin with HSP90 inhibitors based on the degradation of Fanconi anemia pathway factors upon HSP90 inhibition. Treatment with the drug combination results in increased DNA damage and chromosome fragmentation, as we have reported previously for ovarian cancer cells. On top of this, HSP90 inhibition also enhanced the accumulation of DNA-bound platinum. We next investigated an animal model consisting of tumours arising from orthotopic transplantation of KPC cells (LSL-KrasG12D/+; LSL-Trp53R172H/+; Pdx-1-Cre, C57/BL6 genetic background). Here again, when treating established tumours, the combination of cisplatin with the HSP90 inhibitor onalespib was highly effective and almost completely prevented further tumour growth. We propose that the combination of platinum drugs and HSP90 inhibitors might be worth testing in the clinics for the treatment of basal-like, cisplatin-resistant PDACs.

3.2 Highlights

- Basal-like PDAC cells are not responsive to cisplatin treatment
- miRNA-200 and GATA6 may serve as biomarkers, not only for classical subtype but also for cisplatin sensitivity
- A combination of HSP90 inhibitors and cisplatin can sensitise basal-like subtype
- Cisplatin cooperates with HSP90 inhibitor in the KPC mouse model of PDAC

3.3 Introduction

Pancreatic ductal adenocarcinoma (PDAC) represents one of the most devastating malignancies, with a 5-year survival rate below 5 %, raising the need for novel therapies (Bengtsson et al., 2020). Most tumours are inoperable at the time of detection. Concerning chemotherapy, gemcitabine has long been used, albeit with limited success, i.e. extending survival by a few months (Burris et al., 1997). More recently, platinum-based drugs such as cisplatin or oxaliplatin were employed with somewhat better success, at least when compared to gemcitabine (Conroy et al., 2011; Golan et al., 2019; Jameson et al., 2020). However, the extent of response strongly varies with either drug, or reliable predictive markers for therapeutic efficacy remain to be determined. Such biomarkers would be important to avoid futile attempts of chemotherapy and to maintain a reasonable balance of therapeutic benefit and drug-induced toxicities.

As an approach towards personalised treatment, PDACs were classified based on genomic alterations and gene expression patterns. In particular, the distinction between ‘classical’ and ‘basal-like’ subtypes emerged. The basal-like subtype partially – but not entirely – coincides with a squamous cell type and with epithelial-to-mesenchymal transition (Aiello et al., 2018; Bailey et al., 2016; Collisson et al., 2011; Moffitt et al., 2015; Puleo et al., 2018). A characteristic gene set was distilled from a number of gene expression analyses to distinguish the classical vs. the basal-like subtype most accurately (Rashid et al., 2020). In particular, the transcription factor GATA6 is mostly found in classical but not in basal-like PDAC (O’Kane et al., 2020). Basal-like PDACs tend to be more resistant to various chemotherapeutics, but there is still a need for strongly predictive biomarkers (Collisson et al., 2011; Moffitt et al., 2015; O’Kane et al., 2020).

Importantly, alternative therapeutic approaches are desperately needed in those cases where tumour cells turn out resistant against currently established chemotherapeutics. In this context, we have reported a way to fortify platinum-based therapy by combining it with inhibitors of the chaperone HSP90. This combination was strongly synergistic when treating a panel of ovarian cancer cells. Inhibiting HSP90 led to the degradation of the Fanconi anemia pathway factors, thus abolishing the major repair pathway for adducts between DNA and platinum. As a consequence, tumour cells treated by platinum drugs and HSP90 inhibitors turned these adducts into double-stranded DNA breaks, leading to extensive fragmentation of chromosomes, failed mitosis, and cell death (Kramer et al., 2017). This raises the question of whether the same

combination might also be active against PDACs, and in particular against those cells that are resistant to cisplatin alone.

Here we show that the expression of markers of the classical PDAC subtype GATA6 and the newly identified markers miRNA-200a and miRNA-200b strongly predict the sensitivity of PDAC cell lines towards cisplatin. On the other hand, basal-like PDAC cells, albeit resistant to cisplatin alone, respond synergistically to the combination of cisplatin and HSP90 inhibitors. Employing the KPC mouse model, this drug combination almost entirely restricted the growth of established, orthotopically transplanted PDAC tumours.

3.4 Methods and Material

Lead contact and materials availability

Further information and requests for reagents and protocols should be directed to and will be fulfilled by the Lead Contact Matthias Dobbelstein (mdobbel@uni-goettingen.de).

Cell culture and treatment

Human pancreatic MIA Paca-2 and Panc-1 cells, and murine KPC cells were maintained in Dulbecco's modified Eagle's medium (DMEM). The medium was supplemented with 10 % fetal bovine serum (FBS), antibiotics and 1 % non-essential amino acids for KPC cells. The cell lines PaTu8988T and Suit-028 were cultured in DMEM with 5 % FBS. ASPC-1, BxPC-3 and Capan-1 cells were maintained in RPMI medium containing 10 % or 20 % FBS, respectively, and antibiotics. All cells were kept at 37 °C in a humidified atmosphere with 5 % CO_2. For treatment of the cells, onalespib (100 mM in DMSO, Selleckchem) and cisplatin (1 mg/ml, Teva GmbH) were diluted in the corresponding medium and added to the cells for the indicated concentration and time.

Transfections

In MIA PaCa-2 and Panc-1 cells, transfection of miRNA precursors was performed using 10 nM Pre-miR™ miRNA Precursors (200a-3p and 200b-3p) (ThermoFisher Scientific) or a Pre-miR™ miRNA precursor negative control with Lipofectamine 3000 (Invitrogen) for reverse transfection. The Pre-miR™ miRNA inhibitor (200a-3p and 200b-3p) and the Pre miR™ miRNA inhibitor negative control was used in Capan-1, As-PC-1 and BxPC-3 cells. The medium was changed 24 hours after transfection followed by 24 hours further incubation and a second transfection for 24 hours. Afterwards, cells were treated for 72 hours.

Immunofluorescence

For immunofluorescence analysis, treated cells were fixed with 4 % formaldehyde for 30 min. After permeabilization with 0.5 % Triton X-100/PB, the cells were blocked in PB buffer containing 10 % normal goat serum (NGS, Sigma Aldrich) for 1 hour and incubated at 4 °C with an antibody against phospho-H2AX (05-636, Millipore) over night at 4 °C. Washing steps were followed by staining with the secondary antibody (AlexaFluor568, Invitrogen) and nuclei counterstained with DAPI (Sigma Aldrich). The coverslips were mounted with ImmuMount (ThermoFisher Scientific).

Immunoblot analysis

Cells were harvested in protein lysis buffer (20 mM TRIS-HCl pH 7.5, 150 mM NaCl, 10 mM EDTA, 0.1 % SDS, 1 % deoxycholic acid, 1 % Triton X 100, 2 M urea) containing protease inhibitor cocktail (Roche). After 30 min of lysis on ice, the samples were sonicated to disrupt DNA-protein complexes and centrifuged to obtain the protein lysates in the supernatant. Total protein concentration was determined by BCA Protein assay kit (ThermoFisher Scientific). After boiling the samples in Laemmli buffer at 95 °C for 5 min, equal amounts of protein samples were separated by SDS-PAGE and transferred onto nitrocellulose (0.4 µM, GE Healthcare) blocked in 5 % of non-fat milk in PBS containing 0.1 % Tween 20. The primary antibody was incubated overnight at 4 °C followed by 1 hour incubation with the peroxidase-conjugated secondary antibodies (donkey anti-rabbit or donkey anti-mouse, Jackson Immunoresearch or mouse anti-goat, Santa Cruz). The proteins were visualised with either Immobilion Western Substrate (Millipore) or Super Signal West Femto Maximum Sensitivity Substrate (ThermoFisher Scientific).

Antibodies	**Source (Catalog number)**
E-Cadherin	BD (610181)
FancA	Bethyl (A301-980A)
Phosho-H2AX (S139)	Cell Signaling (#2577)
GAPDH	Abcam (ab8245)
GATA6	R&D (AF1700)
HSP70	Cell signaling (#4872)
PARP1	Cell signaling (#9542)
Vimentin	Santa Cruz (#6260)
Zeb1	Santa Cruz (#25388)

Viability assays and determination of drug synergism

Cell viability assays were performed using the Cell TiterGlo Kit (Promega). Therefore, cells were seeded according to cell growth 24 hours before treatment. IC_{50} drug concentration of onalespib and cisplatin was determined after incubation of increasing concentrations for 72 hours. Cell viability was assessed by luminometry, setting vehicle control to 100 % cell viability, and the relative cell viability on drug treatment was calculated from three independent biological replicates for each drug concentration.

Synergism between HSP90 inhibitors and cisplatin was assessed by combined treatment of these drugs. Control treated cells were set to 100 %, whereas the fraction affected (Fa) of each treatment was calculated by the difference of remaining cell viability and control-treated cells. The combination index (CI) was calculated according to the Chou-Talalay algorithm, along with the Fa. A CI below 1.0 indicates synergism of the drug combination, CI equals 1 additive effect, and CI value greater than 1 corresponds to antagonistic or non-synergistic effects (Chou and Talalay 1984).

RNA isolation and RT-PCR

Total RNA was extracted from cells using TRIzol® (Invitrogen). The mRNA was reverse-transcribed with random hexameric primers and oligo-dT, followed by SYBR Green-based qRT-PCR (Invitrogen). For the reverse transcription of the miRNA, the miRNA was reverse transcribed using TaqMan™ microRNA Kit (ThermoFisher Scientific). For the real-time PCR analysis, the TaqMan™ MicroRNA-Assay with target-specific stem-loop primer was used. Gene expression levels were normalized to 36B4 or U6 snRNA (for miRNA) as a reference gene and calculated using the ΔΔCt method. qRT-PCR primer sets were chosen as follows:

	Forward	Reverse
hRPLP0 (36B4)	5'-GATTGGCTACCCAACTGTTG	5'-CAGGGGCAGCAGCCACAAA
hZeb1	5'-GCGCAGAAAGCAGGCGAACCC	5'-CCCTTCCTTTCCTGTGTCATCCTCC
hGATA6	5'-TCTACAGCAAGATGAATGGCC	5'-CTCACCCTCAGCATTTCTACG
hVimentin	5'-CGTGTATGCCACGCGCTCCT	5'-TCGAGCTCGGCCAGCAGGAT
hEcadherin	5'-CTTTGACGCCGAGAGCTACA	5'-AAATTCACTCTGCCCAGGACG

hsa-miR-200a-3p	Thermo Fisher	000502
hsa-miR-200a-3p	Thermo Fisher	002251
U6 snRNA	Thermo Fisher	001973

Chromosome spreads

Chromosomal structures were analysed after 24 hours of incubation with the indicated onalespib concentration in the presence of 20 µM zVad. To drive the cells in mitotic arrest with condensed chromosomes, the cells were treated with 2 µM Dimethylenastron for 4.5 hours before harvest. After 15 min incubation in hypotonic solution (40 % supplement-free medium,

60 % dest. H_2O), the cells were fixed with Carnoy's fixative (3 acetic acid: 1 methanol). The cells were then taken up in 100 % acetic acid and spread on slides. The staining was performed with 8 % Giemsa solution (Carl Roth). Analysis was performed with a × 100 objective in oil on a Zeiss AxioVert microscope (Carl Zeiss, Jena, Germany). For quantification, 40 random cells from three independent experiments were counted per treatment group.

Immuno-cytological assay for Pt-(GpG)adducts in DNA

Cells were treated with cisplatin for 4 hours, washed with PBS and placed onto microscopic adhesion slides (Super-frost Plus Gold Adhesion Slides; Thermo Fisher Scientific). The DNA platination product Pt-(GpG) was stained, visualised, and quantified as described (Melnikova and Thomale, 2018). Briefly, cells were fixed at -20 °C in methanol and denatured in an alkaline solution (60 % 70 mM NaOH/140 mM NaCl; 40 % methanol; 5 min at 0 °C). The digestion with pepsin and proteinase K (400 µg/mL) was performed at 37 °C for 10 min each. After blocking in 5 % non-fat milk in PBS, the cells were stained with Pt-(GpG)-specific rat antibody R-C18 (20 ng/mL in PBS/BSA overnight at 4 °C) (Liedert et al. 2006). Slides were stained with Cy3-labeled rabbit anti-(rat IgG) antibody (#312-165-003; Dianova) for 1 hour at 37 °C, and the nuclear DNA was counterstained with DAPI (1 µg/mL in PBS). The Cy3 and DAPI signals were measured for each nucleus and integrated separately using a microscope-coupled digital image analysis system (Zeiss Axioplan; ACAS 6.0 Image Analysis System). Cy3 fluorescence signal was normalized to corresponding DAPI signal and expressed as arbitrary fluorescence units (AFU). Values were calculated as means of > 100 measured cells per sample.

In vivo study using a syngenic orthotopic mouse model

C57BL/6-J mice (Janvier labs) were used for syngenic orthotopic transplantation studies. Mice were transplanted at the age of 8 weeks. 200.000 viable KPC-BL6 PDAC cells (20 µL) were mixed with an equal volume of matrigel (Matrigel GF R Red/F, Th. Geyer). This 40 µL mixture was injected into the tail of the pancreas of each mouse (Hingorani et al., 2005). After 10 days, high-resolution ultrasound was performed on each mouse to detect the tumour (Goetze et al., 2018). Briefly, mice were anaesthetized with isoflurane, and Visual Sonics Vevo 2100 high-resolution ultrasound system with a Vevo 2100 MicroScan Transducer MS-550-D was used to scan the mouse abdomen to detect tumour formation in the pancreas. Before treatment, mice were randomized into 4 groups with 8 mice per group: vehicle (10 % DMSO, 18 % Cremophor RH40 (Sigma-Aldrich), 3.6 % Dextrose, 68.4 % H_2O) 3 times a week, 25 mg/kg onalespib in vehicle solution 3 times a week, 4 mg/kg cisplatin in 0.9 % saline once a week and combination

of 25 mg/kg onalespib (three times) with 4 mg/kg cisplatin (once). The mice were treated for 10 days and weighed three times a week. To compare the tumour weight, only the pancreatic tumours were removed after scarification of the mice and weight.

Immunofluorescence staining

The paraffin blocks were cut in 4 µM thick slices and dewaxed and rehydrated. For immunofluorescence, the paraffin sections were boiled in 10 mM citric acid pH 6.0 for antigen retrieval. After washing steps with TB buffer, the slides were blocked with 10 % normal goat serum (NGS, Abcam) in 0.4 % PBT solution for 2 hours. The slides were incubated with both primary antibodies, phosho-H2AX (#2577, Cell Signaling) and with E-cadherin (610181, BD Science). Sections were washed, incubated with secondary fluorophore (Alexa-488, Alexa 568, ThermoFisher Scientific) for 2 hours, counterstained with DAPI and mounted with ImmuMount (ThermoFisher Scientific). For apoptosis determination, a TUNEL assay kit (Promega) was used. 10 pictures per mouse were taken on a Zeiss AxioVert microscope (Carl Zeiss) with a magnification of 40x. The intrinsic phospho-H2AX and TUNEL intensity was quantified using Image J software.

RNA-seq data analysis

RNA-seq data was obtained from GEO (https://www.ncbi.nlm.nih.gov/geo/) under accession GSE64558 (Diaferia et al., 2016). SRA files were converted to fastq files using a fastq-dump tool (version: 2.8.2), and the resultant reads were then mapped against hg38 using STAR (version: 2.6.0c, (Dobin et al., 2013)). Subsequently, PCR duplicates were removed using samtools (version: 1.9, (Li et al., 2009)). Reads counting was done using HTSeq (version: 0.11.2, (Anders et al., 2015)), and DESeq2 (version:1.24.0,(Love et al., 2014)) was utilized to normalize read counts and conduct the differential analysis.

Quantification and Statistical Analysis

Nuclear quantification of immunofluorescence

Images were taken with the Axio Scope A1 microscope (Zeiss) equipped with an Axio Cam MRc/503 camera with the same exposure time for all images for each fluorescent channel. For automated analysis and quantification of phospho-H2AX intensity, the Fiji software was used. As a nuclear counterstain, DAPI was used to mask the region of interest prior to the measurement of the mean intensity of the Alexa Fluor 568 staining (phospho-H2AX). At least 200 cells were subjected to analysis and quantification.

Statistical analysis

Statistical testing was performed using Graph Pad Prism v5.04 software (GraphPad Software Inc). Data were analyzed with one-way ANOVA or two-way ANOVA. Bonferroni post-tests were also applied for multiple comparisons. Significance was assumed where p-values ≤ 0.05. Asterisks represent significance in the following way: *$p \leq 0.05$, **$p \leq 0.01$, ***$p \leq 0.005$, ****$p \leq 0.0001$.

3.5 Results

Human PDAC-derived cell lines segregate in two distinct groups regarding their sensitivity towards cisplatin

We first analysed the response to human cell lines derived from PDAC toward treatment with cisplatin in parallel and standardized assays. After incubating the cells with cisplatin at a series of concentrations, we determined cell viability by measuring the ATP content of the cells through a luciferase assay. This revealed a characteristic dichotomy in that one class of cells responded to roughly 10-fold lower concentrations of cisplatin than the other class, with no intermediate responders (Figure 1A). We refer to the first class as cisplatin-sensitive and the other class as cisplatin-resistant from here on. Assessing another major chemotherapeutic used to treat PDAC, gemcitabine, also yielded a range of sensitivities, but not the same sharp distinction of two different groups with the classical cell line AsPC-1 as an intermediate responder. No classification applies for the chemotherapeutics doxorubicin and irinotecan (Supplemental Figure 1A-C). We further characterized the response of these cells by determining the DNA damage response upon cisplatin treatment through detecting phosphorylated Histone 2AX (phospho-H2AX), again identifying the same classes (Figure 1B, C). Thus, cisplatin-sensitive cells show a two- to four-fold increased DNA damage response to the same concentration of 20 µM cisplatin than the resistant class. Finally, we determined the formation of platinum adducts upon short-term treatment with cisplatin, using antibodies that specifically detect platinated DNA. And again, sensitive cells showed a two- to three-fold stronger signal than resistant ones (Figure 1D, E). An inhibitor of platinum export, diphenhydramine (DIPH), restored the accumulation of platinised DNA in resistant cells, perhaps suggesting that drug export represents a mechanism of resistance in these cells. In any case, these observations argue that the two classes of PDAC cells not only differ by platinum-induced cell killing but also by the formation of platinated DNA in the first place.

GATA6 and microRNAs of the miRNA-200 family serve as biomarkers to predict not only the classical subtype but also cisplatin sensitivity

Next, we sought to determine if the expression of specific genes correlates with the sensitivity of human PDAC cells towards cisplatin. Based on previous characterizations of these cell lines (Adams et al., 2019; Kloesch et al., 2021), we suspected that the basal-like vs. classical subtypes correlated with the resistant vs. sensitive group of cells respectively. In particular, the two subtypes were previously distinguished by the expression levels of the master regulator of

transcription, GATA6 (O'Kane et al., 2020). RNA-seq analysis revealed a differential expression for members of the miRNA-200 family in classical and basal-like PDAC cells (Supplemental Fig. 2A). And indeed, the expression of GATA6, miRNA-200a and 200b were found almost exclusively in the cisplatin-sensitive set of cells (Figure 2A-D), arguing that the expression levels of these genes are not only characteristic for the classical subtype but can also serve to identify cisplatin-sensitive cells. Thus, the detection of these genes might be further developable into biomarkers for PDAC cells that respond to cisplatin, thus contributing to a personalised use of platinum-based therapy of this tumour.

In contrast to previous studies of Arumugam et al., we did *not* observe a significant correlation of markers of epithelial-mesenchymal transition (EMT) with cisplatin sensitivity (Figure 2E) (Arumugam et al., 2009). For instance, the sensitive cells AsPC-1 and Suit-028 still expressed readily detectable amounts of vimentin, a typical marker of a mesenchymal phenotype. Moreover, the re-expression of miRNA-200 in the cisplatin-resistant Panc-1 cells led to the re-expression of E-cadherin, an epithelial marker; nonetheless, this did not alter the response of the cells towards cisplatin (Figure 2F, G). In conclusion, miRNA-200a and 200b as well as GATA6 expression are characteristic for cisplatin-sensitive cells as well as for the classical subtype of PDAC, perhaps making them suitable as biomarkers. In contrast, this degree of correlation was not found for epithelial vs. mesenchymal markers.

HSP90 inhibitors synergize with cisplatin, reduce Fanconi anemia pathway mediators, enhance platinum-DNA adduct formation and sensitise basal-like PDAC cells

Next, we sought to evaluate an approach to sensitize the resistant, basal-like PDAC cells towards cisplatin therapy. We applied a strategy that we had previously found effective in ovarian cancer cells, i.e. combining a platinum drug with inhibitors of the HSP90 chaperone (Kramer et al., 2017). Indeed, this combination also decreased the viability of basal-like PDAC cells in a synergistic fashion, as determined by the remaining ATP content of the cells after treatment (Figure 3A). The combination index, calculated according to the algorithm by Chou and Talalay (Chou and Talalay, 1984), was less than 1, corroborating the synergistic activity of the drugs (Figure 3B). Furthermore, we found that HSP90 inhibitors reduced the levels of Fanconi anemia factors such as FANCA, defining a plausible mechanism of how HSP90 inhibition compromises the repair of platinum-DNA adducts and thus sensitizes the cells towards cisplatin. Interestingly, the sensitive cell lines did not display a strong reduction of FANCA protein after HSP90 inhibition (Figure 3C). Accordingly, damage signaling, as

revealed by phospho-H2AX, was enhanced when both drugs were combined (Figure 3D-F). Further, the combination of both drugs led to chromosome fragmentation, compatible with the triggering of double-strand DNA breaks by unrepaired platinum adducts (Figure 3G-I). All these features had been found and characterized in a completely analogous fashion when investigating ovarian cancer cells (Kramer et al., 2017). Finally, the combination of cisplatin and HSP90 inhibitor onalespib enhanced platinum-DNA adduct formation after short-term treatment (Figure 3J). Curiously, the sensitive class of PDAC cells was hardly further sensitized by HSP90 inhibition (Supplemental Figure 3A, B, G-I, K, L). This raises the perspective that PDACs might be amenable to differential therapy depending on their subtype. Classical PDACs appear sensitive to cisplatin as such, whereas basal-like PDACs seem resistant against cisplatin but synergistically respond to a combination of cisplatin with HSP90 inhibitors.

Cisplatin and HSP90 inhibition synergistically induce DNA damage, chromosome fragmentation, and death in cells derived from the murine PDAC model KPC

To further elaborate the combination of cisplatin and HSP90 inhibitors *in vivo*, we first established the synergism of both drugs in cells from a murine PDAC model, i.e. KPC cells that contain $Kras^{G12D}$ and $Trp53^{R172H}$ mutations. (Hingorani et al., 2005). These cells represent a very widespread PDAC model and readily form tumours upon transplantation. Their assignment to basal vs. classical subtypes remains subject to further investigations since they can be manipulated to become more squamous (Somerville et al., 2018)but also to get closer to a classical phenotype (Candido et al., 2018). In any case, we found that these cells respond to cisplatin and HSP90 inhibitors in a highly synergistic fashion (Figure 4A, B). This was accompanied by a strong accumulation of phospho-H2AX when the drugs were combined (Figure 4C-E). Strikingly, the drug combination led to the accumulation of hundreds of DNA breaks (Figure 4F, G), as revealed by the dramatic fragmentation of chromosomes. We conclude that the combination of cisplatin and HSP90 inhibitors act in a highly synergistic fashion on KPC cells.

An HSP90 inhibitor and cisplatin cooperate to counteract the growth of KPC tumours in an orthotopic and syngeneic PDAC transplant model

Finally, we tested whether cisplatin, along with the HSP90 inhibitor onalespib, could reduce the growth of pancreatic carcinoma *in vivo*. To test this, we first transplanted KPC cells orthotopically into the pancreas of syngeneic mice. When palpable tumours occurred, we

treated the animals with the two drugs, either alone or in combination (Figure 5A). While both drugs had a moderate effect when used individually, their combination prevented the outgrowth of palpable tumours and almost completely restricted the tumour mass by nearly 50 % in a postmortem analysis (Figure 5B, C). When tumours were removed briefly after the last drug treatment, the combination of cisplatin and onalespib also led to the strong accumulation of phospho-H2AX and induction of apoptosis *in vivo* (Figure 5D-G). Hence, cisplatin and HSP90 inhibitors cooperatively and strongly restricts the growth of pancreatic carcinoma in an animal model, further moving this approach towards its clinical perspective.

3.6 Discussion

The sharp, dichotomous distinction of sensitivities between two separated groups of PDAC cell lines, with ca. 10-fold differences in effective drug concentrations, suggests that the efficacy of cisplatin might be predictable even in patients. Along this line, the clinical response of PDACs to chemotherapy in patients also correlates with molecular subtypes (Collisson et al., 2011; Moffitt et al., 2015; O'Kane et al., 2020). Using GATA6, miRNA-200 family members and additional gene products as biomarkers, it may become possible to tailor platinum-based therapies for use only in patients with sensitive tumour cells. This would save resistant patients from demanding toxicities in cases where tumours are unlikely to respond anyway.

What mechanism(s) might render classical PDAC cells so much more sensitive towards cisplatin? Even though expression levels of GATA6 and miRNA-200 appear to correlate exquisitely with drug sensitivity, this does not imply that the differential expression of these genes is also *causing* different drug response. On the contrary, we observed that manipulating the levels of miRNA-200a and 200b did not alter the drugs response, unlike in other tumour species (Brozovic et al., 2015; Chen et al., 2016) although it did shift the cells regarding EMT markers (Figure 2E). This also implies that EMT is not the same as a shift from classical to basal subtype, despite some overlapping aspects (Aiello et al., 2018). The precise nature and molecular mechanisms conferring a basal vs. classical cell phenotype thus remain to be defined.

Interestingly, not only the cellular response but also the extent of adduct formation between cisplatin and the DNA was found reduced in resistant cells. Considering the short exposure to cisplatin in these experiments, we hypothesise that the cisplatin repair mechanism contributes little if anything to adduct reduction. Instead, we propose that either the uptake of cisplatin, the excretion of the drug, or the metabolism to form adducts, might be different between sensitive and resistant cells.

Targeting the cisplatin export transporter by the antihistaminic agent DIPH, which has been shown to inhibit the cisplatin efflux (Melnikova et al., 2020), revealed an enhanced cisplatin-DNA adduct formation in basal-like PDAC cells. Therefore, we propose that cisplatin efflux might contribute to differential cisplatin response in the two classes of PDAC cells.

The clear distinction between resistant and sensitive cancer cells leaves the necessity to find novel treatments for patients suffering from cisplatin-resistant PDACs. Here, the combination of cisplatin with HSP90 inhibitor onalespib shows remarkable promise. This is further supported by the fact that the repair of cisplatin-DNA adducts requires a specific cellular pathway that is not needed to repair most other DNA lesions. Specifically, the Fanconi anemia

pathway first removes those stretches of DNA that are covalently linked to platinum. Next, the gap is filled, e.g. by the machinery of homologous recombination repair (Niraj et al., 2019). Our previous studies and the results reported here indicate that the stability of Fanconi anemia pathway factors strongly depends on the HSP90 chaperone (Kramer et al., 2017). Thus, HSP90 inhibitors essentially abolish the ability of cells to remove platinum-DNA adducts. Hence, it is particularly the platinum drugs (rather than other chemotherapeutics) that cooperate with HSP90 inhibitors. The recent introduction of such drugs into PDAC therapy raises the perspective of further fortifying their impact by HSP90 inhibitors. On top of this, HSP90 inhibition may compromise the functionality of cisplatin exporters, further contributing to increased platinum-DNA adduct formation.

Curiously, cells derived from the classical subtype of PDAC did not allow strong synergisms of cisplatin and onalespib while displaying sensitivity towards cisplatin alone. We can only speculate about the reasons. One possibility would be that the DNA repair mechanisms for platinum adducts might be less active to begin with in the classical subtype. This would explain both the high initial cisplatin sensitivity and the lack of further improvement by HSP90 inhibition and subsequent impairment of the Fanconi anemia pathway.

Many proteins depend on HSP90 as a chaperone, and HSP90 inhibition often leads to the proteasomal degradation of such 'HSP90 clients' (Schopf et al., 2017). Thus, the general impact of HSP90 on cells is likely pleiotropic. Of note, however, tumour cells tend to depend more strongly on HSP90 than their normal counterparts, possibly as a result of aneuploidy and resulting non-stoichiometric synthesis of protein complex components (Dobbelstein and Moll, 2014). In tumour cells, we anticipate that, on top of interfering with the Fanconi anemia pathway, HSP90 inhibition compromises PDAC cell proliferation and survival by additional mechanisms. For instance, HSP90 inhibition negatively regulates the levels of mutant p53 (Alexandrova et al., 2015; Li et al., 2011; Schulz-Heddergott et al., 2018) as well as Macrophage migration inhibitory factor MIF (Klemke et al., 2021; Schulz et al., 2012). Such mechanisms might further enhance the efficacy of HSP90 inhibitors, on top of their cooperation with cisplatin.

In the case of ovarian cancer, we have previously reported the strongly synergistic activity of platinum drugs in combination with HSP90 inhibitors. Furthermore, these results have led to the establishment of a phase II clinical study involving 120 patients (NCT03783949). Pending the results of this study, we hope to expand the approach to other tumours, including PDAC. Another tumour commonly treated with cisplatin but with frequent resistance formation is small

cell lung cancer, the response of which to the drug combination remains to be studied. In each case, however, we anticipate that identifying tumour subtypes with the enhanced response towards the combination will further increase the clinical benefit.

3.7 Acknowledgement

We thank the Deutsche Forschungsgemeinschaft (KFO 5002), the Wilhelm Sander Stiftung and the Deutsche Krebshilfe for financial support. KE was a member of the Göttingen Graduate Center for Neurosciences, Biophysics, and Molecular Biosciences (GGNB) during this work.

3.8 Author contributions

K.M.E. and M.D. designed research, K.M.E. performed most experiments, K.M.E, S.P., W.K. and E.H. conducted the *in vivo* experiments, K.M.E, A.M. and T.Q performed *in vitro* experiments. X.W. performed RNAseq analysis, J.T analysed immuno-cytological assay. K.M.E analyzed data, K.M.E and M.D. wrote the paper. All the authors read and approved the manuscript.

3.9 Declaration of interest

The authors declare no conflict of interest.

FIGURE 1

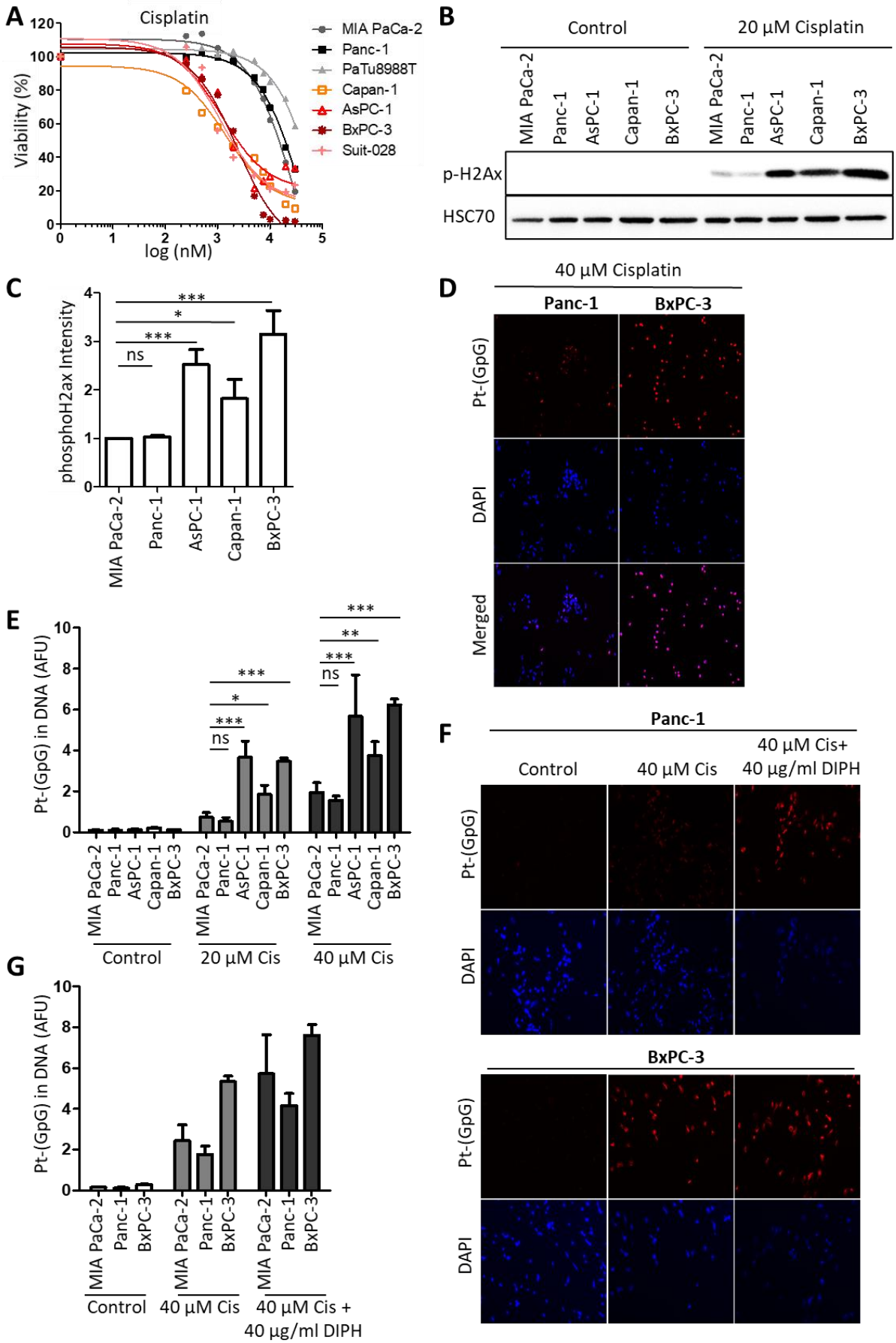
A
Cisplatin
Viability (%)
log (nM)
MIA PaCa-2
Panc-1
PaTu8988T
Capan-1
AsPC-1
BxPC-3
Suit-028
B
Control
20 µM Cisplatin
MIA PaCa-2
Panc-1
AsPC-1
Capan-1
BxPC-3
p-H2Ax
HSC70
C
phosphoH2ax Intensity
ns
***
*
D
40 µM Cisplatin
Panc-1
BxPC-3
Pt-(GpG)
DAPI
Merged
E
Pt-(GpG) in DNA (AFU)
Control
20 µM Cis
40 µM Cis
F
Panc-1
Control
40 µM Cis
40 µM Cis+
40 µg/ml DIPH
Pt-(GpG)
DAPI
BxPC-3
G
Pt-(GpG) in DNA (AFU)
Control
40 µM Cis
40 µM Cis +
40 µg/ml DIPH

FIGURE LEGENDS

Manuscript Fig. 1: Distinction of human PDAC cells based on cisplatin response.

A Treatment of PDAC cell panel with 0.25 µM to 30 µM cisplatin for 72 h. The viability of cells was measured with an ATP-based luminescence assay.

B Immunoblot analysis of DNA damage marker phospho-H2AX in insensitive cell lines MIA PaCa-2 and Panc-1 and in sensitive cell lines AsPC-1, Capan-1 and BxPC-3 after treatment with 20 µM Cisplatin for 24 h. HSP70 served as a loading control.

C Quantification of phospho-H2AX immunoblot signal normalised to HSP70. ± SD of 3 biological replicates. *p* values were calculated with 1way ANOVA. ns = not significant, *p ≤ 0.05, **p ≤ 0.01, ***p ≤ 0.001.

D Representative images of Pt-(GpG) adduct formation in the DNA of pancreatic cancer cell lines BxPC-3 (right) and the cisplatin-resistant Panc-1 (left) after exposure to cisplatin (40 µM for 4 h).

E Platinum-adduct level quantification of pancreatic cancer cell lines measured after ± SD of 3 biological replicates. *p* values were calculated with 2way ANOVA. ns = not significant, *p ≤ 0.05, **p ≤ 0.01, ***p ≤ 0.001.

F Representative images of Pt-(GpG) adduct formation in the DNA of pancreatic cancer cell lines after 1 h exposure to 40 µg/mL DIPH prior to 5 h treatment of 40 µM cisplatin.

G Platinum-adduct level quantification of PDAC cell lines measured after 1 h preincubation with 40 µg/mL DIPH followed by ± SD of 3 biological replicates.

FIGURE 2

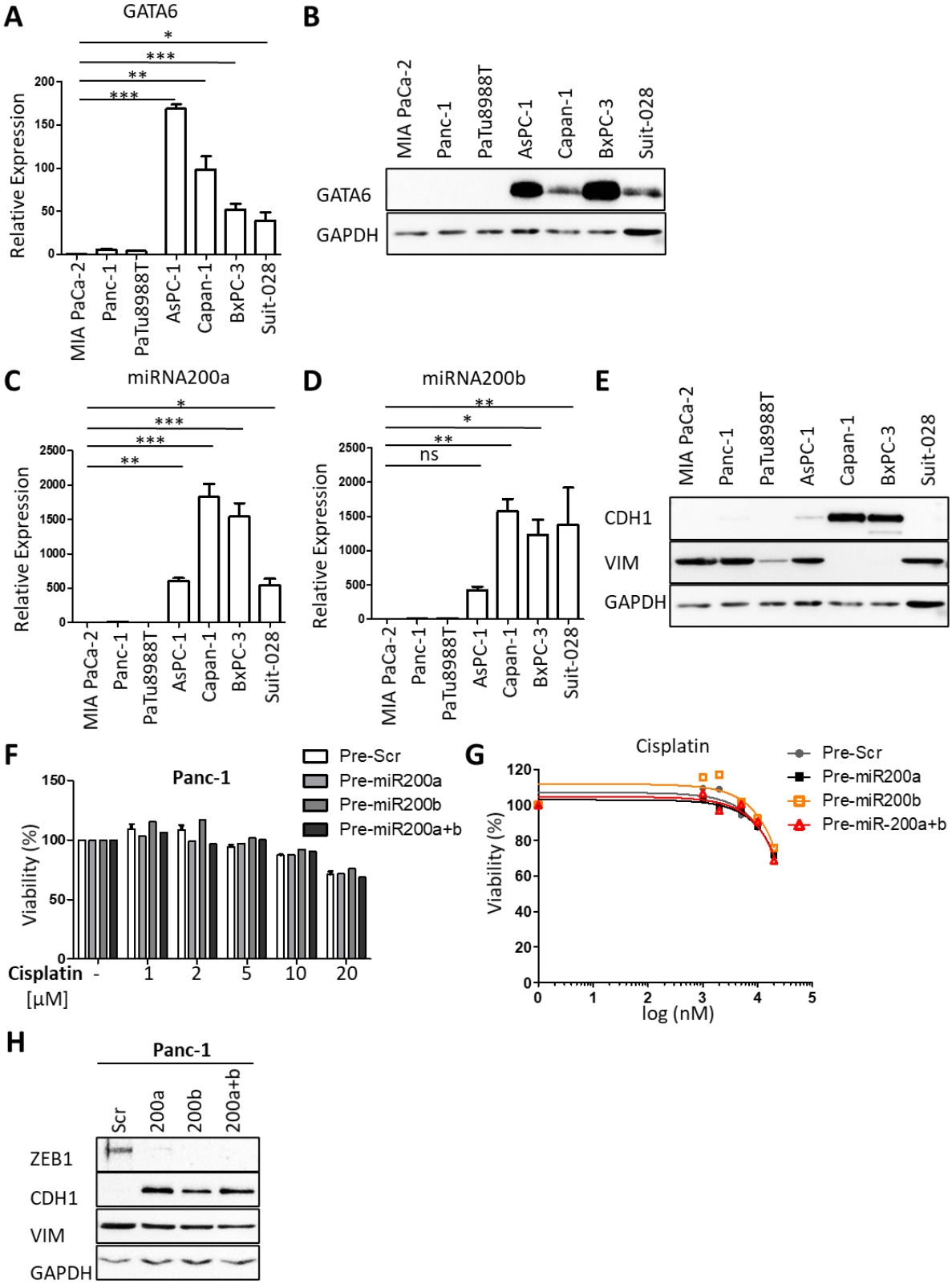
A
GATA6
Relative Expression
MIA PaCa-2
Panc-1
PaTu8988T
AsPC-1
Capan-1
BxPC-3
Suit-028
B
GATA6
GAPDH
C
miRNA200a
D
miRNA200b
ns
E
CDH1
VIM
GAPDH
F
Panc-1
Pre-Scr
Pre-miR200a
Pre-miR200b
Pre-miR200a+b
Viability (%)
Cisplatin
[µM]
G
Cisplatin
Pre-miR-200a+b
log (nM)
H
Panc-1
Scr
200a
200b
200a+b
ZEB1
CDH1
VIM
GAPDH

Manuscript Fig. 2: GATA6, miRNA-200a, and b serve as marker for cisplatin sensitivity.

A Expression analysis of GATA6 in PDAC cell lines. qRT-PCR was normalised to *RPLP0* mRNA. Means ± SD of three biological replicates.

B Immunoblot analysis of GATA6 om PDAC cell lines. GAPDH served as a loading control.

C, D miRNA-200a and b expression analysis on cell panel. snRNA U6 was used for normalization. Means ± SD of three biological replicates.

E Immunoblot of PDAC panel for epithelial to mesenchymal transition marker (EMT) ZEB1, E cadherin (CDH1) and vimentin (VIM). GAPDH was used as a loading control.

F, G Panc-1 cells were transfected with Pre-miRNA-200a and 200b for 48 h and re-transfected for 24 h. After treatment with different concentrations (1 µM to 20 µM) of cisplatin for 72 h, cell viability was measured. Mean ± SD of three biological replicates.

H Immunoblot analysis of Panc-1 cells after transfection as described in **F**. Staining of Zeb-1, E-cadherin (CDH1), Vimentin (VIM) and GATA6, GAPDH as a loading control.

A, C, D *p* values were calculated with 1way ANOVA comparing the indicated groups. ns = not significant, *p ≤ 0.05, **p ≤ 0.01, ***p ≤ 0.001.

FIGURE 3

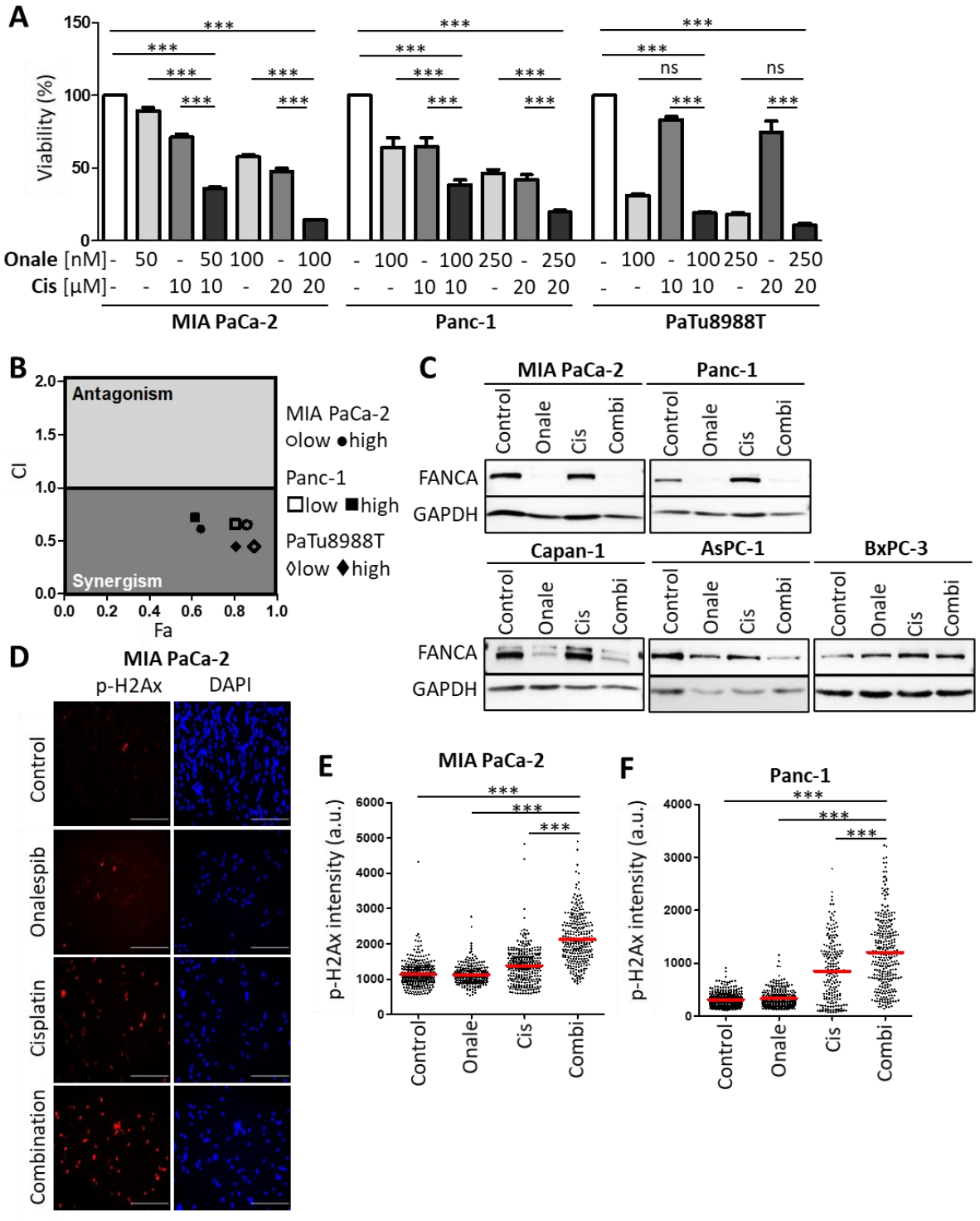
A
Viability (%)
Onale [nM]
Cis [µM]
MIA PaCa-2
Panc-1
PaTu8988T
B
Antagonism
Synergism
CI
Fa
MIA PaCa-2 ○low ●high
Panc-1 □low ■high
PaTu8988T ◊low ♦high
C
MIA PaCa-2
Panc-1
Capan-1
AsPC-1
BxPC-3
Control
Onale
Cis
Combi
FANCA
GAPDH
D
MIA PaCa-2
p-H2Ax
DAPI
Control
Onalespib
Cisplatin
Combination
E
MIA PaCa-2
p-H2Ax intensity (a.u.)
F
Panc-1
p-H2Ax intensity (a.u.)

FIGURE 3 (continued)

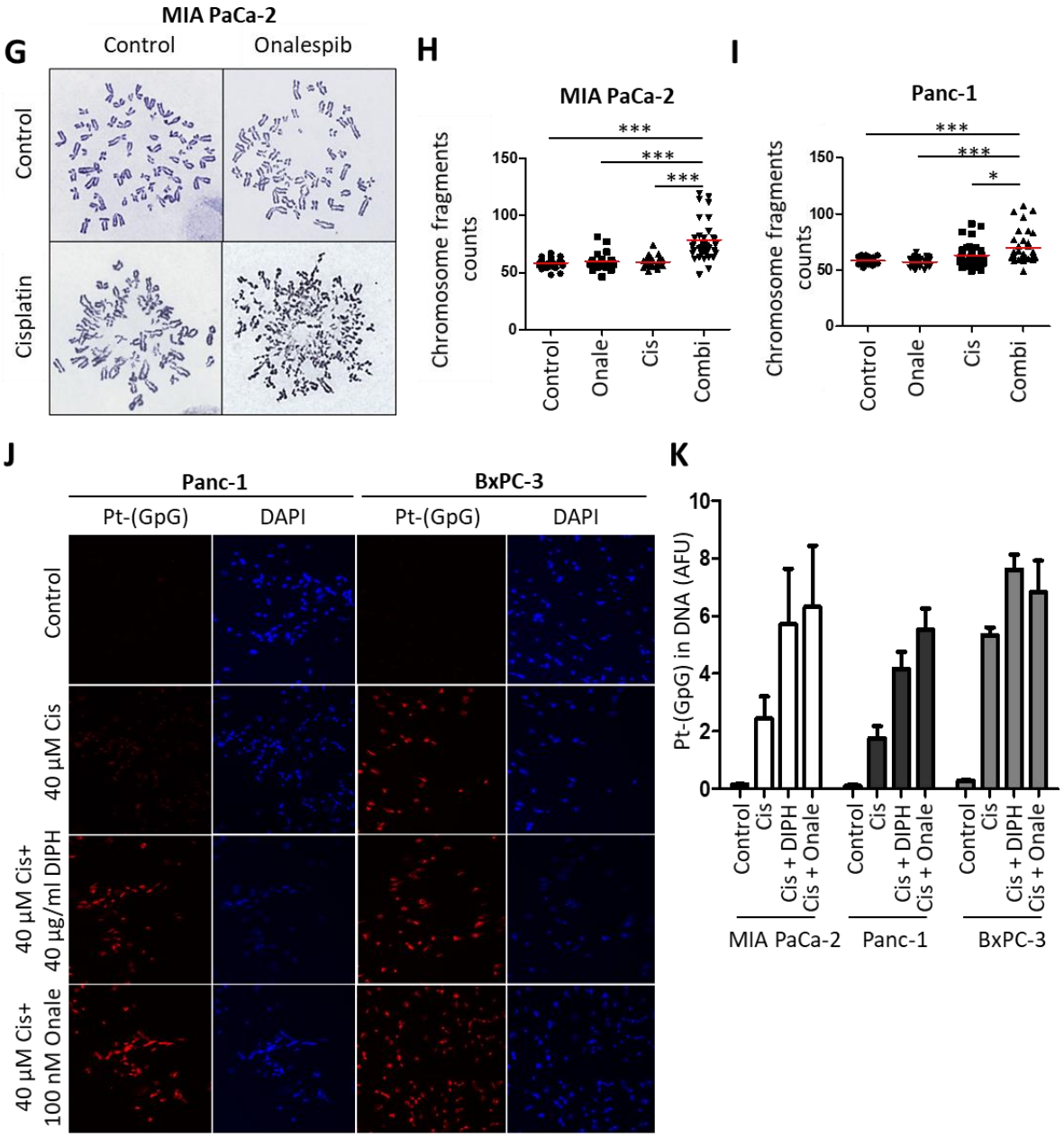

Manuscript Fig. 3: Resistant human PDAC cells can be sensitised by HSP90 inhibiton.

A Human MIA PaCa-2, Panc-1 and PaTu8988T cells were treated with onalespib or cisplatin and a combination for 72 h with concentrations as indicated. Viability was determined by quantifying the ATP concentration.

B Combination index (CI) was calculated for the combinations from **A** and plotted against the fraction affected (Fa).

C Immunoblot analysis of FANCA. Cells were treated with onalespib and cisplatin for 24 h: MIA PaCa-2 (150 nM; 20 µM), Panc-1 (150 nM; 20 µM), Capan-1 (400 nM; 2 µM), AsPC-1 (400 nM; 2 µM) and BxPC-3 (400 nM; 5 µM). GAPDH was used as a loading control.

D Representative staining of the DNA damage marker phospho-H2AX in MIA PaCa-2 cells treated with onalespib (100 nM), cisplatin (20 µM) or in combination for 24 h. Scale bar: 200 µm.

E, F Fluorescence intensity per nucleus is shown in a scatter plot for **E** MIA PaCa-2 and **F** Panc-1. The red lines indicate the mean intensity. Phospho-H2Ax intensity per nucleus (arbitrary units) was calculated by quantification one of two independent experiments.

G Representative images of metaphase spreads. MIA PaCa-2 cells were treated with onalespib (100 nM) and cisplatin (20 µM) for 24 h together with 20 µM zVad to block apoptosis. Chromosomes were stained with Gimsea.

H, I Number of **H** MIA PaCa-2 and **I** Panc-1 chromosome fragments per cell shown as box plot analysed in 40 randomly chosen cells from three independent experiments Panc-1 cells were treated equally to MIA Paca-2 from **G**. Red line indicates the mean.

J Representative images of Pt-(GpG) adduct formation in the DNA of pancreatic cancer cell lines Panc-1 (left) and the cisplatin-resistant BxPC-3 (right) after 24 h treatment with 100 nM onalespib or 40 µg/mL DIPH

K Platinum-adduct level quantification of pancreatic cancer cell lines from **J**. ± SD of 3 biological replicates.

A, E, F, H, I *p* values were calculated with 1way ANOVA comparing the indicated groups. ns = not significant, *$p \leq 0.05$, **$p \leq 0.01$, ***$p \leq 0.001$.

FIGURE 4

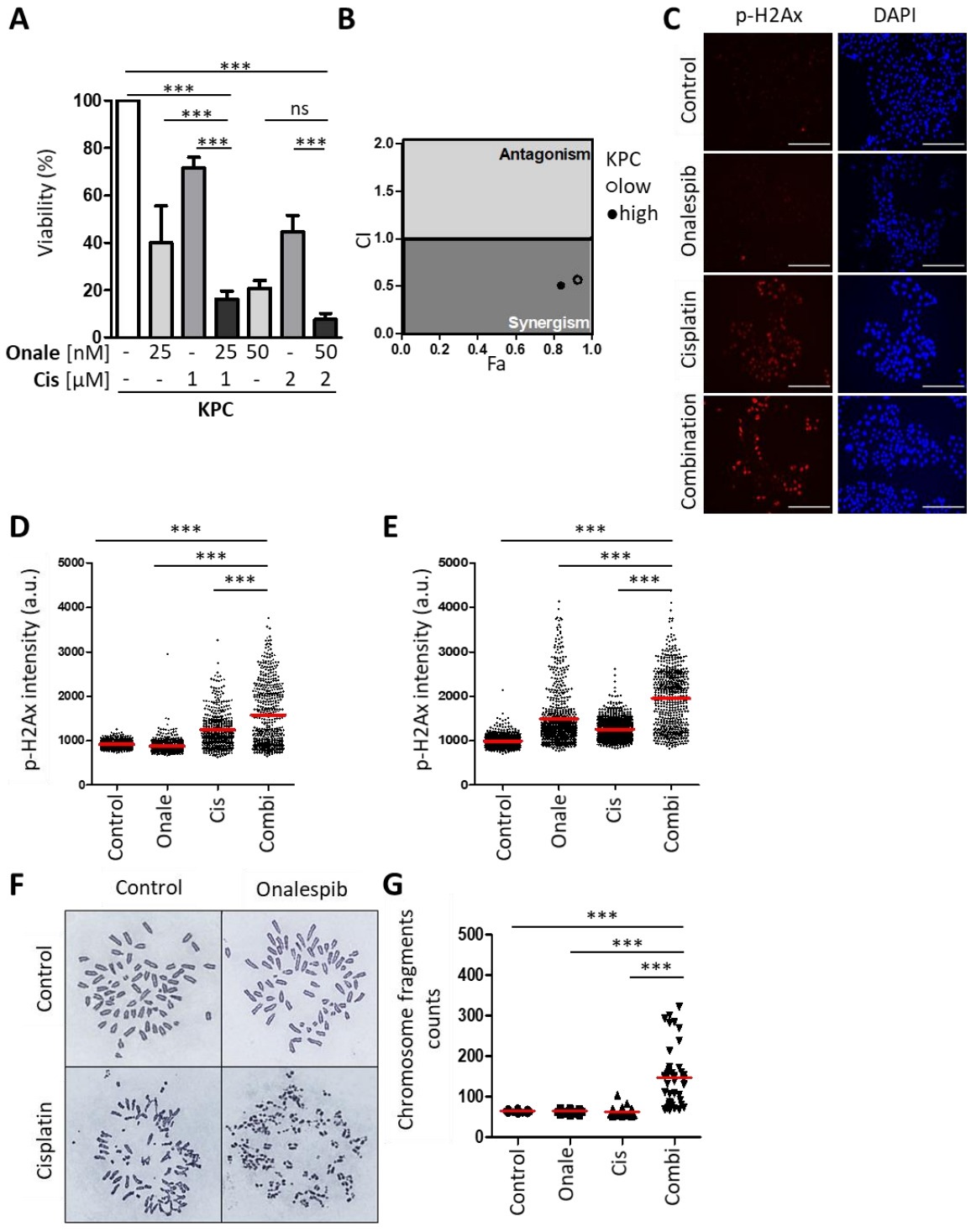
A
B
C
p-H2Ax
DAPI
Control
Onalespib
Cisplatin
Combination
Viability (%)
Onale [nM] - 25 - 25 50 - 50
Cis [µM] - - 1 1 - 2 2
KPC
ns
Antagonism
Synergism
CI
Fa
KPC
low
high
D
E
p-H2Ax intensity (a.u.)
Control
Onale
Cis
Combi
F
Control
Onalespib
Cisplatin
G
Chromosome fragments counts

Manuscript Fig. 4: Synergistic effect of HSP90 inhibitors and cisplatin in KPC cells.

A KPC cells (LSL-KrasG12D/+; LSL-Trp53R172H/+; Pdx-1-Cre, C57/BL6 genetic background) were treated with two different concentrations of onalespib and cisplatin for 48 h, followed by the assessment of cell viability by quantification of ATP. Means ± SD.

B Combination index (CI) calculated from **A** plotted against the fraction affected (Fa) for the combination of HSP90 inhibitors onalespib and cisplatin.

C Representative immunofluorescence staining for phosho-H2Ax with DAPI as counterstain. Cells were treated with onalespib and cisplatin for 24 h. Scale bar: 200 µm.

D, E Scatter plot of phospho-H2AX intensity per nucleus (arbitrary units), calculated by quantification of **C** from one of two independent experiments. The Red line indicates the mean nuclear phospho-H2AX staining.

F KPC cells were treated with onalespib (100 nM) and/or cisplatin (2 µM) for 24 h in the presence of 20 µM zVad. The chromosomes were stained with Giemsa staining. Representative images of metaphase spreads are shown.

G The chromosome fragmentation was analyzed by counting the number of fragments shown in **F** in 40 randomly chosen cells from three independent experiments depicted as box blot. The mean is indicated with the red line.

A, D, F *p* values were calculated with 1way ANOVA comparing the indicated groups. ns = not significant, *p ≤ 0.05, **p ≤ 0.01, ***p ≤ 0.001.

FIGURE 5

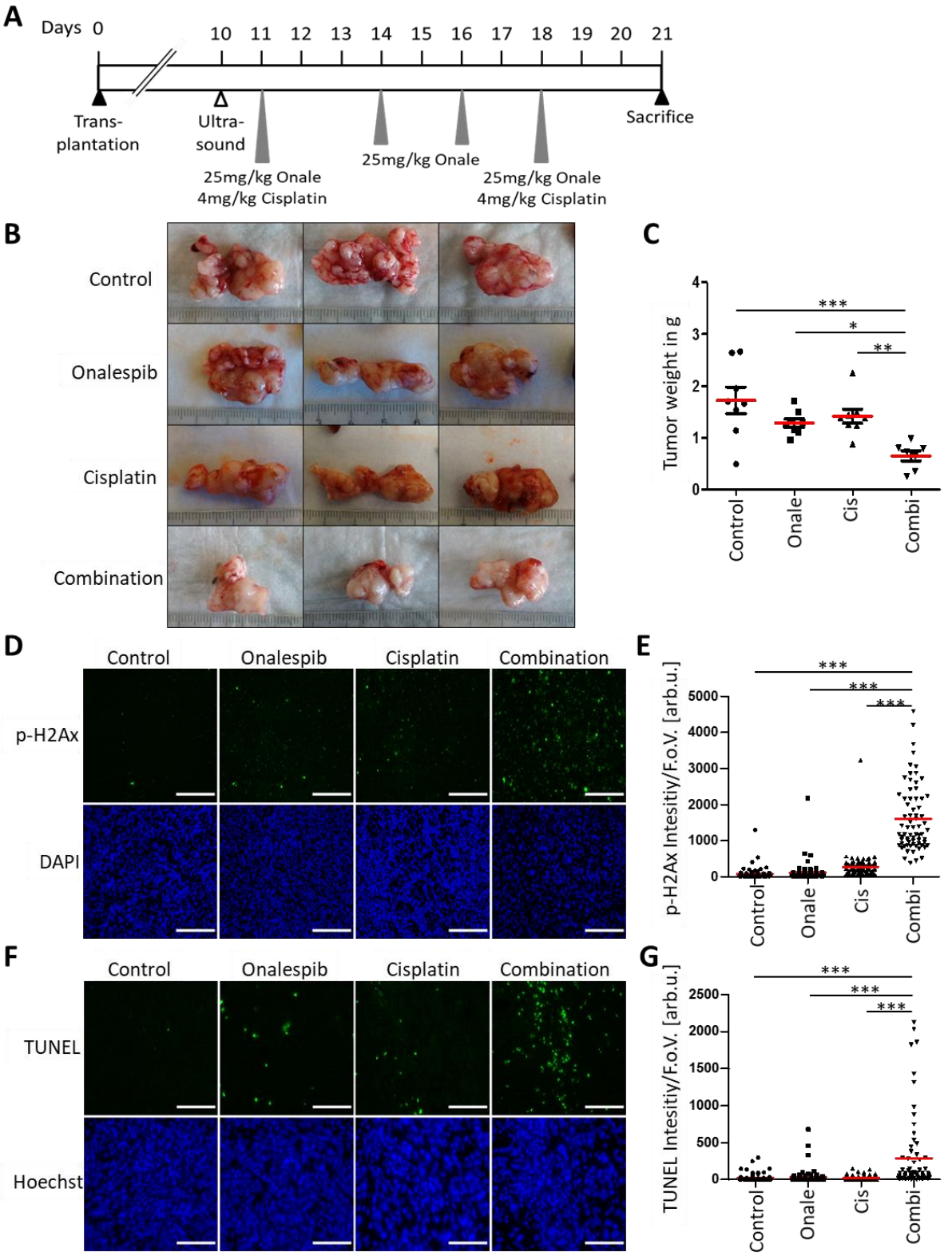
A
Days 0
10 11 12 13 14 15 16 17 18 19 20 21
Trans-plantation
Ultra-sound
25mg/kg Onale
4mg/kg Cisplatin
25mg/kg Onale
25mg/kg Onale
4mg/kg Cisplatin
Sacrifice
B
Control
Onalespib
Cisplatin
Combination
C
Tumor weight in g
***
*
**
Control
Onale
Cis
Combi
D
Control
Onalespib
Cisplatin
Combination
p-H2Ax
DAPI
E
p-H2Ax Intesitiy/F.o.V. [arb.u.]
***
***
***
Control
Onale
Cis
Combi
F
Control
Onalespib
Cisplatin
Combination
TUNEL
Hoechst
G
TUNEL Intesitiy/F.o.V. [arb.u.]
***
***
***
Control
Onale
Cis
Combi

Manuscript Fig. 5: Antitumor efficiency of onalespib and cisplatin *in vivo*.

A Treatment scheme for C57BL/6-J mice, which were orthotopically transplanted with 200.000 KPC cells. Ten days after transplantation, tumour formation was confirmed by ultrasound. The treatment with 25 mg/kg onalespib and 4 mg/kg cisplatin was started on day 11 and repeated on day 18. On day 14 and 16, the mice received the single treatment with 25 mg/kg onalespib. 21 days after transplantation, the mice were sacrificed for the removal of the tumours.

B Images of three representative pancreatic tumours were collected from mice treated according to **A** at the endpoint of the experiment (day 21).

C Tumor weight was determined after sacrifice on day 21. Red lines indicated the mean weight. Control, onalespib and cisplatin-treated group (n=8), combination (n=7).

D, F Tumor sections from **B** were stained for **D** phospho-H2AX and **F** apoptosis using a TUNEL assay. Representative images are shown. Scale bar: 200 µm.

E, G Calculated intensity of **E** intrinsic phospho-H2AX and **G** apoptosis per field of view depicted as scatter blot. Ten images were randomly taken per mouse. The red line indicates the mean intensity.

C, E, G *p* values were calculated with 1way ANOVA comparing the indicated groups. *$p \leq 0.05$, **$p \leq 0.01$, ***$p \leq 0.001$.

SUPPLEMENTAL FIGURE 1

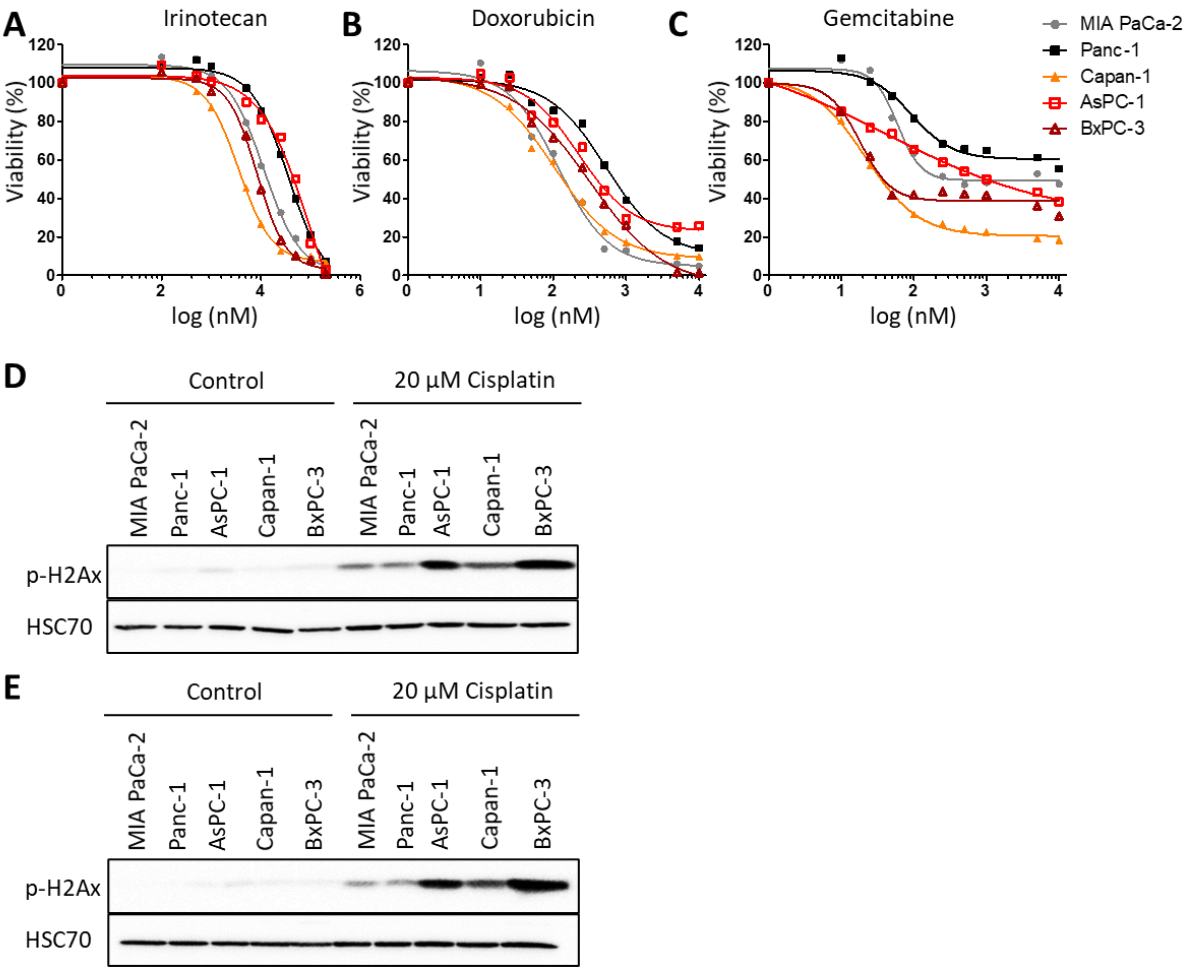

SUPPLEMENTAL FIGURE LEGENDS

Supplemental Fig. 1: Chemosensitivity of PDAC cells

Related to Manuscript Fig.1.

A-C Treatment of PDAC cell panel with **A** 0.25 µM to 30 µM irinotecan, **B** 0.1 µM to 200 µM doxorubicin and **C** 10 nM to 10 µM gemcitabine for 72 h. The viability of cells was measured with an ATP-based luminescence assay.

D, E Immunoblot for the DNA damage marker phospho-H2AX after treatment with 20 µM Cisplatin for 24 h. HSP70 as a loading control. Replicate experiments for **Fig. 1 B**. Blots were used for quantification; see **Fig. 1 C**.

SUPPLEMENTAL FIGURE 2

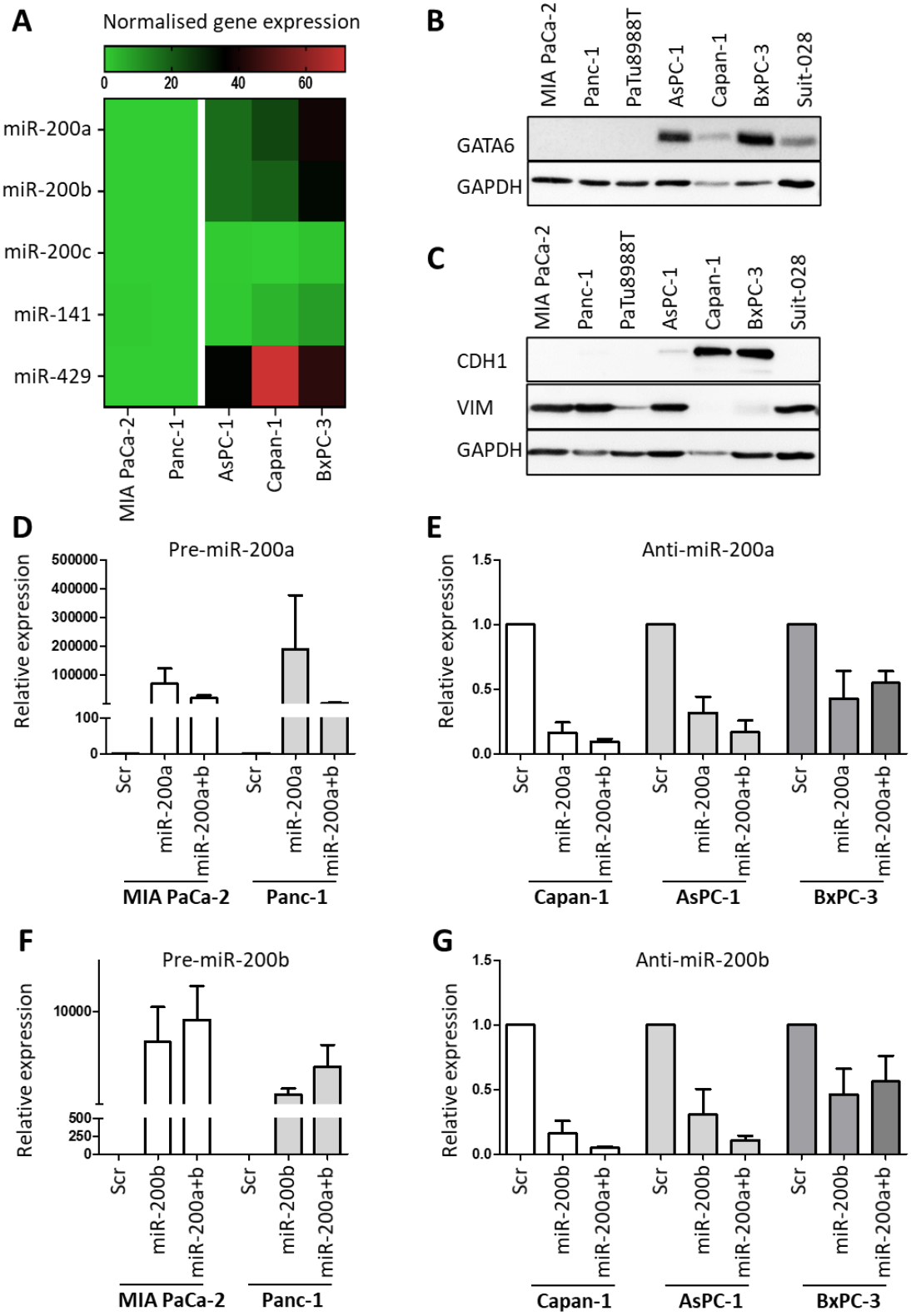

SUPPLEMENTAL FIGURE 2 (continued)

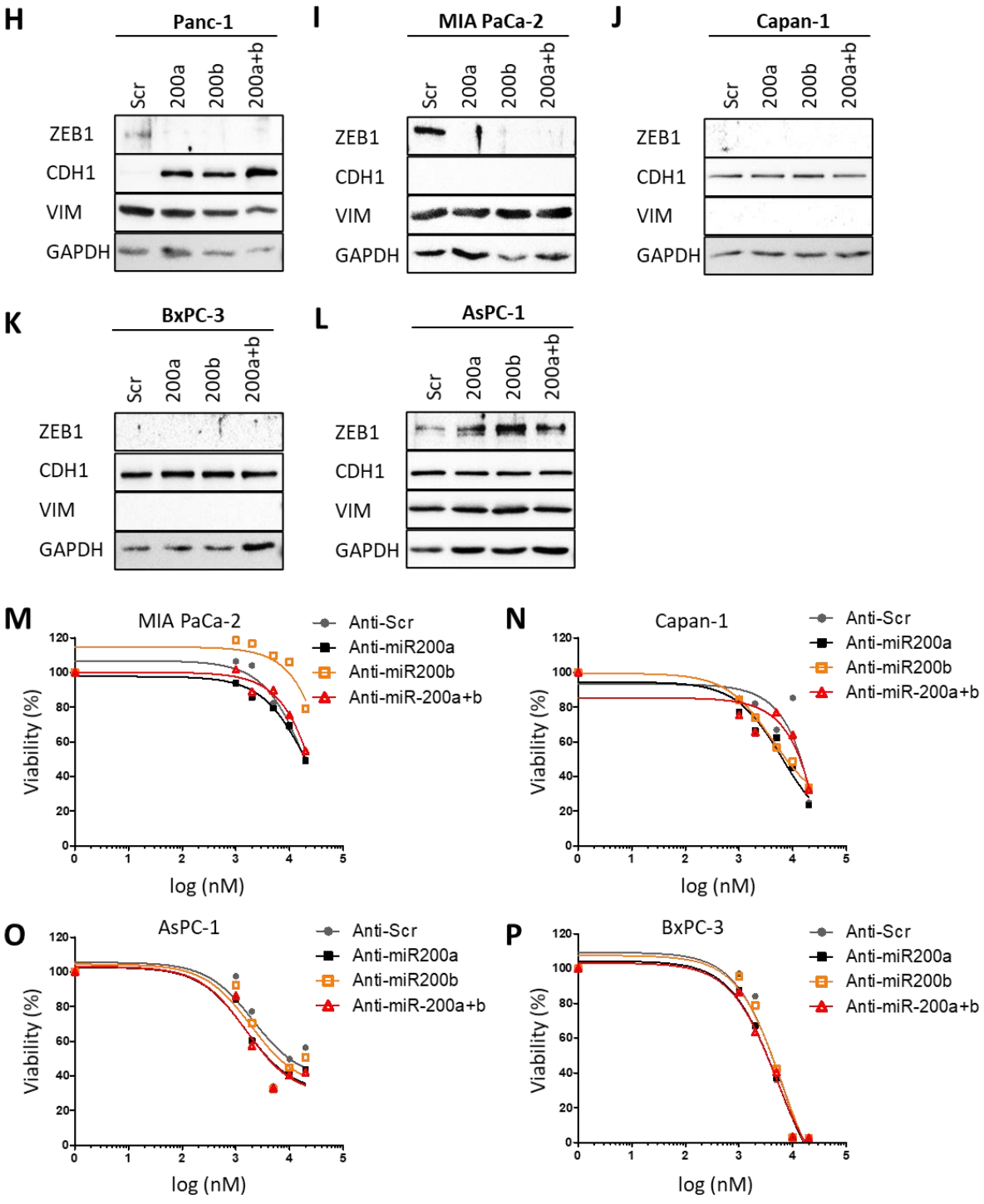

Supplemental Fig. 2: miRNA-200 and EMT not involved in cisplatin resistance in PDAC

Related to Manuscript Fig.2.

A Heat map of microRNA-200 family genes. Differentially expressed between basal-like (MIA PaCa 2, Panc-1) and classical (Capan-1, AsPC-1 and BxPC-3) except miRNA-200c.

B Biological replicate to **Fig. 2 B** of immunoblot analysis of GATA6 on PDAC cell lines. GAPDH served as a loading control.

C Immunoblot analysis of Vimentin (VIM) and E-cadherin (E-cad). GAPDH served as a loading control. Biological replicate to **Fig. 2 E**.

D, F miRNA-200a and b expression analysis on MIA PaCa-2 and Panc-1 cells after the transfection with Pre-miR™ miRNA Precursors (**D** 200a-3p and **F** 200b-3p) for 72 h (48 h and 24 h). snRNA U6 was used for normalization. Means ± SD of three biological replicates.

E, G miRNA-200a and b expression analysis on Capan-1, AsPC-1 and BxPC-3 cells after the transfection with Pre-miR™ miRNA inhibitor (**E** 200a-3p and **G** 200b-3p) for 72 h (48 h and 24 h). snRNA U6 was used for normalization. Means ± SD of three biological replicates.

H, I Immunoblot analysis of MIA PaCa-2 and Panc-1 cells after transfection as described in **D, F**. Staining of Zeb-1, E-cadherin (CDH1), Vimentin (VIM) and GATA6, GAPDH as a loading control.

J-L Immunoblot analysis of Capan-1, AsPC-1 and BxPC-3 cells after transfection as described in **E, G**. Staining of Zeb-1, E-cadherin (CDH1), Vimentin (VIM) and GATA6, GAPDH as a loading control.

M Cell viability assay of MIA PaCa-2 cells after transfection described in **D,F** and treated with 1 µM to 20 µM cisplatin for 72 h.

N-P Cell viability assay of **N** Capan-1, **O** AsPC-1 and **P** BxPC-3 cells after transfection described in **E, G** and treated with 1 µM to 20 µM cisplatin for 72 h.

SUPPLEMENTAL FIGURE 3

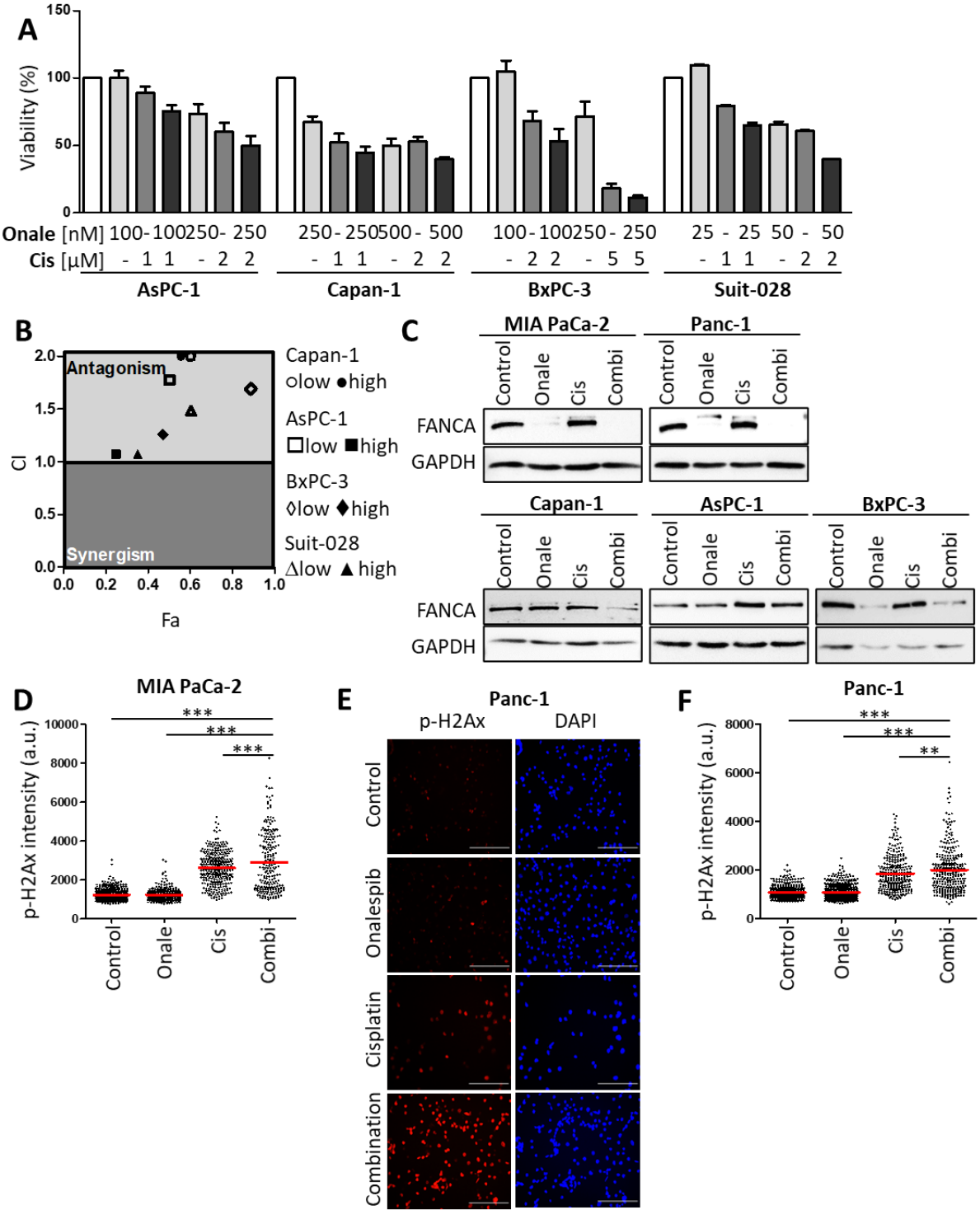

SUPPLEMENTAL FIGURE 3 (continued)

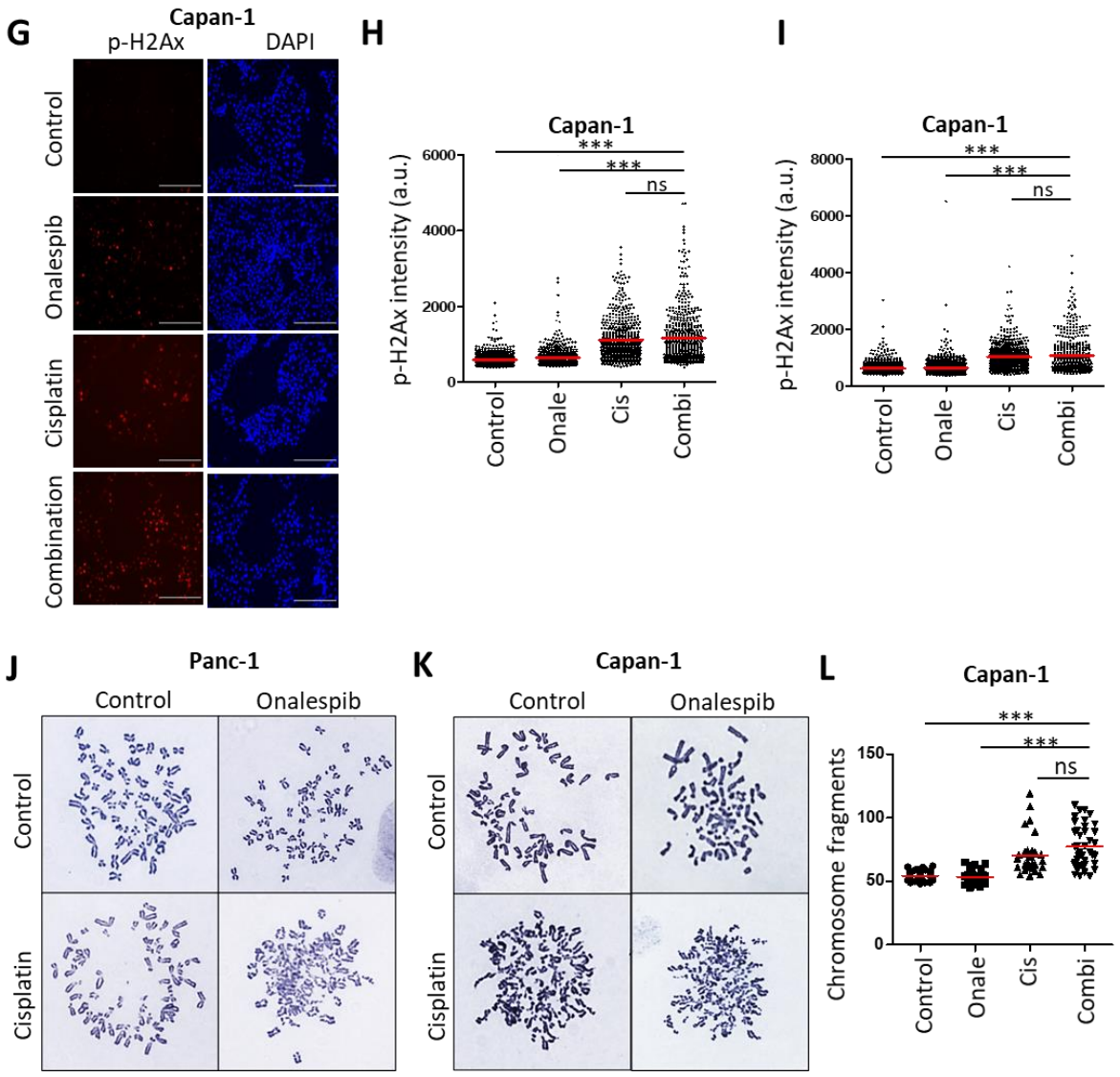

Supplemental Fig. 3: Sensitive PDAC cells revealed no synergism upon HSP90 inhibition

Related to Manuscript Fig. 3

A PDAC cell panel (AsPC-1, Capan-1, BxPC-3 and Suit-028) were treated with onalespib or cisplatin and a combination for 72 h with concentrations as indicated. Viability was determined by quantifying the ATP concentration.

B Combination index (CI) calculated from **A** plotted against the fraction affected (Fa) for the combination of HSP90 inhibitors onalespib and cisplatin.

C Biological replicate to **Fig. 3 C**. Immunoblot for FANCA, cells were treated as described in Fig 3 C. GAPDH served as a loading control.

D Biological replicate of fluorescence intensity per nucleus depicted as scatter plot for MIA Paca-2. Phosho-H2AX intensity per nucleus (arbitrary units) was calculated by quantification one of two independent experiments. The red lines indicate the mean intensity. Corresponding to **Fig. 3 E**.

E, G Representative immunofluorescence staining for phosho-H2AX in **E** Panc-1 cells and **G** Capan-1 with DAPI as counterstain. Cells were treated with onalespib and cisplatin for 24 h. Scale bar: 200 µm.

F, H, I Scatter plot of phosho-H2AX intensity per nucleus (arbitrary units), calculated by quantification of **E** and **G** from one of two independent experiments. The red line indicates the mean nuclear phospho-H2AX staining.

J Representative images of metaphase Panc-1 spreads related to **Fig. 3I**. Cells were treated with onalespib (100 nM) and cisplatin (20 µM) for 24 h together with 20 µM zVad to block apoptosis. Chromosomes were stained with Gimsea.

K Representative images of metaphase spreads. Capan-1 cells were treated with onalespib (250 nM) and cisplatin (2 µM) for 24 h together with 20 µM zVad to block apoptosis. Chromosomes were stained with Gimsea.

L The chromosome fragmentation was analyzed by counting the number of fragments shown in **K** in 40 randomly chosen cells from three independent experiments depicted as box blot. The mean red lines indicate the mean.

4 Discussion

In this study, we investigated the response of PDAC cell lines to cisplatin treatment. In particular, we discovered that the response of the cells could be categorised into two distinct groups, which are simultaneously reflected by the classical and basal-like subtypes. The expression of the markers GATA6 and miRNA-200 could further be linked to the subtype-specific response, potentially serving as biomarkers. Overall, we propose a treatment strategy that can not only be applied to cisplatin-sensitive cells but also to initially cisplatin-resistant cells by combining them with an HSP90 inhibitor (Figure 13). This strategy was successfully applied in PDAC cell lines and an orthotopically transplanted syngeneic mouse model. In the following sections, the details of our findings are discussed in more detail.

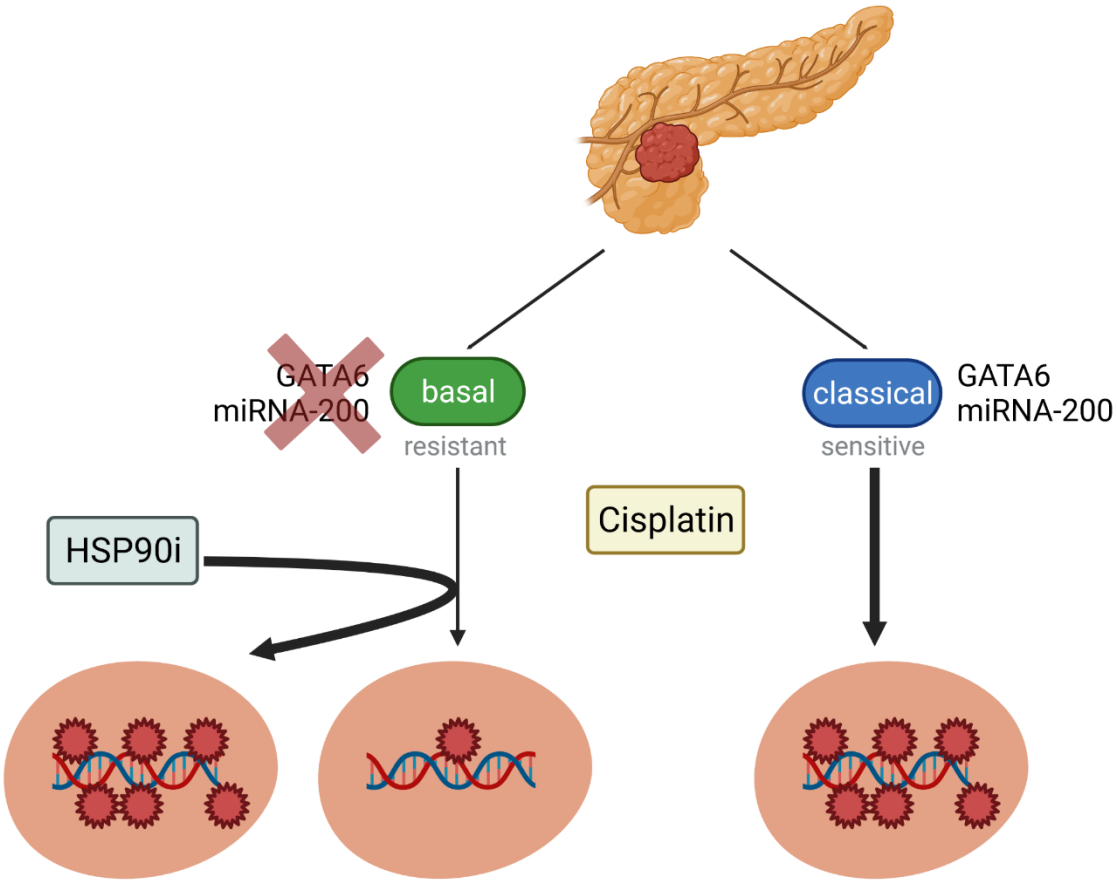

Figure 13: Proposed model for the treatment of PDAC with cisplatin and HSP90 inhibitor. Pancreatic cancer can be divided into two subtypes: the more epithelial, chemo-sensitive classical subtype and the more mesenchymal, chemo-resistant basal-like subtype. Both subtypes can be distinguished among their expression of the transcription factor GATA6 and the miRNA-200. Cell lines of the classical subtype revealed a cisplatin sensitivity with the formation of platinum-DNA adducts (depicted as red circles on the DNA). Basal-like PDAC cells responded to cisplatin with strongly reduced sensitivity and platinum adduct formation. This cisplatin resistance could be overcome by adding the HSP90 inhibitor onalespib, leading to increased DNA plantation. Created with BioRender.com.

4.1 Subtype dependent cisplatin-response

4.1.1 Cisplatin response of PDAC cell lines

Pancreatic cancer is predicted to be the second leading cause of cancer-related deaths within the next decade. Despite intensive research, the overall survival only slightly improved over the past years (Rawla et al., 2019; Tavakkoli et al., 2020). A significant problem of successful PDAC treatment is the low therapy response due to chemoresistance (Orth et al., 2019). It is therefore essential to understand which patients benefit from which treatment, thereby improving therapy outcome. The standard therapy of PDAC involves the nucleoside analogue gemcitabine (Burris et al., 1997). Patients with good performance status receive the more toxic but slightly more efficient therapy gemcitabine with the cytoskeletal inhibitor nab-paclitaxel or a combination of folinic acid, 5-fluorouracil (5-FU), irinotecan and oxaliplatin (FOLFIRINOX). However, the therapy options for metastatic pancreatic cancer are still limited, with a median survival of 11.1 months, and new treatment strategies are strongly required to improve the clinical outcome (Conroy et al., 2011).

Cisplatin, the most used chemotherapeutic agent, was already tested on pancreatic cancer cell lines (Arumugam et al., 2009; Danilov et al., 2011; Fujiwara et al., 2008). However, the response of PDAC cells was very heterogeneous and could not be correlated to any pathway, mutational change, or markers. Further, exploring cisplatin efficacy in clinical trials, PDAC patients were treated with a combination of cisplatin and gemcitabine versus gemcitabine alone. The median overall survival (7.5 vs. 6.0 months) and progression-free survival (5.3 months vs. 3.1 months) were favourable, however, the benefit of these trials displayed no statistically significant prolongation of the patient survival (Heinemann et al., 2006).

Although the cisplatin response has already been studied in some PDAC cell lines, we investigated the sensitivity towards cisplatin in a panel of seven commonly used PDAC cell lines (Manuscript Fig. 1A) (Mezencev et al., 2016; Michel et al., 2018). Interestingly, two clearly distinct groups were identified, which responded with a 10-fold concentration difference in cisplatin. In the following, the group treated with lower concentrations will be called cisplatin-sensitive and the group with higher concentrations cisplatin-resistant group. Interestingly, this sharp distinction in sensitivity could only be achieved by cisplatin treatment and not with other chemotherapeutics as the intercalating agent doxorubicin and the topoisomerase inhibitor irinotecan, hinting towards a cisplatin specific reaction. (Supplemental Fig. 1A, B). In response to the standard therapy agent gemcitabine, this separation into sensitive and resistance categories was also possible. However, the segregation between the two groups

was less clear following gemcitabine treatment, with the cell line AsPC-1 showing an intermediate response (Supplemental Fig. 1C). Thus, the resistance mechanisms for cisplatin must involve a specific feature that is only relevant for this class of drugs but not for other therapeutics.

4.1.2 Cisplatin resistance in basal-like pancreatic cancer cells

An essential step for the improved understanding and treatment of PDAC is the classification into distinct subtypes. These subtypes share similar molecular patterns and are assumed to share resemblance regarding chemo-response and survival rate. Essentially, two main transcriptomic subtypes are described: the classical/progenitor and basal-like/squamous subtype (hereafter referred to as classical and basal-like subtype) (Bailey et al., 2016; Collisson et al., 2019; Moffitt et al., 2015). Adams et al. and Kloesch et al. investigated a set of PDAC cell lines to assign them to the molecular PDAC subtypes (Adams et al., 2019; Kloesch et al., 2021). Further, Rashid et al. published a list of genes that assist in distinguishing classical and basal-like subtypes (Rashid et al., 2020). Based on the classification of Adams et al. and Kloesch et al. as well as our RNAseq analysis obtained from Diaferia et al., we could show that the response of cisplatin is correlated to the molecular subtype of PDAC cell lines with the basal-like PDAC cell lines displaying a cisplatin resistance (Adams et al., 2019; Diaferia et al., 2016; Kloesch et al., 2021). Our RNA-seq analysis revealed a downregulation of seven out of eight classical-associated genes in basal-like cell lines (Rashid et al., 2020) (https://owncloud.gwdg.de/index.php/s/SN091sU3FVlWgt3).

The basal-like subtype could be linked to a poor patient outcome. Further, basal-like tumours were shown to be resistant to FOLFIRINOX treatment in two independent clinical trials (O'Kane et al., 2020; Rashid et al., 2020). Since the platinum analogue oxaliplatin is part of FOLFIRINOX and in combination with the identified cisplatin resistance in basal-like PDAC cell lines, we hypothesise that basal-like pancreatic cancer patients are resistant to platinum-based chemotherapy in general. Indeed, a clinical trial assessing the response of PDAC patients to cisplatin within the context of subtype classification would be more conclusive.

4.2 Mechanisms contributing to cisplatin sensitivity

4.2.1 Predictive marker for cisplatin sensitivity

The best possible outcome for cancer patients is the early detection and correct therapy. Many cancer types, as PDAC, are diagnosed at a late stage, as they are asymptomatic at early stages (Adamska et al., 2017). For improved detection, biomarkers are a helpful tool. Biomarkers are quantifiable, objective characteristics, which indicate pathogenic processes, biological activities or response to interference or exposure, however, biomarkers are hard to identify (Califf, 2018; Strimbu and Tavel, 2010).

Besides the diagnostic markers, which assist in detecting or confirming a disease, prognostic markers help indicate a likely therapy outcome (e.g., disease recurrence, disease progression or death), independent of the treatment. Another class of biomarkers are the predictive biomarkers, representing the likelihood of the response to a certain therapy. This biomarker presents an improved tool to prevent unnecessary side effects by ineffective therapies (Califf, 2018).

Analysis of the COMPASS trial, a study to find predictive mutational and transcriptional signatures for better treatment strategies, revealed a strong correlation between the expression of the transcription factor GATA6 and the classical subtype (O'Kane et al., 2020). GATA6 contains two highly conserved zinc-finger DNA-binding domains, which bind to the (A/T)GATA(A/G) consensus sequence, thereby regulating gene expression. It is an important factor for normal pancreas development and endodermal lineage differentiation (Shi et al., 2017). High GATA6 expression is associated with well-differentiated tumours and the classical subtype, based on Moffitt subtyping. Low expression of GATA6, on the other hand, can be linked to poor prognosis and reduced response to 5-FU based chemotherapy (Martinelli et al., 2017). Thus, GATA6 was validated as a biomarker to differentiate basal-like and classical PDAC subtypes. As the cisplatin sensitivity is subtype dependent and GATA6 an indicator for the classical subtype, we conclude that GATA6 can also serve as a predictive marker for cisplatin response.

Analysing our RNA-seq data (Supplemental Fig. 2A), a distinct expression of miRNA-200 family members miRNA-200a, miRNA-200b, miRNA-141 and miRNA-429 but not miRNA-200c among the classical and basal-like PDAC cell lines could be observed. For further investigations, we decided to investigate miRNA-200a and miRNA-200b further, as they were already described to play a role in pancreatic cancer and epithelial to mesenchymal transition (Chen and Zhang, 2017; Daoud et al., 2019; Diaz-Riascos et al., 2019; Humphries and Yang,

2015). Validation of the miRNA-200a and miRNA-200b expression by qPCR revealed a 500-to-2500-fold decreased expression in basal-like cell lines (Manuscript Fig. 2C, D). Jin et al. could also show that high grade and metastasised tumours exhibit a reduced miRNA-200 expression (Jin et al., 2020). Further, they revealed an increased cisplatin sensitivity in cells with a high miRNA-200 expression. Also, the breast cancer cell line MCF-7 displayed reduced miRNA-200 levels after acquired cisplatin resistance (Piperigkou et al., 2020). Previous explorations of the miRNA-200 family in pancreatic cancer were mostly restricted to comparison of the expression between the pancreatic ducts to stroma but not between the different molecular subtypes (Diaz-Riascos et al., 2019).

Funamizu et al. investigated the expression levels of miRNA-200 in PDAC cell lines in the context of gemcitabine response and could show that gemcitabine resistance is correlated with the low expression of miRNA-200b (Funamizu et al., 2019). These results are partly in line with the response towards gemcitabine in our tested PDAC cell lines, as the cell line AsPC-1 revealed an intermediate gemcitabine response while expressing high levels of miRNA-200a and miRNA-200b (Manuscript Fig. 2C, D, Supplemental Fig. 1C). However, we could clearly show that increased miRNA-200 levels were correlated to a high cisplatin sensitivity in PDAC cells, whereas insensitive cells displayed a low expression of miRNA-200. As the expression pattern of miRNA-200a and 200b in pancreatic cancer is comparable to the GATA6, our results suggest that miRNA-200 expression can also serve as a predictive marker for cisplatin sensitivity and molecular PDAC subtypes.

One major role for the miRNA-200 family comprises of the regulation of epithelial to mesenchymal transition (EMT) by repression of transcription factor ZEB1/2 and therefore the expression of the epithelial marker E-cadherin (Lu et al., 2014; Mongroo and Rustgi, 2010; O'Brien et al., 2018). In the absence of miRNA-200, ZEB1/2 is upregulated, leading to a repression of E-cadherin. As the expression of miRNA-200 varies among the basal-like and classical subtypes of PDAC cell lines, we investigated whether the EMT can also be used as a predictive marker for cisplatin sensitivity, as Huang et al. could show, that EMT plays a role in chemoresistance (Huang et al., 2016). However, the expression of epithelial and mesenchymal markers did not show this distinct separation, as classical cell lines AsPC-1 and Suit-028 express mesenchymal marker vimentin and lack the epithelial marker E-cadherin (Manuscript Fig. 2E). Even though a tight connection between the basal-like subtype and EMT could be shown, EMT does not overlap with the basal-like subtype and is therefore unsuitable as a predictive marker for cisplatin response.

4.2.2 EMT or miRNA-200 expression does not contribute to cisplatin resistance

Due to the heterogeneity of PDAC, it is of high importance to understand which and why cells do not respond to the administered therapy to optimise the treatment. This deeper understanding also opens the possibility of targeting resistant cells and thereby increasing the response rate. After identifying predictive markers for cisplatin sensitivity in PDAC, the question arises, whether the sensitivity is dependent on miRNA-200 expression, which is involved in maintaining the sensitivity to certain chemotherapy (Chen and Zhang, 2017). Rui et al. investigated the miRNA-200 expression in docetaxel-resistant non-small cell lung carcinoma cells and could show that these cells exhibit a low miRNA-200b expression (Neves et al., 2010). By restoring the levels of miRNA-200b, Chen et al. were able to sensitise docetaxel resistant lung adenocarcinoma cells (Chen et al., 2014). The role of miRNA-200 in chemosensitivity comprises several factors: besides EMT, the miRNA-200 is involved in the regulation of cancer stem cell maintenance, apoptosis and cell cycle control (Korpal et al., 2008; Kurashige et al., 2012; Lim et al., 2013; Park et al., 2008).

Similar effects were observed by Funamizu et al., which revealed a sensitisation in gemcitabine resistant pancreatic cancer cells after the upregulation of miRNA-200b (Funamizu et al., 2019). This sensitisation is accompanied by a change in epithelial and mesenchymal markers. miRNA-200, an inhibitor of the EMT master regulator ZEB1/2, can induce the mesenchymal to epithelial transition (Korpal et al., 2008). Not only changes of miRNA-200 levels, but also altered expression of EMT markers like high vimentin and low E-cadherin displayed reduced chemosensitivity in breast cancer, oral squamous carcinoma, and pancreatic cancer cells towards taxanes, doxorubicin and cisplatin (Arumugam et al., 2009; Fang et al., 2018; Yang et al., 2014). Targeting the EMT by miRNA-200 or master regulator ZEB1/2 is expected to induce the mesenchymal to epithelial transduction, sensitising the cells to chemotherapy.

Even though we could observe the reduction of ZEB1 in the basal-like cell lines Panc-1 and MIA PaCa-2, only the Panc-1 cells revealed an increased level of E-cadherin upon the restoration of miRNA-200a or 200b. The reduction of miRNA-200a and b did not alter the EMT marker in the classical PDAC cell lines. Further, we could not determine any changes of cisplatin sensitivity in the basal-like PDAC cells with upregulation of miRNA-200 or classical cells with downregulation of miRNA-200 (Manuscript Fig. 2F-H, Supplemental Fig. 2 H-P). Our results differ from the findings of Funamizu et al., who were able to reverse the EMT by restoring miRNA-200 in Panc-1 cells resulting in enhanced gemcitabine sensitivity (Funamizu

et al., 2019). Further, Arumugam et al. were also able to sensitise Panc-1 cells towards cisplatin, gemcitabine, and 5-FU by knockdown of ZEB1 (Arumugam et al., 2009).

GATA6 stabilises, similar to miRNA-200, the epithelial state of the cell. Loss of GATA-6 results in the downregulation of GATA6 and the increase of vimentin. Restoration of GATA6 induces mesenchymal-to-epithelial transition in pancreatic cancer cells (O'Kane et al., 2020). Since the reversal of EMT did not result in sensitisation of PDAC cells to cisplatin, we assume that GATA6 also serve as a marker and is not involved in the mediation of cisplatin resistance. Hence, based on our current knowledge, we conclude another mechanism responsible for cisplatin resistance in basal-like PDAC cell lines.

4.2.3 Cisplatin resistance can be mediated by drug exporters

Different mechanisms can mediate the cisplatin resistance in tumour cells, as extensively described in section 2.2.4. The varying degree of cisplatin-DNA adduct formation in sensitive and resistant cells suggests a difference in cisplatin uptake, export, metabolism, or DNA repair mechanism (Manuscript Fig. 1E). This raises the question, which of these mechanisms is responsible for the cisplatin resistance? Answering that, the cells were treated with diphenhydramine (DIPH), an agent initially discovered to possess antihistaminic properties and currently used as cough medicine, hypnotic or against motion sickness (Garnett, 1986; Pathy, 2018). Interestingly, studies from Melnikova et al. in ovarian cancer cells showed an increased platinum uptake and decreased export activity, indicating an exporter blockage caused by DIPH treatment (Melnikova et al., 2020). Consequently, resistant PDAC cell lines were treated with a combination of DIPH and cisplatin, leading to a strong increase of cisplatin-DNA adduct formation (Manuscript Fig. 1F). Based on this observation we hypothesise, that blocking of export channels increases the intracellular cisplatin concentration resulting in enhanced sensitivity. Thus, the cisplatin export mechanism might contribute to the cisplatin resistance in basal-like PDAC cells.

Interestingly, our RNA-seq analysis revealed an elevated expression of the ABC transporter p-glycoprotein (p-gp) in basal-like PDAC cells which was shown to be involved in cisplatin resistance in non-small cell lung cancer and osteosarcoma (He et al., 2019; Vesel et al., 2017). Overexpression of p-gp can be linked to poor therapy response and low survival rates in osteosarcoma, non-small cell lung cancer and breast cancer patients (Chang et al., 2009; He et al., 2019). Even though it could be shown that cisplatin is no substrate of p-gp (Vesel et al.,

2017), the overexpression is correlated with resistance to cisplatin in sarcoma (Ren et al., 2007). However, knockdown or inhibition of the transporter leads to a re-sensitisation of the cells to cisplatin treatment (He et al., 2019). Resistance to cisplatin mediated by p-gp might be attributed to repression of caspase-3 activity (Gibalová et al., 2012)

Further, based on the RNA-seq analysis, we identified strong differences in the expression of the copper-transporting P-type ATPase (ATP7B) between the basal-like cell lines and two of the classical cell lines. However, the classical cell line Capan-1 displayed an intermediate ATP7B expression. This will be further elaborated in the discussion section 4.3.3. ATP7B was found to be involved in the efflux of platinum drugs, and increased levels lead to cisplatin resistance in ovarian and non-small cell lung cancer (Mangala et al., 2009; Nakagawa et al., 2008). In oral squamous cell carcinoma patients, the high expression of the transporters correlated with reduced platinum levels and decreased survival rate (Miyashita et al., 2003). The exact transport mechanism is still unrevealed; however, it is assumed that ATB7B sequesters platinum compounds into vesicles, transporting them to the cell membrane and secreting the drug from the cell (Safaei et al., 2008).

Another class of drug exporter proteins are the ATP-binding cassette (ABC) transporters. Mainly the ABC transporter multidrug resistance-associated protein 2 (MRP2/ABCC2) was found to be linked to cisplatin resistance (Guminski et al., 2006). Cisplatin conjugated to the antioxidant glutathione is exported by MRP2. An increased expression could be associated with cisplatin resistance in human carcinoma cell lines (Kool et al., 1997; Liedert et al., 2006; Materna et al., 2005). Also, patients with oesophagal squamous cell carcinoma and non-small lung cancer revealed a correlation of the expression of MRP2 and poor prognosis or cisplatin resistance, respectively (Yamasaki et al., 2011). Even though no correlation between the cisplatin sensitivity and export mechanism could be shown so far, inhibition of export transporters by DIPH reveal a positive impact on cisplatin-DNA adduct formation. Thus, this approach suggests a promising treatment strategy.

4.3 Sensitisation by targeting HSP90

4.3.1 Sensitisation of cisplatin-resistant PDAC cells by HSP90 inhibition

Besides identifying and classifying sensitive cells, it is important to find strategies for treating resistant cells. These cells often display cross-resistance to other chemotherapeutics, leaving a little if any option for efficient therapies (Pan et al., 2016). Further, it might allow the treatment

of initially sensitive cells with acquired resistance. An appropriate target for this approach is the heat shock protein 90 (HSP90). Its involvement in nearly all hallmarks of cancers and interaction with over 800 clients might be the suitable strategy to target cancer cells and reverse the resistance (Echeverría et al., 2011; Miyata et al., 2013; Picard, 2021). Further, HSP90 exhibits a special role in cancer cells, as it stabilises mutant oncoproteins and maintains the cancerous environment (Mahalingam et al., 2009). As a single agent, HSP90 inhibitors did not reveal an efficacy for cancer therapy in patients so far, however, in combination with radiotherapy or cross-linking agents as carbo- or cisplatin, it could be shown to increase the induction of apoptosis in soft tissue sarcoma, glioblastoma, ovarian, colon and pancreatic cancer *in vitro* and *in vivo* (Ernst et al., 2015; Kramer et al., 2017; Nagaraju et al., 2019; Orth et al., 2021; Spiegelberg et al., 2020). Clinical efficacy is under investigation, but so far, no HSP90 inhibitor has entered the clinics.

Based on these results, we investigated the response of the basal-like cell lines towards the combination of cisplatin and the HSP90 inhibitor onalespib. We could show that the combination of both drugs leads to the sensitisation of the cisplatin-resistant cells and a synergistic reduction of cell viability (Manuscript Fig. 3A, B). These findings are in line with the response of ovarian cancer cells to the combination of the HSP90 inhibitor ganetespib and carboplatin published by Kramer et al. (Kramer et al., 2017). The following sections will discuss possible mechanisms by which HSP90 inhibition contributes to cisplatin sensitisation in pancreatic cancer.

4.3.2 Mechanisms for sensitisation of cancer cells to cisplatin by HSP90 inhibition

4.3.2.1 Impaired DNA repair increases DNA damage in cisplatin-resistant cells

The main mechanism behind treating cancer cells with cisplatin is the formation of inter-strand crosslinks in the DNA (Wang and Lippard, 2005). These lesions are toxic for the cells, as they inhibit replication as well as transcription processes and further require an elaborate repair mechanism as extensively described in section 2.2.3 (Kee and D'Andrea, 2010). It could be shown that defects or deficiencies of the DNA damage repair pathway, e.g., in BRCA1, BRCA2 and PALB, result in a sensitisation towards platinum compounds (Chirnomas et al., 2006). BRCA1/2 and PALB are components of the Fanconi anemia (FA) pathway, linking the FA proteins to the homologous recombination repair (Michl et al., 2016). Liu et al. indicated that a

deficiency of other Fanconi anaemia, complementation (FANC) proteins can also induce the sensitisation to platinum chemotherapy (Liu et al., 2020).

Fanconi anemia describes a rare genetic disease that is characterised by a deficiency in DNA damage response. Patients with this disorder are prone to bone marrow failure, cancer development and are highly sensitive to DNA crosslinking agents as mitomycin C and platinum compounds (Chirnomas et al., 2006). The most altered gene is FANCA, and the protein is part of the FA core complex, responsible together with FANCG for the nuclear localization and stability of the FA core complex proteins (Castella et al., 2011). Mutations or deficiency of FANCA result in the lack of FANCD2/I monoubiquitination and subsequently no activation of homologous recombination proteins. Thus, the cell is not able to repair double-strand breaks and accumulates chromosomal aberrations (Pfeiffer et al., 2000).

HSP90 acts as a chaperone of FANCA, thereby regulating the FA pathway (Yamashita et al., 2007). In ovarian and head and neck cancer, it could be shown that pharmacological inhibition of HSP90 by ganetespib or AUY922 resulted in a degradation of FANCA by the ubiquitin-proteasome pathway (Kramer et al., 2017; McLaughlin et al., 2017). In basal-like PDAC cells, we observed degradation of FANCA after treatment with the HSP90 inhibitor onalespib (Manuscript Fig. 3C). Besides the reduction of FANCA levels, we obtained a significant increase of the DNA damage marker phospho-H2Ax upon combination treatment (Manuscript Fig. 3D-F).

Beside the increased DNA damage by downregulation of FANCA, Kramer et al. could show that HSP90 inhibition also affects the cell cycle progression, forcing cells to proceed the cell cycle independent of DNA damage by downregulation of the kinases cyclin-dependent kinase 1 (CDK1) and Wee1 (Kramer et al., 2017). We could confirm in basal-like PDAC cells that the impaired DNA repair by reduced FANCA, increased DNA damage and potential cell cycle progression by downregulation of CDK1 result in the accumulation of chromosomal aberrations, which climax in the pulverisation of the chromosomes (Manuscript Fig. 3G-I).

4.3.2.2 HSP90 inhibition increases the cisplatin-adduct formation

Besides the impaired DNA damage repair by downregulation of FANCA, HSP90 might regulate other mechanisms involved in cisplatin resistance in PDAC. One mechanism contributing to decreased cisplatin sensitivity is the increased drug efflux which consequently causes a reduction of cytotoxic intracellular cisplatin concentration (Zhou et al., 2020). We

observed that inhibition of drug export mechanism by DIPH increased the platinum-DNA adduct formation (Manuscript Fig. 1F). This effect could be reproduced by combining cisplatin with the HSP90 inhibitor onalespib, suggesting a potential role of HSP90 in the regulation of cisplatin export (Manuscript Fig. 2J). It is tempting to speculate that an HSP90 client protein enhances the export of cisplatin and that HSP90 inhibition leads to the destabilization of such a protein, resulting in sensitization towards cisplatin. If this is true, the question remains which protein(s) fulfil(s) such criteria.

The ABC transporter p-glycoprotein was found differentially expressed between resistant and sensitive PDAC cells. However, cisplatin was not described as a substrate of this transporter so far, although overexpression could be correlated to cisplatin resistance, while inhibition resulted in sensitisation towards cisplatin in osteosarcoma cells (He et al., 2019). Also, inhibition of HSP90 was shown to reduce the expression of p-gp and sensitise the non-small cell lung cancer cells to cisplatin treatment (Bacon et al., 2020). Even though no direct interaction of cisplatin and p-gp was described, it might be possible that HSP90 inhibition contributes to sensitisation by regulating p-gp. Further, we could identify differences in the expression of ATP7B between PDAC subtypes. ATP7B plays a pivotal role in the efflux of cisplatin, and overexpression could be linked to cisplatin resistance (Dmitriev, 2011). However, no interaction of HSP90 and ATP7B was described so far.

Beyond that, the enhanced platinum-adduct formation might also be induced by impaired DNA damage response. However, both mechanisms can lead to increased adduct formation by either increased intranuclear cisplatin concentrations or reduced DNA damage repair. Since we could show that blocking cisplatin export with DIPH and HSP90 inhibition revealed similar levels of adduct formation, we assume that the cisplatin efflux contributes to the effect.

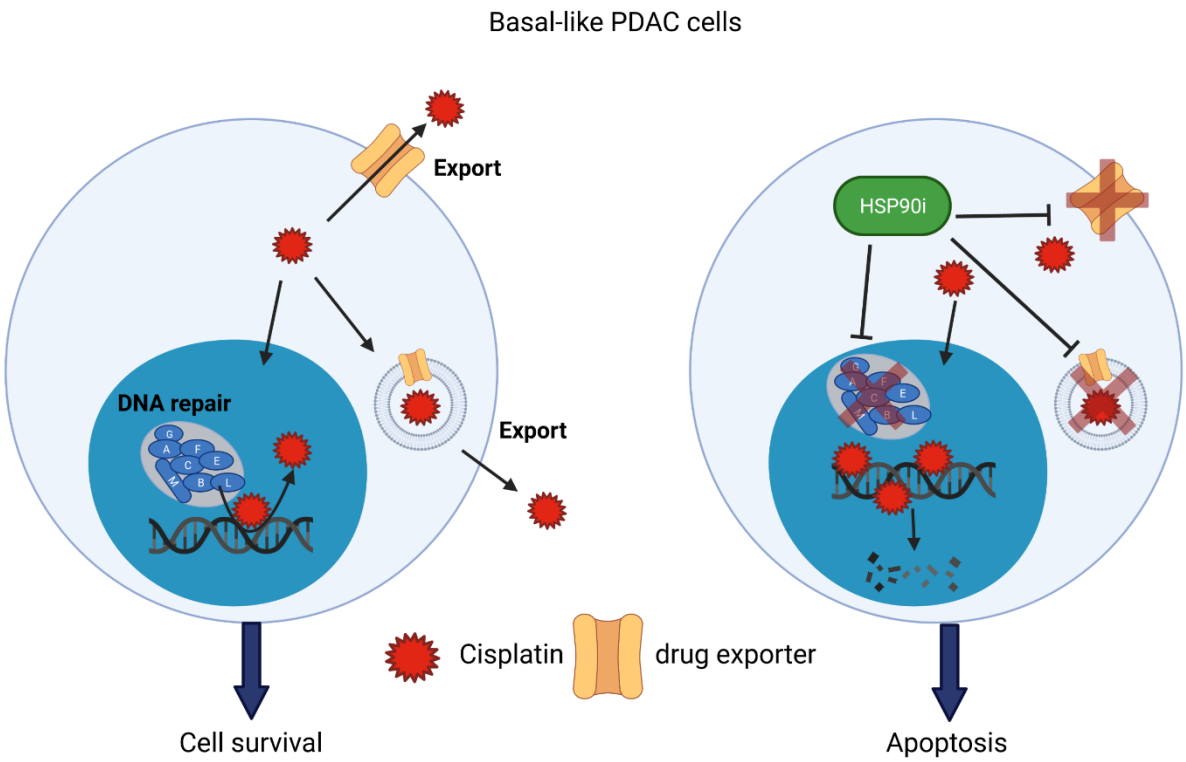

Figure 14: Proposed mechanism of cisplatin resistance and sensitisation in resistant PDAC. Basal-like PDAC cells display cisplatin resistance by interfering with the cisplatin export and DNA repair mechanisms. Thus, less cisplatin can induce DNA damage which leads to the survival of the cells. Combining the cisplatin treatment with HSP90 inhibition, the efflux of cisplatin is reduced, and the DNA repair machinery is inhibited, leading to enhanced platinum-DNA adduct formation and accumulation of chromosomal aberrations. Created with BioRender.com.

4.3.2.3 Other possible mechanisms

Apart from the impaired DNA damage response and inhibition of the cisplatin export mechanism, further pathway alterations by HSP90 inhibition might be involved in cisplatin sensitisation, which we did not further elaborate on. However, due to the pleiotropic effects of HSP90, also other pathways might additionally contribute to enhanced sensitivity upon HSP90 inhibition.

One factor which might play a role in cisplatin response is the hypoxia-inducible factor 1 alpha (HIF-1α), controlling oxygen regulation as a transcription factor in the cell (Long et al., 2018). Since oxygen supply is essential for tumour growth, elevated levels of HIF-1α can be found in many tumours, leading to tumour promotion, inhibition of apoptosis and angiogenesis (Masoud and Li, 2015). Long et al. revealed that hypoxia could inhibit cisplatin-induced apoptosis in ovarian cancer cells, which was linked to HIF-1α induced autophagy (Long et al., 2018). In lung cancer cells, the nucleotide excision repair protein XPA, which high expression levels

correlate with cisplatin resistance, is a target of HIF-1α and therefore enhanced HIF-1α expression leads to high XPA levels resulting in cisplatin resistance (Liu et al., 2012). Nagaraju et al. could show that the combination of HSP90 inhibition with radiotherapy or 5-FU lead to a reduction of HIF-1α in pancreatic cancer cells and was able to overcome HIF-1α mediated resistance (Nagaraju et al., 2019). Thus, we assume that HSP90 inhibition and subsequent HIF-1α reduction might also sensitise the pancreatic cancer cells to cisplatin.

Different studies have shown that overexpression of HSP90 contributes to multi-drug resistance (Kumar et al., 2020; Piper and Millson, 2011; Yin et al., 2021). Besides the already mentioned pathways, the evasion of apoptosis is also regulated by HSP90. The activity of pro-survival factors Bcl-2 and survivin were shown to correlate with increased HSP90 levels in ovarian, breast and lung cancer mediate the drug resistance. In ovarian cancer, the high expression of HSP90 lead to the increased activation of the Akt/GSK3β/β-catenin pathway resulting in high expression of Bcl-2 and survivin. Targeting HSP90 sensitised the ovarian cancer cells to cisplatin and paclitaxel (Yin et al., 2021). It thus remains possible that differential, HSP90-dependent stability of anti-apoptotic factors in PDAC cells might also contribute to their sensitivity towards cisplatin.

The mutant form of the tumour suppressor p53 is also a client of HSP90 and could be shown to mediate chemo- and radioresistance, also for cisplatin treatment (Lin et al., 2008a; Tung et al., 2015). While chemotherapy would lead to p53 accumulation and apoptosis in a wildtype background, some p53 mutants were shown to inhibit caspase activity and p63/73-dependent induction of the anti-apoptotic proteins Bcl-2-associated X (Bax) and Phorbol-12-myristate-13-acetate-induced protein 1 (Noxa) contributing to insensitivity to radio- and chemotherapy (Chee et al., 2013; Liu et al., 2011). Thus, inhibition of the pleiotropic function of HSP90 might add to the reduced DNA repair and cisplatin export leading to successful treatment of basal-like PDAC cells, influencing the cisplatin resistance by interfering with various pathways.

4.3.3 No synergism in classical subtype upon combination treatment

We found that the classical subtype is sensitive towards cisplatin treatment, and the initially cisplatin-resistant basal-like cells could be sensitised by HSP90 inhibition with onalespib. Curiously, we could not see an enhanced efficacy in the classical PDAC cells upon the combination treatment (Supplemental Fig. 3A, B). Unfortunately, the mechanism by which

some cells evade HSP90 inhibition remains to be elucidated, leaving us speculating about the reasons.

Interestingly, only a slight reduction in FANCA protein levels was detected after HSP90 inhibition and no further increase of the DNA damage signal phospho-H2AX in classical Capan-1 cells (Manuscript Fig. 3C, Supplemental Fig. 3G-I). A possible explanation could be that HSP90 is not upregulated in classical PDAC cells, which therefore experience no enhanced effects when combining HSP90 inhibitors with cisplatin. Further, the cells might be less dependent on the HSP90 function, and upon inhibition, a reduced client degradation can be achieved, resulting in reduced FANCA degradation and intact DNA damage response. Another possibility besides the reduced expression level of HSP90 might be the aneuploidy and the subsequent imbalance in proteostasis. Overexpression of proteins that tend to form aggregates can also lead to a stronger dependency on HSP90. For specific HSP90 clients, e.g., fms like tyrosine kinase 3 (FLT-3) in leukaemia or Myc in AML, a direct correlation between the expression level and the sensitivity to HSP90 inhibitors could be shown (Echeverria et al., 2019). Our finding that classical PDAC cells show a reduced sensitivity towards onalespib compared to basal-like cells is in line with the assumptions mentioned above.

Further, no strong increase in cisplatin-DNA adducts could be detected after inhibition of the cisplatin exporter by DIPH in the classical cell line (Manuscript Fig. 1F). We hypothesise that the maximum amount of cisplatin is already bound to the DNA, and the inhibition of cisplatin exporter could not further sensitise the cells. Capan-1 cells displayed a reduced platinum-DNA adduct formation, and the expression of the ATP7B transporter was slightly enhanced compared to both other classical cell lines, however, the sensitivity to cisplatin is comparable. It is important to know that Capan-1 cells harbour a BRCA2 mutation, so even though less cisplatin is bound to the DNA than the other classical cell lines, the impaired DNA repair results in the same sensitivity to cisplatin (Manuscript Fig. 1A, E) (McCabe et al., 2009).

4.4 Clinical relevance

4.4.1 Mouse study

To further elaborate on our hypothesis and bring the combination of cisplatin and HSP90 inhibitor closer to the clinical application, we aimed to investigate the combination in an *in vivo* mouse model. Therefore, we firstly explored the response in KPC (LSL-KrasG12D/+; LSL-Trp53R172H/+; Pdx-1-Cre, C57/BL6 genetic background) cells *in vitro*. Treatment of these

cells with the combination of cisplatin and onalespib resembles the response of basal-like PDAC cells in terms of synergy and DNA damage marker expression (Manuscript Fig. 4B-D), even though the KPC cells were cisplatin responsive (Manuscript Fig. 4A)

There are different types of PDAC mouse models available: xenograft, genetically engineered or orthotopic mouse models (Lee et al., 2016). We decided on the syngeneic orthotopic mouse model, as it has an intact immune system, and the tumours are formed after a short period of time with comparable sizes. Furthermore, KPC models could be shown to share common genetic mutations with human pancreatic cancer (Niknafs et al., 2019). However, the syngeneic mouse model is less desmoplastic than human tumours, while the desmoplastic stroma contributes to therapeutic resistance in human PDAC (Grbovic-Huezo et al., 2020). After transplantation of the KPC cells into a syngeneic orthotopic mouse model, the combination resulted in a strong tumour reduction *in vivo* (Manuscript Fig. 5B). Also, enhanced DNA damage marker levels could be detected in the combination group, resulting in increased apoptosis (Manuscript Fig. 5D-G). So far, the subtype classification of KPC could not be clearly defined since they can be manipulated to become more squamous (Somerville et al., 2018) but also to get closer to a classical phenotype (Candido et al., 2018). Hence, cisplatin and HSP90 inhibitors cooperatively and strongly restrict pancreatic carcinoma growth in an animal model, further moving this approach towards its clinical perspective.

4.4.2 Cisplatin versus Oxaliplatin

For the treatment of pancreatic cancer, the third-generation compound oxaliplatin is used as first-line therapy in combination with folinic acid, 5-FU and irinotecan (FOLFIRINOX) (Conroy et al., 2011). Oxaliplatin was approved in 1996 by the FDA and is applied for the treatment of metastatic colon cancer, gastric cancer and relapsed refractory lymphoma (Bécouarn et al., 1998). In 2011, the combination FOLFIRINOX became an option in metastatic pancreatic cancer with a survival benefit of 11.1 months versus 6.8 months compared to the standard therapy gemcitabine (Conroy et al., 2011). As oxaliplatin is already used for the treatment of PDAC, the question arises whether a combination of HSP90 inhibitor and oxaliplatin would also be beneficial.

Even though cisplatin and oxaliplatin are both platinum compounds, the active form of both drugs differ in structure and causes distinct mechanisms of action, with the exact mechanism remaining to be elucidated (Alcindor and Beauger, 2011). Nevertheless, Woynarowski et al.

could show that oxaliplatin causes a diminished induction of DNA damage signals and reduced double-strand breaks compared to cisplatin (Woynarowski et al., 2000). Further, oxaliplatin does not affect cell cycle control, whereas cisplatin-treated cells arrest in S-phase after 24 h treatment and in G2/M phase after 48 h, speculating about a different mode of action for oxaliplatin (Schoch et al., 2020).

Kramer et al. revealed that HSP90 inhibition reduces the DNA damage repair by preventing the repair of double-strand breaks. Further, HSP90 is involved in cell cycle control, and upon inhibition, the cyclin-dependent kinase 1 (CDK1) and Wee1 are inhibited, forcing the cell to proceed through the cell cycle. Simultaneous treatment with cisplatin or similar reagent carboplatin increases the DNA double-strand breaks, resulting in fragmented chromosomes after forced progression of the cell cycle (Kramer et al., 2017). Oxaliplatin is assumed to trigger apoptosis in cells by inducing ribosomal biogenesis stress (Riddell, 2018). Thus, we hypothesise that the combination of HSP90 inhibitor and oxaliplatin will show alterations compared to cisplatin. Indeed, an investigation of oxaliplatin together with onalespib would be more conclusive.

4.4.3 HSP90 inhibitors in clinical trails

The approval of HSP90 inhibitors in patients was not successful so far, even though promising results were achieved in several *in vitro* and *in vivo* studies (Acquaviva et al., 2014; Caldas-Lopes et al., 2009; Garon et al., 2013; Jiao et al., 2011; Lazenby et al., 2015). The lack of convincing anti-tumour activity and organ-specific toxicities, as hepato- or ocular toxicity, prevented the FDA approval (Park et al., 2020). Even in combination with other agents as chemotherapy (5-FU, paclitaxel, carboplatin and cisplatin) or targeted therapy (multi-kinase inhibitor sorafenib, epidermal growth factor receptor (EGFR) inhibitor erlotinib and Bruton's tyrosine kinase (BTK) inhibitor), HSP90 inhibition did not yet achieve the meaningful anti-tumour efficacy(Daunys et al., 2019; Jacobson et al., 2016; Kramer et al., 2017; Liao and Yang, 2017; Ono et al., 2013; Yin et al., 2021). Based on a strong synergy of HSP90 inhibitor ganetespib and carboplatin in ovarian cancer cell lines, a phase II clinical trial involving 120 high-grade ovarian cancer patients (NCT03783949) was conducted, however, the results are still pending.

One possible explanation for the efficacy failure in patients can be the upregulation of the heat shock response pathway (HSR). Upon inhibition of the N-terminal ATP binding site, the heat

shock factor 1 (HSF1) is induced, which leads to an increased expression of HSP70, HSP27 and HSP90 (Kijima et al., 2018). Chen et al. could show that the upregulation of HSP70 and HSF1 induces resistance to HSP90 inhibitors and activates a pro-survival pathway in malignant cells (Chen et al., 2013). All clinically tested HSP90 inhibitors target the N-terminal site of the protein, however, novel inhibitors were developed which block the C-terminal nucleotide-binding domain of HSP90, leading to client protein release and degradation (Park et al., 2020). In fact, testing the C-terminal HSP90 inhibitors together with cisplatin could be of interest, having the advantages of HSP90 inhibition without activation of the HSR.

4.5 Concluding remarks and further perspective

In summary, our work revealed a correlation between the cisplatin response and the molecular subtypes of PDAC. While classical PDAC cells displayed cisplatin sensitivity, the basal-like cells were resistant. Differences in response are reflected by the amount of cisplatin bound to the DNA identified with immuno-cytological staining. Identifying subtype and response specific biomarkers would help avoid toxic therapies in patients who are unlikely to respond. The expression of the biomarker GATA6, which has already been correlated to the classical subtype, and the expression of miRNA-200a and miRNA-200b could be linked to cisplatin sensitivity. In contrast, the resistant basal-like PDAC cells lack these markers (O'Kane et al., 2020). Furthermore, we were able to sensitise cisplatin-resistant basal-like PDAC cells by treatment with a combination of the HSP90 inhibitor onalespib and cisplatin. The combination resulted in a synergistic anti-tumour effect with reduced expression of the DNA damage repair protein FANCA and increased cisplatin-DNA adduct formation.

In the future, further investigations of the mechanism behind the synergy of the drug combination would be helpful. Of particular interest is the question of whether an export mechanism is involved in the resistance process and, if so, which exporter protein mediates the cisplatin efflux in an HSP90-dependent fashion. Knockdown experiments or specific exporter inhibition might help to elaborate on this question. It would be interesting to know whether a combination of HSP90 inhibitor and the drug export blocker DIPH together with cisplatin might enhance the platinum-DNA adduct formation even more.

Some HSP90 inhibitors lack efficacy due to upregulation of the resistance-associated heat shock response pathway by disrupting the HSP90/HSF1 interaction. N-terminal HSP90 inhibitors remain in the closed state, increasing the binding duration of HSF1 to the *hsp70* promotor

(Kijima et al., 2018). To avoid such a scenario, it might be helpful to evaluate the efficacy of cisplatin together with novel HSP90 inhibitors, like Novobiocin, which inhibit the C-terminal nucleotide-binding pocket of HSP90 without inducing the heat shock response. (Donnelly and Blagg, 2008).

The combination of cisplatin and HSP90 inhibitors might be advantageous when transferred to other cisplatin-treated tumours with frequent resistance formation, such as small cell lung cancer or cervical cancer (Gaponova et al., 2016; Jiao et al., 2011). These tumours revealed already sensitivity to HSP90 inhibition alone, however, the combination with cisplatin remains to be studied.

To bring our findings closer to the clinical application, we performed a mouse study using the syngeneic orthotopic KPC mouse model. Treatment of the mice with the combination of cisplatin and HSP90 inhibitor onalespib resulted in reduced tumour size and increased apoptosis induction. However, it would be even more stringent to evaluate this approach in autochthonous tumours rather than transplanted ones.

As the first step, it is essential to analyse the correlation of cisplatin response and molecular subtype in patients. Furthermore, it is important to verify the applicability of the marker GATA6, miRNA-200a and miRNA-200b in patients since we identified them as predictors for cisplatin sensitivity. Finally, based on our promising findings, investigation of the combination therapy might be beneficial for cisplatin-resistant PDAC patients.

5 References

Acquaviva, J., Smith, D.L., Jimenez, J.P., Zhang, C., Sequeira, M., He, S., Sang, J., Bates, R.C., and Proia, D.A. (2014). Overcoming acquired BRAF inhibitor resistance in melanoma via targeted inhibition of hsp90 with ganetespib. Mol. Cancer Ther. *13*, 353–363.

Adamo, P., Cowley, C.M., Neal, C.P., Mistry, V., Page, K., Dennison, A.R., Isherwood, J., Hastings, R., Luo, J.L., Moore, D.A., et al. (2017). Profiling tumour heterogeneity through circulating tumour DNA in patients with pancreatic cancer. Oncotarget *8*, 87221–87233.

Adams, C.R., Htwe, H.H., Marsh, T., Wang, A.L., Montoya, M.L., Subbaraj, L., Tward, A.D., Bardeesy, N., and Perera, R.M. (2019). Transcriptional control of subtype switching ensures adaptation and growth of pancreatic cancer. Elife *8*, 1–25.

Adamska, A., Domenichini, A., and Falasca, M. (2017). Pancreatic ductal adenocarcinoma: Current and evolving therapies. Int. J. Mol. Sci. *18*.

Aiello, N.M., Maddipati, R., Norgard, R.J., Balli, D., Li, J., Yuan, S., Yamazoe, T., Black, T., Sahmoud, A., Furth, E.E., et al. (2018). EMT Subtype Influences Epithelial Plasticity and Mode of Cell Migration. Dev. Cell *45*, 681-695.e4.

Alcindor, T., and Beauger, N. (2011). Oxaliplatin: A review in the era of molecularly targeted therapy. Curr. Oncol. *18*, 18–25.

Alderden, R.A., Hall, M.D., and Hambley, T.W. (2006). The discovery and development of cisplatin. J. Chem. Educ. *83*, 728–734.

Alexandrova, E.M., Yallowitz, A.R., Li, D., Xu, S., Schulz, R., Proia, D.A., Lozano, G., Dobbelstein, M., and Moll, U.M. (2015). Improving survival by exploiting tumour dependence on stabilized mutant p53 for treatment. Nature *523*, 352–356.

Altieri, D.C., Stein, G.S., Lian, J.B., and Languino, L.R. (2012). TRAP-1, the mitochondrial Hsp90. Biochim. Biophys. Acta - Mol. Cell Res. *1823*, 767–773.

Altuvia, Y., Landgraf, P., Lithwick, G., Elefant, N., Pfeffer, S., Aravin, A., Brownstein, M.J., Tuschl, T., and Margalit, H. (2005). Clustering and conservation patterns of human microRNAs. Nucleic Acids Res. *33*, 2697–2706.

Anders, S., Pyl, P.T., and Huber, W. (2015). HTSeq-A Python framework to work with high-throughput sequencing data. Bioinformatics *31*, 166–169.

Ansari, D., Althini, C., Ohlsson, H., and Andersson, R. (2019). Early-onset pancreatic cancer: a population-based study using the SEER registry. Langenbeck's Arch. Surg. *404*, 565–571.

Arango, D., Wilson, A.J., Shi, Q., Corner, G.A., Arañes, M.J., Nicholas, C., Lesser, M., Mariadason, J.M., and Augenlicht, L.H. (2004). Molecular mechanisms of action and prediction of response to oxaliplatin in colorectal cancer cells. Br. J. Cancer *91*, 1931–1946.

Arumugam, T., Ramachandran, V., Fournier, K.F., Wang, H., Marquis, L., Abbruzzese, J.L., Gallick, G.E., Logsdon, C.D., McConkey, D.J., and Choi, W. (2009). Epithelial to Mesenchymal Transition Contributes to Drug Resistance in Pancreatic Cancer. Cancer Res. *69*, 5820–5828.

Aung, K.L., Fischer, S.E., Denroche, R.E., Jang, G., Dodd, A., Creighton, S., Southwood, B., Liang, S., Chadwick, D., Kane, G.M.O., et al. (2019). HHS Public Access Cancer : Early Results from the COMPASS Trial. *24*, 1344–1354.

Bacon, N.A., Larre, I., Lawag, A.A., Merritt, C., Smith, M., Rosolen, M., and Sollars, V.E. (2020). Low dose HSP90 inhibition with AUY922 blunts rapid evolution of metastatic and drug resistant phenotypes induced by TGF-β and paclitaxel in A549 cells. Biomed. Pharmacother. *129*.

Bailey, P., Chang, D.K., Nones, K., Johns, A.L., Patch, A.M., Gingras, M.C., Miller, D.K., Christ, A.N., Bruxner, T.J.C., Quinn, M.C., et al. (2016). Genomic analyses identify molecular subtypes of pancreatic cancer. Nature *531*, 47–52.

Bartel, D.P. (2004). MicroRNAs. Cell *116*, 281–297.

Barton, C.M., and Staddon, S.L. (1991). Abnormalities of the p53. Br. J. Cancer *64*, 1076–1082.

Bécouarn, Y., Ychou, M., Ducreux, M., Borel, C., Bertheault-Cvitkovic, F., Seitz, J.F., Nasca, S., Nguyen, T.D., Paillot, B., Raoul, J.L., et al. (1998). Phase II trial of oxaliplatin as first-line chemotherapy in metastatic colorectal cancer patients. J. Clin. Oncol. *16*, 2739–2744.

Beger, H.G., Gansauge, F., and Leder, G. (2002). Pancreatic cancer: Who benefits from curative resection? Can. J. Gastroenterol. *16*, 117–120.

Bengtsson, A., Andersson, R., and Ansari, D. (2020). The actual 5-year survivors of pancreatic ductal adenocarcinoma based on real-world data. Sci. Rep. *10*, 1–9.

Bhayani, M.K., Calin, G.A., and Lai, S.Y. (2012). Functional relevance of miRNA* sequences in human disease. Mutat. Res. - Fundam. Mol. Mech. Mutagen. *731*, 14–19.

Biankin, A. V., Waddell, N., Kassahn, K.S., Gingras, M.C., Muthuswamy, L.B., Johns, A.L., Miller, D.K., Wilson, P.J., Patch, A.M., Wu, J., et al. (2012). Pancreatic cancer genomes reveal aberrations in axon guidance pathway genes. Nature *491*, 399–405.

Bisht, K.S., Bradbury, C.M., Mattson, D., Kaushal, A., Sowers, A., Markovina, S., Ortiz, K.L., Sieck, L.K., Isaacs, J.S., Brechbiel, M.W., et al. (2003). Geldanamycin and 17-Allylamino-17-demethoxygeldanamycin Potentiate the in Vitro and in Vivo Radiation Response of Cervical Tumor Cells via the Heat Shock Protein 90-Mediated Intracellular Signaling and Cytotoxicity. Cancer Res. *63*, 8984–8995.

Blacklock, K., and Verkhivker, G.M. (2014). Allosteric regulation of the Hsp90 dynamics and stability by client recruiter cochaperones: Protein structure network modeling. PLoS One *9*.

Borchert, G.M., Lanier, W., and Davidson, B.L. (2006). RNA polymerase III transcribes human microRNAs. Nat. Struct. Mol. Biol. *13*, 1097–1101.

Borst, P., Evers, R., Kool, M., and Wijnholds, J. (2000). A family of drug transporters: The multidrug resistance-associated proteins. J. Natl. Cancer Inst. *92*, 1295–1302.

Brozovic, A., Duran, G.E., Wang, Y.C., Francisco, E.B., and Sikic, B.I. (2015). The miR-200 family differentially regulates sensitivity to paclitaxel and carboplatin in human ovarian carcinoma OVCAR-3 and MES-OV cells. Mol. Oncol. *9*, 1678–1693.

Buchner, J. (1999). Hsp90 and Co. - A holding for folding. Trends Biochem. Sci. *24*, 136–141.

Burris, H.A., Moore, M.J., Andersen, J., Green, M.R., Rothenberg, M.L., Modiano, M.R., Cripps, M.C., Portenoy, R.K., Storniolo, A.M., Tarassoff, P., et al. (1997). Improvements in survival and clinical benefit with gemcitabine as first- line therapy for patients with advanced pancreas cancer: A randomized trial. J. Clin. Oncol. *15*, 2403–2413.

Butler, L.M., Ferraldeschi, R., Armstrong, H.K., Centenera, M.M., and Workman, P. (2015). Maximizing the therapeutic potential of HSP90 inhibitors. Mol. Cancer Res. *13*, 1445–1451.

Byun, S.S., Kim, S.W., Choi, H., Lee, C., and Lee, E. (2005). Augmentation of cisplatin sensitivity in cisplatin-resistant human bladder cancer cells by modulating glutathione concentrations and glutathione-related enzyme activities. BJU Int. *95*, 1086–1090.

Caldas-Lopes, E., Cerchietti, L., Ahn, J.H., Clement, C.C., Robles, A.I., Rodina, A., Moulick, K., Taldone, T., Gozrnan, A., Guo, Y., et al. (2009). Hsp90 inhibitor PU-H71, a multimodal inhibitor of malignancy, induces complete responses in triple-negative breast cancer models. Proc. Natl. Acad. Sci. U. S. A. *106*, 8368–8373.

Caldas, C., Hahn, S.A., da Costa, L.T., Redston, M.S., Schutte, M., Seymour, A.B., Weinstein, C.L., Hruban, R.H., Yeo, C.J., and Kern, S.E. (1994). Frequent somatic mutations and homozygous deletions of the p16 (MTS1) gene in pancreatic adenocarcinoma. Nat. Genet. *8*, 27–32.

Califf, R.M. (2018). Biomarker definitions and their applications. Exp. Biol. Med. *243*, 213–221.

Candido, J.B., Morton, J.P., Bailey, P., Campbell, A.D., Karim, S.A., Jamieson, T., Lapienyte, L., Gopinathan, A., Clark, W., McGhee, E.J., et al. (2018). CSF1R+ Macrophages Sustain Pancreatic Tumor Growth through T Cell Suppression and Maintenance of Key Gene Programs that Define the Squamous Subtype. Cell Rep. *23*, 1448–1460.

Castella, M., Pujol, R., Callén, E., Trujillo, J.P., Casado, J.A., Gille, H., Lach, F.P., Auerbach, A.D., Schindler, D., Benítez, J., et al. (2011). Origin, functional role, and clinical impact of fanconi anemia fanca mutations. Blood *117*, 3759–3769.

Chang, H., Rha, S.Y., Jeung, H.-C., Im, C.-K., Ahn, J.B., Kwon, W.S., Yoo, N.C., Roh, J.K., and Chung, H.C. (2009). Association of the ABCB1 gene polymorphisms 2677G>T/A and 3435C>T with clinical outcomes of paclitaxel monotherapy in metastatic breast cancer patients. Ann. Oncol. *20*, 272–277.

Chee, J.L.Y., Saidin, S., Lane, D.P., Leong, S.M., Noll, J.E., Neilsen, P.M., Phua, Y.T., Gabra, H., and Lim, T.M. (2013). Wild-type and mutant p53 mediate cisplatin resistance through interaction and inhibition of active caspase-9. Cell Cycle *12*, 278–288.

Chen, S.H., and Chang, J.Y. (2019). New insights into mechanisms of cisplatin resistance: From tumor cell to microenvironment. Int. J. Mol. Sci. *20*.

Chen, Y., and Zhang, L. (2017). Members of the microRNA-200 family are promising therapeutic targets in cancer (Review). Exp. Ther. Med. *14*, 10–17.

Chen, B., Zhong, D., and Monteiro, A. (2006). Comparative genomics and evolution of the HSP90 family of genes across all kingdoms of organisms. BMC Genomics *7*, 1–19.

Chen, B., Li, H., Zeng, X., Yang, P., Liu, X., Zhao, X., and Liang, S. (2012). Roles of microRNA on cancer cell metabolism. J. Transl. Med. *10*, 1–12.

Chen, B., Xu, M., Zhang, H., Wang, J. xu, Zheng, P., Gong, L., Wu, G. jue, and Dai, T. (2013). Cisplatin-induced non-apoptotic death of pancreatic cancer cells requires mitochondrial cyclophilin-D-p53 signaling. Biochem. Biophys. Res. Commun. *437*, 526–531.

Chen, D.Q., Huang, J.Y., Feng, B., Pan, B.Z., De, W., Wang, R., and Chen, L.B. (2014). Histone deacetylase 1/Sp1/MicroRNA-200b Signaling accounts for maintenance of cancer stem-like cells in human lung adenocarcinoma. PLoS One *9*, 1–17.

Chen, X., Lu, P., Wu, Y., Wang, D. dan, Zhou, S., Yang, S. jin, Shen, H.Y., Zhang, X. hui, Zhao, J. hua, and Tang, J. hai (2016). MiRNAs-mediated cisplatin resistance in breast cancer. Tumor Biol. *37*, 12905–12913.

Chirnomas, D., Taniguchi, T., De La Vega, M., Vaidya, A.P., Vasserman, M., Hartman, A.R., Kennedy, R., Foster, R., Mahoney, J., Seiden, M. V., et al. (2006). Chemosensitization to cisplatin by inhibitors of the Fanconi anemia/BRCA pathway. Mol. Cancer Ther. *5*, 952–961.

Chisholm, C.L., Wang, H., Wong, A.H.H., Vazquez-Ortiz, G., Chen, W., Xu, X., and Deng, C.X. (2016). Ammonium tetrathiomolybdate treatment targets the copper transporter ATP7A and enhances sensitivity of breast cancer to cisplatin. Oncotarget *7*, 84439–84452.

Choi, Y.C., Yoon, S., Jeong, Y., Yoon, J., and Baek, K. (2011). Regulation of vascular endothelial growth factor signaling by miR-200b. Mol. Cells *32*, 77–82.

Chou, T., and Talalay, P. (1984). Quantitative Dose-Effect Relationships : the Combined Effects of Multiple. Adv Enzym. Regul *22*, 27–55.

Cintron, N.S., and Toft, D. (2006). Defining the requirements for Hsp40 and Hsp70 in the Hsp90 chaperone pathway. J. Biol. Chem. *281*, 26235–26244.

Citri, A., Harari, D., Shohat, G., Ramakrishnan, P., Gan, J., Lavi, S., Eisenstein, M., Kimchi, A., Wallach, D., Pietrokovski, S., et al. (2006). Hsp90 recognizes a common surface on client kinases. J. Biol. Chem. *281*, 14361–14369.

Clegg, L.X., Reichman, M.E., Miller, B.A., Hankey, B.F., Singh, G.K., Lin, Y.D., Goodman, M.T., Lynch, C.F., Schwartz, S.M., Chen, V.W., et al. (2009). Impact of socioeconomic status on cancer incidence and stage at diagnosis: selected findings from the surveillance, epidemiology, and end results: National Longitudinal Mortality Study. Cancer Causes Control *20*, 417–435.

Collisson, E.A., Sadanandam, A., Olson, P., Gibb, W.J., Gu, S., Cooc, J., Weinkle, J., Kim, G.E., Jakkula, L., Feiler, H.S., et al. (2011). Differing Responses to Therapy. Nat Med *17*, 500–503.

Collisson, E.A., Bailey, P., Chang, D.K., and Biankin, A. V. (2019). Molecular subtypes of pancreatic cancer. Nat. Rev. Gastroenterol. Hepatol. *16*, 207–220.

Conroy, T., Desseigne, F., Ychou, M., Bouché, O., Guimbaud, R., Bécouarn, Y., Adenis, A., Raoul, J.-L., Gourgou-Bourgade, S., de la Fouchardière, C., et al. (2011). FOLFIRINOX versus Gemcitabine for Metastatic Pancreatic Cancer. N. Engl. J. Med. *364*, 1817–1825.

Dai, C.H., Li, J., Chen, P., Jiang, H.G., Wu, M., and Chen, Y.C. (2015a). RNA interferences targeting the Fanconi anemia/BRCA pathway upstream genes reverse cisplatin resistance in drug-resistant lung cancer cells. J. Biomed. Sci. *22*, 1–13.

Dai, X., Li, T., Bai, Z., Yang, Y., Liu, X., Zhan, J., and Shi, B. (2015b). Breast cancer intrinsic subtype classification, clinical use and future trends. Am. J. Cancer Res. *5*, 2929–2943.

Danilov, A. V., Neupane, D., Nagaraja, A.S., Feofanova, E. V., Humphries, L.A., DiRenzo, J., and Korc, M. (2011). DeltaNp63alpha-mediated induction of Epidermal growth factor receptor promotes pancreatic cancer cell growth and chemoresistance. PLoS One *6*.

Daoud, A.Z., Mulholland, E.J., Cole, G., and McCarthy, H.O. (2019). MicroRNAs in Pancreatic Cancer: Biomarkers, prognostic, and therapeutic modulators. BMC Cancer *19*, 1–13.

Dasari, S., and Tchounwou, P.B. (2014). Cisplatin in cancer therapy: Molecular mechanisms of action. Eur. J. Pharmacol. *740*, 364–378.

Daunys, S., Matulis, D., and Petrikaitė, V. (2019). Synergistic activity of Hsp90 inhibitors and anticancer agents in pancreatic cancer cell cultures. Sci. Rep. *9*, 1–8.

Davies, M.S., Berners-Price, S.J., and Hambley, T.W. (2000). Slowing of cisplatin aquation in the presence of DNA but not in the presence of phosphate: Improved understanding of sequence selectivity and the roles of monoaquated and diaquated species in the binding of cisplatin to DNA. Inorg. Chem. *39*, 5603–5613.

DeBoer, C., Meulman, P.A., Wnuk, R.J., and Peterson, D.H. (1970). GELDANAMYCIN, A NEW ANTIBIOTIC. J. Antibiot. (Tokyo). *23*, 442–447.

Delmotte, P., and Delmotte-Plaquee, J. (1953). A New Antifungal Substance of Fungal Origin. Nature *171*, 344–344.

Diaferia, G.R., Balestrieri, C., Prosperini, E., Nicoli, P., Spaggiari, P., Zerbi, A., and Natoli, G. (2016). Dissection of transcriptional and cis -regulatory control of differentiation in human pancreatic cancer . EMBO J. *35*, 595–617.

Diaz-Riascos, Z.V., Ginesta, M.M., Fabregat, J., Serrano, T., Busquets, J., Buscail, L., Cordelier, P., and Capellá, G. (2019). Expression and Role of MicroRNAs from the miR-200 Family in the Tumor Formation and Metastatic Propensity of Pancreatic Cancer. Mol. Ther. - Nucleic Acids *17*, 491–503.

Dijk, F., Veenstra, V.L., Soer, E.C., Dings, M.P.G., Zhao, L., Halfwerk, J.B., Hooijer, G.K., Damhofer, H., Marzano, M., Steins, A., et al. (2020). Unsupervised class discovery in pancreatic ductal adenocarcinoma reveals cell-intrinsic mesenchymal features and high concordance between existing classification systems. Sci. Rep. *10*, 1–12.

Dijt, F.J., Fichtinger-Schepman, A.M.J., Berends, F., and Reedijk, J. (1988). Formation and Repair of Cisplatin-Induced Adducts to DNA in Cultured Normal and Repair-deficient Human Fibroblasts. Cancer Res. *48*, 6058–6062.

Dmitriev, O.Y. (2011). Mechanism of tumor resistance to cisplatin mediated by the copper transporter ATP7B. Biochem. Cell Biol. *89*, 138–147.

Do, K., Speranza, G., Chang, L.C., Polley, E.C., Bishop, R., Zhu, W., Trepel, J.B., Lee, S., Lee, M.J., Kinders, R.J., et al. (2015). Phase I study of the heat shock protein 90 (Hsp90) inhibitor onalespib (AT13387) administered on a daily for 2 consecutive days per week dosing schedule in patients with advanced solid tumors. Invest. New Drugs *33*, 921–930.

Dobbelstein, M., and Moll, U. (2014). Targeting tumour-supportive cellular machineries in anticancer drug development. Nat. Rev. Drug Discov. *13*, 179–196.

Dobin, A., Davis, C.A., Schlesinger, F., Drenkow, J., Zaleski, C., Jha, S., Batut, P., Chaisson, M., and Gingeras, T.R. (2013). STAR: Ultrafast universal RNA-seq aligner. Bioinformatics *29*, 15–21.

Dongre, A., and Weinberg, R.A. (2019). New insights into the mechanisms of epithelial–mesenchymal transition and implications for cancer. Nat. Rev. Mol. Cell Biol. *20*, 69–84.

Donnelly, A., and Blagg, B.S.J. (2008). Novobiocin and additional inhibitors of the Hsp90 C-terminal nucleotide-binding pocket. Curr. Med. Chem. *15*, 2702–2717.

Du, Y., Liu, Z., You, L., Hou, P., Ren, X., Jiao, T., Zhao, W., Li, Z., Shu, H., Liu, C., et al. (2017). Pancreatic cancer progression relies upon mutant p53-induced oncogenic signaling mediated by NOP14. Cancer Res. *77*, 2661–2673.

Duan, W., Gao, L., Zhao, W., Leon, M., Sadee, W., Webb, A., Resnick, K., Wu, X., Ramaswamy, B., Cohn, D.E., et al. (2013). Assessment of FANCD2 nuclear foci formation in paraffin-embedded tumors: A potential patient-enrichment strategy for treatment with DNA interstrand crosslinking agents. Transl. Res. *161*, 156–164.

Dutta, R., and Inouye, M. (2000). GHKL , an emergent ATPase / kinase superfamily Rinku Dutta and. Trends Biochem. Sci. *25*, 24–28.

Eastman, A. (1987). Cross-linking of glutathione to DNA by cancer chemotherapeutic platinum coordination complexes. Chem. Biol. Interact. *61*, 241–248.

Echeverria, P.C., Bhattacharya, K., Joshi, A., Wang, T., and Picard, D. (2019). The sensitivity to Hsp90 inhibitors of both normal and oncogenically transformed cells is determined by the equilibrium between cellular quiescence and activity. PLoS One *14*, 1–20.

Echeverría, P.C., Bernthaler, A., Dupuis, P., Mayer, B., and Picard, D. (2011). An interaction network predicted from public data as a discovery tool: Application to the Hsp90 molecular chaperone machine. PLoS One *6*.

El-Khateeb, M., Appleton, T.G., Gahan, L.R., Charles, B.G., Berners-Price, S.J., and Bolton, A.M. (1999). Reactions of cisplatin hydrolytes with methionine, cysteine, and plasma ultrafiltrate studied by a combination of HPLC and NMR techniques. J. Inorg. Biochem. *77*, 13–21.

Ellis, C.A., and Clark, G. (2000). The importance of being K-Ras. Cell. Signal. *12*, 425–434.

Ernst, A., Anders, H., Kapfhammer, H., Orth, M., Hennel, R., Seidl, K., Winssinger, N., Belka, C., Unkel, S., and Lauber, K. (2015). HSP90 inhibition as a means of radiosensitizing resistant, aggressive soft tissue sarcomas. Cancer Lett. *365*, 211–222.

Fang, C. Bin, Wu, H.T., Zhang, M.L., Liu, J., and Zhang, G.J. (2020). Fanconi Anemia Pathway: Mechanisms of Breast Cancer Predisposition Development and Potential Therapeutic Targets. Front. Cell Dev. Biol. *8*, 1–15.

Fang, L., Gao, L., Xie, L., and Xiao, G. (2018). Eukaryotic translation initiation factor 5A-2 involves in doxorubicin-induced epithelial-mesenchymal transition in oral squamous cell carcinoma cells. J. Cancer *9*, 3479–3488.

Ferrarini, M., Heltai, S., Zocchi, M.R., and Rugarli, C. (1992). Unusual expression and localization of heat-shock proteins in human tumor cells. Int. J. Cancer *51*, 613–619.

Ferry, K. V., Hamilton, T.C., and Johnson, S.W. (2000). Increased nucleotide excision repair in cisplatin-resistant ovarian cancer cells: Role of ERCC1-XPF. Biochem. Pharmacol. *60*, 1305–1313.

Fujiwara, M., Izuishi, K., Sano, T., Hossain, M.A., Kimura, S., Masaki, T., and Suzuki, Y. (2008). Modulating effect of the PI3-kinase inhibitor LY294002 on cisplatin in human pancreatic cancer cells. J. Exp. Clin. Cancer Res. *27*, 1–9.

Funamizu, N., Ray Lacy, C., Kamada, M., Yanaga, K., and Manome, Y. (2019). MicroRNA-200b and -301 are associated with gemcitabine response as biomarkers in pancreatic carcinoma cells. Int. J. Oncol. *54*, 991–1000.

Gaponova, A. V, Nikonova, A.S., Deneka, A.Y., Kopp, M.C., Kudinov, A.E., Skobeleva, N., Khazak, V., Ogawa, L.S., Cai, K.Q., Duncan, K.E., et al. (2016). A Novel HSP90 Inhibitor–Drug Conjugate to SN38 Is Highly Effective in Small Cell Lung Cancer. Clin. Cancer Res. *22*, 5120–5129.

Garnett, W.R. (1986). Diphenhydramine. Am. Pharm. *26*, 35–40.

Garon, E.B., Finn, R.S., Hamidi, H., Dering, J., Pitts, S., Kamranpour, N., Desai, A.J., Hosmer, W., Ide, S., Avsar, E., et al. (2013). The HSP90 inhibitor NVP-AUY922 potently inhibits non-small cell lung cancer growth. Mol. Cancer Ther. *12*, 890–900.

Georgakopoulos-Soares, I., Chartoumpekis, D. V., Kyriazopoulou, V., and Zaravinos, A. (2020). EMT Factors and Metabolic Pathways in Cancer. Front. Oncol. *10*, 1–20.

Gibalová, L., Šereš, M., Rusnák, A., Ditte, P., Labudová, M., Uhrík, B., Pastorek, J., Sedlák, J., Breier, A., and Sulová, Z. (2012). P-glycoprotein depresses cisplatin sensitivity in L1210 cells by inhibiting cisplatin-induced caspase-3 activation. Toxicol. Vitr. *26*, 435–444.

Goetze, R.G., Buchholz, S.M., Patil, S., Petzold, G., Ellenrieder, V., Hessmann, E., and Neesse, A. (2018). Utilizing high resolution ultrasound to monitor tumor onset and growth in genetically engineered pancreatic cancer models. J. Vis. Exp. *2018*.

Golan, T., Hammel, P., Reni, M., Van Cutsem, E., Macarulla, T., Hall, M.J., Park, J., Hochhauser, D., Arnold, D., Oh, D.-Y., et al. (2019). Maintenance Olaparib for Germline BRCA -Mutated Metastatic Pancreatic Cancer. N. Engl. J. Med. *381*, 317–327.

Grbovic-Huezo, O., Pitter, K.L., Lecomte, N., Saglimbeni, J., Askan, G., Holm, M., Melchor, J.P., Chandwani, R., Joshi, S., Haglund, C., et al. (2020). Unbiased in vivo preclinical evaluation of anticancer drugs identifies effective therapy for the treatment of pancreatic adenocarcinoma. Proc. Natl. Acad. Sci. U. S. A. *117*, 30670–30678.

Grimson, A., Farh, K.K.H., Johnston, W.K., Garrett-Engele, P., Lim, L.P., and Bartel, D.P. (2007). MicroRNA Targeting Specificity in Mammals: Determinants beyond Seed Pairing. Mol. Cell *27*, 91–105.

Guminski, A.D., Balleine, R.L., Chiew, Y.E., Webster, L.R., Tapner, M., Farrell, G.C., Harnett, P.R., and DeFazio, A. (2006). MRP2 (ABCC2) and cisplatin sensitivity in hepatocytes and human ovarian carcinoma. Gynecol. Oncol. *100*, 239–246.

Guo, J., Xie, K., and Zheng, S. (2016). Molecular Biomarkers of Pancreatic Intraepithelial Neoplasia and Their Implications in Early Diagnosis and Therapeutic Intervention of Pancreatic Cancer. Int. J. Biol. Sci. *12*, 292–301.

Hahn, S.A., Schutte, M., Hoque, A.T.M.S., Moskaluk, C.A., da Costa, L.T., Rozenblum, E., Weinstein, C.L., Fischer, A., Yeo, C.J., Hruban, R.H., et al. (1996). DPC4, A Candidate Tumor Suppressor Gene at Human Chromosome 18q21.1. Science (80-.). *271*, 350–353.

Hainzl, O., Lapina, M.C., Buchner, J., and Richter, K. (2009). The charged linker region is an important regulator of Hsp90 function. J. Biol. Chem. *284*, 22559–22567.

Hambley, T.W. (1997). The influence of structure on the activity and toxicity of Pt anti-cancer drugs. Coord. Chem. Rev. *166*, 181–223.

Hammond, S.M. (2015). An overview of microRNAs. Adv. Drug Deliv. Rev. *87*, 3–14.

Hanahan, D., and Weinberg, R.A. (2000). The Hallmarks of Cancer Review Douglas. Cell *100*, 57–70.

Harris, S.F., Shiau, A.K., and Agard, D.A. (2004). The crystal structure of the carboxy-terminal dimerization domain of htpG, the Escherichia coli Hsp90, reveals a potential substrate binding site. Structure *12*, 1087–1097.

Hartl, F.U., Bracher, A., and Hayer-Hartl, M. (2011). Molecular chaperones in protein folding and proteostasis. Nature *475*, 324–332.

Hashimoto, S., Anai, H., and Hanada, K. (2016). Mechanisms of interstrand DNA crosslink repair and human disorders. Genes Environ. *38*, 1–8.

Hashimoto, Y., Akiyama, Y., and Yuasa, Y. (2013). Multiple-to-Multiple Relationships between MicroRNAs and Target Genes in Gastric Cancer. PLoS One *8*.

He, C., Sun, Z., Hoffman, R.M., Yang, Z., Jiang, Y., Wang, L., and Hao, Y. (2019). P-glycoprotein overexpression is associated with cisplatin resistance in human osteosarcoma. Anticancer Res. *39*, 1711–1718.

Heinemann, V., Quietzsch, D., Gieseler, F., Gonnermann, M., Schönekäs, H., Rost, A., Neuhaus, H., Haag, C., Clemens, M., Heinrich, B., et al. (2006). Randomized phase III trial of gemcitabine plus cisplatin compared with gemcitabine alone in advanced pancreatic cancer. J. Clin. Oncol. *24*, 3946–3952.

Higby, D.J., Higby, D.J., Wallace, H.J., Albert, D.J., and Holland, J.F. (1974). Diaminodichloroplatinum: A phase I study showing responses in testicular and other tumors. Cancer *33*, 1219–1225.

Hingorani, S.R., Petricoin, E.F., Maitra, A., Rajapakse, V., King, C., Jacobetz, M.A., Ross, S., Conrads, T.P., Veenstra, T.D., Hitt, B.A., et al. (2003). Preinvasive and invasive ductal pancreatic cancer and its early detection in the mouse. Cancer Cell *4*, 437–450.

Hingorani, S.R., Wang, L., Multani, A.S., Combs, C., Deramaudt, T.B., Hruban, R.H., Rustgi, A.K., Chang, S., and Tuveson, D.A. (2005). Trp53R172H and KrasG12D cooperate to promote chromosomal instability and widely metastatic pancreatic ductal adenocarcinoma in mice. Cancer Cell *7*, 469–483.

Hishikawa, Y., Abe, S., Kinugasa, S., Yoshimura, H., Monden, N., Igarashi, M., Tachibana, M., and Nagasue, N. (1997). Overexpression of Metallothionein Correlates with Chemoresistance to Cisplatin and Prognosis in Esophageal Cancer. Oncology *54*, 342–347.

Hobbs, G.S., Hanasoge Somasundara, A.V., Kleppe, M., Litvin, R., Arcila, M., Ahn, J., McKenney, A.S., Knapp, K., Ptashkin, R., Weinstein, H., et al. (2018). Hsp90 inhibition disrupts JAK-STAT signaling and leads to reductions in splenomegaly in patients with myeloproliferative neoplasms. Haematologica *103*, e5–e9.

Von Hoff, D.D., Ervin, T., Arena, F.P., Chiorean, E.G., Infante, J., Moore, M., Seay, T., Tjulandin, S.A., Ma, W.W., Saleh, M.N., et al. (2013). Increased Survival in Pancreatic Cancer with nab-Paclitaxel plus Gemcitabine. N. Engl. J. Med. *369*, 1691–1703.

Hollstein, M. (1994). Database of p53 and cell lines. Nucleic Acids Res. *22*, 3551–3555.

Holzer, A.K., Manorek, G.H., and Howell, S.B. (2006). Contribution of the major copper influx transporter CTR1 to the cellular accumulation of cisplatin, carboplatin, and oxaliplatin. Mol. Pharmacol. *70*, 1390–1394.

Hong, D.S., Banerji, U., Tavana, B., George, G.C., Aaron, J., and Kurzrock, R. (2013). Targeting the molecular chaperone heat shock protein 90 (HSP90): Lessons learned and future directions. Cancer Treat. Rev. *39*, 375–387.

Hoter, A., El-Sabban, M.E., and Naim, H.Y. (2018). The HSP90 family: Structure, regulation, function, and implications in health and disease. Int. J. Mol. Sci. *19*.

Hruban, R.H., Goggins, M., Parsons, J., and Kern, S.E. (2000). Progression model for pancreatic cancer. Clin. Cancer Res. *6*, 2969–2972.

Hruban, R.H., Adsay, N.V., Albores–Saavedra, J., Compton, C., Garrett, E.S., Goodman, S.N., Kern, S.E., Klimstra, D.S., Klöppel, G., Longnecker, D.S., et al. (2001). Pancreatic Intraepithelial Neoplasia. Am. J. Surg. Pathol. *25*, 579–586.

Huang, D., Duan, H., Huang, H., Tong, X., Han, Y., Ru, G., Qu, L., Shou, C., and Zhao, Z. (2016). Cisplatin resistance in gastric cancer cells is associated with HER2 upregulation-induced epithelial-mesenchymal transition. Sci. Rep. *6*, 1–12.

Humphries, B., and Yang, C. (2015). The microRNA-200 family: Small molecules with novel roles in cancer development, progression and therapy. Oncotarget *6*, 6472–6498.

Jacobson, C., Kopp, N., Layer, J. V., Redd, R.A., Tschuri, S., Haebe, S., Van Bodegom, D., Bird, L., Christie, A.L., Christodoulou, A., et al. (2016). HSP90 inhibition overcomes ibrutinib resistance in mantle cell lymphoma. Blood *128*, 2517–2526.

Jameson, G.S., Borazanci, E., Babiker, H.M., Poplin, E., Niewiarowska, A.A., Gordon, M.S., Barrett, M.T., Rosenthal, A., Stoll-D'Astice, A., Crowley, J., et al. (2020). Response Rate Following Albumin-Bound Paclitaxel Plus Gemcitabine Plus Cisplatin Treatment among Patients with Advanced Pancreatic Cancer: A Phase 1b/2 Pilot Clinical Trial. JAMA Oncol. *6*, 125–132.

Jiao, Y., Ou, W., Meng, F., Zhou, H., and Wang, A. (2011). Targeting HSP90 in ovarian cancers with multiple receptor tyrosine kinase coactivation. Mol. Cancer *10*, 1–12.

Jin, H.F., Wang, J.F., Song, T.T., Zhang, J., and Wang, L. (2020). MiR-200b Inhibits Tumor Growth and Chemoresistance via Targeting p70S6K1 in Lung Cancer. Front. Oncol. *10*, 1–9.

Johnson, J.L. (2012). Evolution and function of diverse Hsp90 homologs and cochaperone proteins. Biochim. Biophys. Acta - Mol. Cell Res. *1823*, 607–613.

Jones, S., Zhang, X., Parsons, D.W., Lin, J.C.H., Leary, R.J., Angenendt, P., Mankoo, P., Carter, H., Kamiyama, H., Jimeno, A., et al. (2008). Core signaling pathways in human pancreatic cancers revealed by global genomic analyses. Science (80-.). *321*, 1801–1806.

Kalluri, R., and Weinberg, R.A. (2009). The basics of epithelial-mesenchymal transition. J. Clin. Invest. *119*, 1420–1428.

Kamal, A., Thao, L., Sensintaffar, J., Zhang, L., Boehm, M.F., Fritz, L.C., and Burrows, F.J. (2003). A high-affinity conformation of Hsp90 confers tumour selectivity on Hsp90 inhibitors. Nature *425*, 407–410.

Kee, Y., and D'Andrea, A.D. (2010). Expanded roles of the Fanconi anemia pathway in preserving genomic stability. Genes Dev. *24*, 1680–1694.

Keitel, U., Scheel, A., Thomale, J., Halpape, R., Kaulfuß, S., Scheel, C., and Dobbelstein, M. (2014). Bcl-xL mediates therapeutic resistance of a mesenchymal breast cancer cell subpopulation. Oncotarget *5*, 11778–11791.

Kenneth Allan, R., and Ratajczak, T. (2011). Versatile TPR domains accommodate different modes of target protein recognition and function. Cell Stress Chaperones *16*, 353–367.

Kijima, T., Prince, T.L., Tigue, M.L., Yim, K.H., Schwartz, H., Beebe, K., Lee, S., Budzynski, M.A., Williams, H., Trepel, J.B., et al. (2018). HSP90 inhibitors disrupt a transient HSP90-HSF1 interaction and identify a noncanonical model of HSP90-mediated HSF1 regulation. Sci. Rep. *8*, 1–13.

Kim, R., Tanabe, K., Uchida, Y., Emi, M., Inoue, H., and Toge, T. (2002). Current status of the molecular mechanisms of anticancer drug-induced apoptosis: The contribution of molecular-level analysis to cancer chemotherapy. Cancer Chemother. Pharmacol. *50*, 343–352.

Kimura, T., and Kambe, T. (2016). The functions of metallothionein and ZIP and ZnT transporters: An overview and perspective. Int. J. Mol. Sci. *17*, 10–12.

Klameth, L., Rath, B., and Hamilton, G. (2017). In vitro cytotoxic activities of the oral platinum(IV) prodrug oxoplatin and HSP90 inhibitor ganetespib against a panel of gastric cancer cell lines. J. Cancer *8*, 1733–1743.

Kleeff, J., Korc, M., Apte, M., La Vecchia, C., Johnson, C.D., Biankin, A. V., Neale, R.E., Tempero, M., Tuveson, D.A., Hruban, R.H., et al. (2016). Pancreatic cancer. Nat. Rev. Dis. Prim. *2*, 1–23.

Klemke, L., De Oliveira, T., Witt, D., Winkler, N., Bohnenberger, H., Bucala, R., Conradi, L.C., and Schulz-Heddergott, R. (2021). Hsp90-stabilized MIF supports tumor progression via macrophage recruitment and angiogenesis in colorectal cancer. Cell Death Dis. *12*.

Kloesch, B., Ionasz, V., Paliwal, S., Hruschka, N., Martinez De Villarreal, J., Öllinger, R., Mueller, S., Dienes, H.P., Schindl, M., Gruber, E.S., et al. (2021). A GATA6-centred gene regulatory network involving HNFs and ΔNp63 controls plasticity and immune escape in pancreatic cancer. Gut 1–12.

Kool, M., Haa, M. De, Scheffer, G.L., Scheper, R.J., Eijk, M.J.T. Van, and Juijn, J. a (1997). of the Multidrug Resistance-associated Protein Gene (MRP1), in Human Cancer Cell Lines1. Cancer Res. *57*, 3537–3547.

Korpal, M., Lee, E.S., Hu, G., and Kang, Y. (2008). The miR-200 family inhibits epithelial-mesenchymal transition and cancer cell migration by direct targeting of E-cadherin transcriptional repressors ZEB1 and ZEB2. J. Biol. Chem. *283*, 14910–14914.

Kramer, D., Stark, N., Schulz-Heddergott, R., Erytch, N., Edmunds, S., Roßmann, L., Bastians, H., Concin, N., Moll, U.M., and Dobbelstein, M. (2017). Strong antitumor synergy between DNA crosslinking and HSP90 inhibition causes massive premitotic DNA fragmentation in ovarian cancer cells. Cell Death Differ. *24*, 300–316.

Krizkova, S., Fabrik, I., Huska, D., Adam, V., Babula, P., Hrabeta, J., Eckschlager, T., Pochop, P., Darsova, D., Kukacka, J., et al. (2010). An adsorptive transfer technique coupled with brdicka reaction to reveal the importance of metallothionein in chemotherapy with platinum based cytostatics. Int. J. Mol. Sci. *11*, 4826–4842.

Kumar, P., Devaki, B., Jonnala, U.K., and Amere Subbarao, S. (2020). Hsp90 facilitates acquired drug resistance of tumor cells through cholesterol modulation however independent of tumor progression. Biochim. Biophys. Acta - Mol. Cell Res. *1867*.

Kuo, M.T., and Chen, H.H.W. (2010). Role of glutathione in the regulation of cisplatin resistance in cancer chemotherapy. Met. Based. Drugs *2010*.

Kurashige, J., Kamohara, H., Watanabe, M., Hiyoshi, Y., Iwatsuki, M., Tanaka, Y., Kinoshita, K., Saito, S., Baba, Y., and Baba, H. (2012). MicroRNA-200b regulates cell proliferation, invasion, and migration by directly targeting ZEB2 in gastric carcinoma. Ann. Surg. Oncol. *19*, 656–664.

Lackie, R.E., Maciejewski, A., Ostapchenko, V.G., Marques-Lopes, J., Choy, W.Y., Duennwald, M.L., Prado, V.F., and Prado, M.A.M. (2017). The Hsp70/Hsp90 chaperone machinery in neurodegenerative diseases. Front. Neurosci. *11*, 1–23.

Lamb, J.R., Tugendreich, S., and Hieter, P. (1995). Tetratrico peptide repeat interactions: to TPR or not to TPR? Trends Biochem. Sci. *20*, 257–259.

Larue, L., and Bellacosa, A. (2005). Epithelial-mesenchymal transition in development and cancer: Role of phosphatidylinositol 3′ kinase/AKT pathways. Oncogene *24*, 7443–7454.

Lazenby, M., Hills, R., Burnett, A.K., and Zabkiewicz, J. (2015). The HSP90 inhibitor ganetespib: A potential effective agent for Acute Myeloid Leukemia in combination with cytarabine. Leuk. Res. *39*, 617–624.

Lee, J.W., Komar, C.A., Bengsch, F., Graham, K., and Beatty, G.L. (2016). Genetically Engineered Mouse Models of Pancreatic Cancer: The KPC Model (LSL-Kras G12D/+ ;LSL-Trp53 R172H/+ ;Pdx-1-Cre), Its Variants, and Their Application in Immuno-oncology Drug Discovery. Curr. Protoc. Pharmacol. *73*, 2089–2103.

Li, D., Marchenko, N.D., Schulz, R., Fischer, V., Velasco-Hernandez, T., Talos, F., and Moll, U.M. (2011). Functional inactivation of endogenous MDM2 and CHIP by HSP90 causes aberrant stabilization of mutant p53 in human cancer cells. Mol. Cancer Res. *9*, 577–588.

Li, H., Handsaker, B., Wysoker, A., Fennell, T., Ruan, J., Homer, N., Marth, G., Abecasis, G., and Durbin, R. (2009). The Sequence Alignment/Map format and SAMtools. Bioinformatics *25*, 2078–2079.

Liao, T.T., and Yang, M.H. (2017). Revisiting epithelial-mesenchymal transition in cancer metastasis: the connection between epithelial plasticity and stemness. Mol. Oncol. *11*, 792–804.

Liedert, B., Pluim, D., Schellens, J., and Thomale, J. (2006). Adduct-specific monoclonal antibodies for the measurement of cisplatin-induced DNA lesions in individual cell nuclei. Nucleic Acids Res. *34*.

Lim, Y.Y., Wright, J.A., Attema, J.L., Gregory, P.A., Bert, A.G., Smith, E., Thomas, D., Lopez, A.F., Drew, P.A., Khew-Goodall, Y., et al. (2013). Epigenetic modulation of the miR-200 family is associated with transition to a breast cancer stem-celllike state. J. Cell Sci. *126*, 2256–2266.

Lin, K., Rockliffe, N., Johnson, G.G., Sherrington, P.D., and Pettitt, A.R. (2008a). Hsp90 inhibition has opposing effects on wild-type and mutant p53 and induces p21 expression and cytotoxicity irrespective of p53/ATM status in chronic lymphocytic leukaemia cells. Oncogene *27*, 2445–2455.

Lin, T.Y., Bear, M., Du, Z., Foley, K.P., Ying, W., Barsoum, J., and London, C. (2008b). The novel HSP90 inhibitor STA-9090 exhibits activity against Kit-dependent and -independent malignant mast cell tumors. Exp. Hematol. *36*, 1266–1277.

Liu, K., Ling, S., and Lin, W.-C. (2011). TopBP1 Mediates Mutant p53 Gain of Function through NF-Y and p63/p73. Mol. Cell. Biol. *31*, 4464–4481.

Liu, W., Palovcak, A., Li, F., Zafar, A., Yuan, F., and Zhang, Y. (2020). Fanconi anemia pathway as a prospective target for cancer intervention. Cell Biosci. *10*, 1–14.

Liu, Y., Bernauer, A.M., Yingling, C.M., and Belinsky, S.A. (2012). HIF1α regulated expression of XPA contributes to cisplatin resistance in lung cancer. Carcinogenesis *33*, 1187–1192.

Long, F., Liu, W., Jia, P., Wang, H., Jiang, G., and Wang, T. (2018). HIF-1α-induced autophagy contributes to cisplatin resistance in ovarian cancer cells. Pharmazie *73*, 533–536.

Love, M.I., Huber, W., and Anders, S. (2014). Moderated estimation of fold change and dispersion for RNA-seq data with DESeq2. Genome Biol. *15*, 1–21.

Lu, Y., Lu, J., Li, X., Zhu, H., Fan, X., Zhu, S., Wang, Y., Guo, Q., Wang, L., Huang, Y., et al. (2014). MiR-200a inhibits epithelial-mesenchymal transition of pancreatic cancer stem cell. BMC Cancer *14*.

Lukanović, D., Herzog, M., Kobal, B., and Černe, K. (2020). The contribution of copper efflux transporters ATP7A and ATP7B to chemoresistance and personalized medicine in ovarian cancer. Biomed. Pharmacother. *129*.

MacFarlane, L.-A., and R. Murphy, P. (2010). MicroRNA: Biogenesis, Function and Role in Cancer. Curr. Genomics *11*, 537–561.

Mahalingam, D., Swords, R., Carew, J.S., Nawrocki, S.T., Bhalla, K., and Giles, F.J. (2009). Targeting HSP90 for cancer therapy. Br. J. Cancer *100*, 1523–1529.

Mangala, L.S., Zuzel, V., Schmandt, R., Leshane, E.S., Halder, J.B., Armaiz-Pena, G.N., Spannuth, W.A., Tanaka, T., Shahzad, M.M.K., Lin, Y.G., et al. (2009). Therapeutic targeting of ATP7B in ovarian carcinoma. Clin. Cancer Res. *15*, 3770–3780.

Martin, H.C., Wani, S., Steptoe, A.L., Krishnan, K., Nones, K., Nourbakhsh, E., Vlassov, A., Grimmond, S.M., and Cloonan, N. (2014). Imperfect centered miRNA binding sites are common and can mediate repression of target mRNAs. Genome Biol. *15*.

Martinelli, P., Carrillo-De Santa Pau, E., Cox, T., Sainz, B., Dusetti, N., Greenhalf, W., Rinaldi, L., Costello, E., Ghaneh, P., Malats, N., et al. (2017). GATA6 regulates EMT and tumour dissemination, and is a marker of response to adjuvant chemotherapy in pancreatic cancer. Gut *66*, 1665–1676.

Martinez-Balibrea, E., Martínez-Cardús, A., Musulén, E., Ginés, A., Manzano, J.L., Aranda, E., Plasencia, C., Neamati, N., and Abad, A. (2009). Increased levels of copper efflux transporter ATP7B are associated with poor outcome in colorectal cancer patients receiving oxaliplatin-based chemotherapy. Int. J. Cancer *124*, 2905–2910.

Martinez-Rivera, M., and Siddik, Z.H. (2012). Resistance and gain-of-resistance phenotypes in cancers harboring wild-type p53. Biochem. Pharmacol. *83*, 1049–1062.

Marzec, M., Eletto, D., and Argon, Y. (2012). GRP94: An HSP90-like protein specialized for protein folding and quality control in the endoplasmic reticulum. Biochim. Biophys. Acta - Mol. Cell Res. *1823*, 774–787.

Masoud, G.N., and Li, W. (2015). HIF-1α pathway: Role, regulation and intervention for cancer therapy. Acta Pharm. Sin. B *5*, 378–389.

Materna, V., Liedert, B., Thomale, J., and Lage, H. (2005). Protection of platinum-DNA adduct formation and reversal of cisplatin resistance by anti-MRP2 hammerhead ribozymes in human cancer cells. Int. J. Cancer *115*, 393–402.

Mayer, M.P., and Le Breton, L. (2015). Hsp90: Breaking the symmetry. Mol. Cell *58*, 8–20.

Mazaira, G.I., Camisay, M.F., De Leo, S., Erlejman, A.G., and Galigniana, M.D. (2016). Biological relevance of Hsp90-binding immunophilins in cancer development and treatment. Int. J. Cancer *138*, 797–808.

McCabe, K.M., Olson, S.B., and Moses, R.E. (2009). DNA interstrand crosslink repair in mammalian cells. J. Cell. Physiol. *220*, 569–573.

McKeage, M.J. (1995). Comparative Adverse Effect Profiles of Platinum Drugs. Drug Saf. *13*, 228–244.

McLaughlin, M., Barker, H.E., Khan, A.A., Pedersen, M., Dillon, M., Mansfield, D.C., Patel, R., Kyula, J.N., Bhide, S.A., Newbold, K.L., et al. (2017). HSP90 inhibition sensitizes head and neck cancer to platin-based chemoradiotherapy by modulation of the DNA damage response resulting in chromosomal fragmentation. BMC Cancer *17*, 1–13.

McLaughlin, S.H., Sobott, F., Yao, Z.P., Zhang, W., Nielsen, P.R., Grossmann, J.G., Laue, E.D., Robinson, C. V., and Jackson, S.E. (2006). The co-chaperone p23 arrests the Hsp90 ATPase cycle to trap client proteins. J. Mol. Biol. *356*, 746–758.

McMillan, D.R., Xiao, X., Shao, L., Graves, K., and Benjamin, I.J. (1998). Targeted disruption of heat shock transcription factor 1 abolishes thermotolerance and protection against heat-inducible apoptosis. J. Biol. Chem. *273*, 7523–7528.

Melnikova, M., Wauer, U.S., Mendus, D., Hilger, R.A., Oliver, T.G., Mercer, K., Gohlke, B.O., Erdmann, K., Niederacher, D., Neubauer, H., et al. (2020). Diphenhydramine increases the therapeutic window for platinum drugs by simultaneously sensitizing tumor cells and protecting normal cells. Mol. Oncol. *14*, 686–703.

Mezencev, R., Matyunina, L. V., Wagner, G.T., and McDonald, J.F. (2016). Acquired resistance of pancreatic cancer cells to cisplatin is multifactorial with cell context-dependent involvement of resistance genes. Cancer Gene Ther. *23*, 446–453.

Micalizzi, D.S., and Ford, H.L. (2009). Epithelial–mesenchymal transition in development and cancer. Futur. Oncol. *5*, 1129–1143.

Michel, O., Kulbacka, J., Saczko, J., Mączyńska, J., Blasiak, P., Rossowska, J., and Rzechonek, A. (2018). Electroporation with cisplatin against metastatic pancreatic cancer: In vitro study on human primary cell culture. Biomed Res. Int. *2018*.

Michl, J., Zimmer, J., and Tarsounas, M. (2016). Interplay between Fanconi anemia and homologous recombination pathways in genome integrity. EMBO J. *35*, 909–923.

Millson, S.H., Truman, A.W., Rácz, A., Hu, B., Panaretou, B., Nuttall, J., Mollapour, M., Söti, C., and Piper, P.W. (2007). Expressed as the sole Hsp90 of yeast, the α and β isoforms of human Hsp90 differ with regard to their capacities for activation of certain client proteins, whereas only Hsp90β generates sensitivity to the Hsp90 inhibitor radicicol. FEBS J. *274*, 4453–4463.

Miyashita, H., Nitta, Y., Mori, S., Kanzaki, A., Nakayama, K., Terada, K., Sugiyama, T., Kawamura, H., Sato, A., Morikawa, H., et al. (2003). Expression of copper-transporting P-type adenosine triphosphatase (ATP7B) as a chemoresistance marker in human oral squamous cell carcinoma treated with cisplatin. Oral Oncol. *39*, 157–162.

Miyata, Y., Nakamoto, H., and Neckers, L. (2013). The Therapeutic Target Hsp90 and Cancer Hallmarks. Curr. Pharm. Des. *19*, 347–365.

Moffitt, R.A., Marayati, R., Flate, E.L., Volmar, K.E., Loeza, S.G.H., Hoadley, K.A., Rashid, N.U., Williams, L.A., Eaton, S.C., Chung, A.H., et al. (2015). Virtual microdissection identifies distinct tumor- and stroma-specific subtypes of pancreatic ductal adenocarcinoma. Nat. Genet. *47*, 1168–1178.

Mongroo, P.S., and Rustgi, A.K. (2010). The role of the miR-200 family in epithelial-mesenchymal transition. 219–222.

Morris, J.P., Wang, S.C., and Hebrok, M. (2010). KRAS, Hedgehog, Wnt and the twisted developmental biology of pancreatic ductal adenocarcinoma. Nat. Rev. Cancer *10*, 683–695.

Müller, P., Ceskova, P., and Vojtesek, B. (2005). Hsp90 is essential for restoring cellular functions of temperature- sensitive p53 mutant protein but not for stabilization and activation of wild-type p53: Implications for cancer therapy. J. Biol. Chem. *280*, 6682–6691.

Nagai, H., and Kim, Y.H. (2017). Cancer prevention from the perspective of global cancer burden patterns. J. Thorac. Dis. *9*, 448–451.

Nagaraju, G.P., Alese, O.B., Landry, J., Diaz, R., and El-Rayes, B.F. (2014). HSP90 inhibition downregulates thymidylate synthase and sensitizes colorectal cancer cell lines to the effect of 5FU-based chemotherapy. Oncotarget *5*, 9980–9991.

Nagaraju, G.P., Zakka, K.M., Landry, J.C., Shaib, W.L., Lesinski, G.B., and El-Rayes, B.F. (2019). Inhibition of HSP90 overcomes resistance to chemotherapy and radiotherapy in pancreatic cancer. Int. J. Cancer *145*, 1529–1537.

Nakagawa, T., Inoue, Y., Kodama, H., Yamazaki, H., Kawai, K., Suemizu, H., Masuda, R., Iwazaki, M., Yamada, S., Ueyama, Y., et al. (2008). Expression of copper-transporting P-type adenosine triphosphatase (ATP7B) correlates with cisplatin resistance in human non-small cell lung cancer xenografts. Oncol. Rep. *20*, 265–270.

Nakanishi, K., Yang, Y.G., Pierce, A.J., Taniguchi, T., Digweed, M., D'Andréa, A.D., Wang, Z.Q., and Jasin, M. (2005). Human Fanconi anemia monoubiquitination pathway promotes homologous DNA repair. Proc. Natl. Acad. Sci. U. S. A. *102*, 1110–1115.

Neves, R., Scheel, C., Weinhold, S., Honisch, E., Iwaniuk, K.M., Trompeter, H.I., Niederacher, D., Wernet, P., Santourlidis, S., and Uhrberg, M. (2010). Role of DNA methylation in miR-200c/141 cluster silencing in invasive breast cancer cells. BMC Res. Notes *3*, 7–10.

Niknafs, N., Zhong, Y., Moral, J.A., Zhang, L., Shao, M.X., Lo, A., Makohon-Moore, A., Iacobuzio-Donahue, C.A., and Karchin, R. (2019). Characterization of genetic subclonal evolution in pancreatic cancer mouse models. Nat. Commun. *10*, 1–10.

Niraj, J., Färkkilä, A., and D'Andrea, A.D. (2019). The Fanconi Anemia Pathway in Cancer. Annu. Rev. Cancer Biol. *3*, 457–478.

O'Brien, M.A., and Kirby, R. (2008). Apoptosis: A review of pro-apoptotic and anti-apoptotic pathways and dysregulation in disease. J. Vet. Emerg. Crit. Care *18*, 572–585.

O'Brien, S.J., Carter, J. V., Burton, J.F., Oxford, B.G., Schmidt, M.N., Hallion, J.C., and Galandiuk, S. (2018). The role of the miR-200 family in epithelial–mesenchymal transition in colorectal cancer: a systematic review. Int. J. Cancer *142*, 2501–2511.

O'Kane, G.M., Grunwald, B.T., Jang, G.H., Masoomian, M., Picardo, S., Grant, R.C., Denroche, R.E., Zhang, A., Wang, Y., Lam, B., et al. (2020). GATA6 Expression Distinguishes Classical and Basal-like Subtypes in Advanced Pancreatic Cancer. Clin. Cancer Res. *26*, 4901–4910.

O'Reilly, E.M., Lee, J.W., Zalupski, M., Capanu, M., Park, J., Golan, T., Tahover, E., Lowery, M.A., Chou, J.F., Sahai, V., et al. (2020). Randomized, multicenter, phase II trial of gemcitabine and cisplatin with or without veliparib in patients with pancreas adenocarcinoma and a germline BRCA/ PALB2 mutation. J. Clin. Oncol. *38*, 1378–1388.

Oettle, H., Neuhaus, P., Hochhaus, A., Hartmann, J.T., Gellert, K., Ridwelski, K., Niedergethmann, M., Zülke, C., Fahlke, J., Arning, M.B., et al. (2013). Adjuvant chemotherapy with gemcitabine and long-term outcomes among patients with resected pancreatic cancer: The CONKO-001 randomized trial. JAMA - J. Am. Med. Assoc. *310*, 1473–1481.

Olive, K.P., and Tuveson, D.A. (2006). The use of targeted mouse models for preclinical testing of novel cancer therapeutics. Clin. Cancer Res. *12*, 5277–5287.

Ono, N., Yamazaki, T., Tsukaguchi, T., Fujii, T., Sakata, K., Suda, A., Tsukuda, T., Mio, T., Ishii, N., Kondoh, O., et al. (2013). Enhanced antitumor activity of erlotinib in combination with the Hsp90 inhibitor CH5164840 against non-small-cell lung cancer. Cancer Sci. *104*, 1346–1352.

Orth, M., Metzger, P., Gerum, S., Mayerle, J., Schneider, G., Belka, C., Schnurr, M., and Lauber, K. (2019). Pancreatic ductal adenocarcinoma: Biological hallmarks, current status, and future perspectives of combined modality treatment approaches. Radiat. Oncol. *14*, 1–20.

Orth, M., Albrecht, V., Seidl, K., Kinzel, L., Unger, K., Hess, J., Kreutzer, L., Sun, N., Stegen, B., Nieto, A., et al. (2021). Inhibition of HSP90 as a Strategy to Radiosensitize Glioblastoma: Targeting the DNA Damage Response and Beyond. Front. Oncol. *11*, 1–15.

Pan, S.T., Li, Z.L., He, Z.X., Qiu, J.X., and Zhou, S.F. (2016). Molecular mechanisms for tumour resistance to chemotherapy. Clin. Exp. Pharmacol. Physiol. *43*, 723–737.

Panaretou, B., Siligardi, G., Meyer, P., Maloney, A., Sullivan, J.K., Singh, S., Millson, S.H., Clarke, P.A., Naaby-Hansen, S., Stein, R., et al. (2002). Activation of the ATPase activity of Hsp90 by the stress-regulated cochaperone Aha1. Mol. Cell *10*, 1307–1318.

Park, J.H., and Shin, C. (2014). MicroRNA-directed cleavage of targets: Mechanism and experimental approaches. BMB Rep. *47*, 417–423.

Park, H.K., Yoon, N.G., Lee, J.E., Hu, S., Yoon, S., Kim, S.Y., Hong, J.H., Nam, D., Chae, Y.C., Park, J.B., et al. (2020). Unleashing the full potential of Hsp90 inhibitors as cancer therapeutics through simultaneous inactivation of Hsp90, Grp94, and TRAP1. Exp. Mol. Med. *52*, 79–91.

Park, S.M., Gaur, A.B., Lengyel, E., and Peter, M.E. (2008). The miR-200 family determines the epithelial phenotype of cancer cells by targeting the E-cadherin repressors ZEB1 and ZEB2. Genes Dev. *22*, 894–907.

Pathy, K. (2018). Antihistamine Drugs Possess some Antiacetylcholine Properties. Nutr. Food Sci. Int. J. *5*.

Peng, Y., Chen, L., Li, C., Lu, W., and Chen, J. (2001). Inhibition of MDM2 by hsp90 Contributes to Mutant p53 Stabilization. J. Biol. Chem. *276*, 40583–40590.

Perkhofer, L., Gout, J., Roger, E., Kude De Almeida, F., Baptista Simões, C., Wiesmüller, L., Seufferlein, T., and Kleger, A. (2021). DNA damage repair as a target in pancreatic cancer: State-of-the-art and future perspectives. Gut *70*, 606–617.

Perone, J.A., Riall, T.S., and Olino, K. (2016). Palliative Care for Pancreatic and Periampullary Cancer. Surg. Clin. North Am. *96*, 1415–1430.

Peyrone, M. (1844). Ueber die Einwirkung des Ammoniaks auf Platinchlorür. Ann. Der Chemie Und Pharm. *51*, 1–29.

Pfeiffer, P., Goedecke, W., and Obe, G. (2000). Mechanisms of DNA double-strand break repair and their potential to induce chromosomal aberrations. Mutagenesis *15*, 289–302.

Picard (2021). https://www.picard.ch/downloads/Hsp90interactors.pdf.

Piper, P.W., and Millson, S.H. (2011). Mechanisms of resistance to Hsp90 inhibitor drugs: A complex mosaic emerges. Pharmaceuticals *4*, 1400–1422.

Piperigkou, Z., Franchi, M., Riethmüller, C., Götte, M., and Karamanos, N.K. (2020). miR-200b restrains EMT and aggressiveness and regulates matrix composition depending on ER status and signaling in mammary cancer. Matrix Biol. Plus *6–7*.

Powers, M. V., and Workman, P. (2006). Targeting of multiple signalling pathways by heat shock protein 90 molecular chaperone inhibitors. Endocr. Relat. Cancer *13*, 125–135.

Prodromou, C. (2000). The ATPase cycle of Hsp90 drives a molecular clamp' via transient dimerization of the N-terminal domains. EMBO J. *19*, 4383–4392.

Prodromou, C., Roe, S.M., O'Brien, R., Ladbury, J.E., Piper, P.W., and Pearl, L.H. (1997). Identification and structural characterization of the ATP/ADP-binding site in the Hsp90 molecular chaperone. Cell *90*, 65–75.

Proia, D.A., Sang, J., He, S., Smith, D.L., Sequeira, M., Zhang, C., Liu, Y., Ye, S., Zhou, D., Blackman, R.K., et al. (2012). Synergistic activity of the Hsp90 inhibitor ganetespib with taxanes in non-small cell lung cancer models. Invest. New Drugs *30*, 2201–2209.

Puleo, F., Nicolle, R., Blum, Y., Cros, J., Marisa, L., Demetter, P., Quertinmont, E., Svrcek, M., Elarouci, N., Iovanna, J., et al. (2018). Stratification of Pancreatic Ductal Adenocarcinomas Based on Tumor and Microenvironment Features. Gastroenterology *155*, 1999-2013.e3.

Rabbie, R., Ferguson, P., Molina-Aguilar, C., Adams, D.J., and Robles-Espinoza, C.D. (2019). Melanoma subtypes: genomic profiles, prognostic molecular markers and therapeutic possibilities. J. Pathol. *247*, 539–551.

Rashid, N.U., Peng, X.L., Jin, C., Moffitt, R.A., Volmar, K.E., Belt, B.A., Panni, R.Z., Nywening, T.M., Herrera, S.G., Moore, K.J., et al. (2020). Purity Independent Subtyping of Tumors (PurIST), A Clinically Robust, Single-sample Classifier for Tumor Subtyping in Pancreatic Cancer. Clin. Cancer Res. *26*, 82–92.

Rawla, P., Sunkara, T., and Gaduputi, V. (2019). Epidemiology of Pancreatic Cancer: Global Trends, Etiology and Risk Factors. World J. Oncol. *10*, 10–27.

Ren, L., Xiao, L., Hu, J., Li, Z., and Wang, Z. (2007). MDR1 and MDR3 genes and drug resistance to cisplatin of ovarian cancer cells. J. Huazhong Univ. Sci. Technol. - Med. Sci. *27*, 721–724.

Richter, K., Walter, S., and Buchner, J. (2004). The co-chaperone Sba1 connects the ATPase reaction of Hsp90 to the progression of the chaperone cycle. J. Mol. Biol. *342*, 1403–1413.

Riddell, I.A. (2018). Cisplatin and Oxaliplatin: Our Current Understanding of Their Actions.

Rocha, C.R.R., Silva, M.M., Quinet, A., Cabral-Neto, J.B., and Menck, C.F.M. (2018). DNA repair pathways and cisplatin resistance: An intimate relationship. Clinics *73*, 1–10.

Roche, J. (2018). The epithelial-to-mesenchymal transition in cancer. Cancers (Basel). *10*, 9–12.

Rodrigo, M.A.M., Michalkova, H., Strmiska, V., Casar, B., Crespo, P., de los Rios, V., Ignacio Casal, J., Haddad, Y., Guran, R., Eckschlager, T., et al. (2021). Metallothionein-3 promotes cisplatin chemoresistance remodelling in neuroblastoma. Sci. Rep. *11*, 1–14.

Roe, S.M., Prodromou, C., O'Brien, R., Ladbury, J.E., Piper, P.W., and Pearl, L.H. (1999). Structural basis for inhibition of the Hsp90 molecular chaperone by the antitumor antibiotics radicicol and geldanamycin. J. Med. Chem. *42*, 260–266.

Rong, B., and Yang, S. (2018). Molecular mechanism and targeted therapy of Hsp90 involved in lung cancer: New discoveries and developments (Review). Int. J. Oncol. *52*, 321–336.

Rosenberg, B., Van Camp, L., and Krigas, T. (1965). Inhibition of Cell Division in Escherichia coli by Electrolysis Products from a Platinum Electrode. Nature *205*, 698–699.

Rozenblum, E., Schutte, M., Goggins, M., Hahn, S.A., Panzer, S., Zahurak, M., Goodman, S.N., Sohn, T.A., Hruban, R.H., Yeo, C.J., et al. (1997). Tumor-suppressive pathways in pancreatic carcinoma. Cancer Res. *57*, 1731–1734.

Rudin, C.M., Poirier, J.T., Byers, L.A., Dive, C., Dowlati, A., George, J., Heymach, J. V., Johnson, J.E., Lehman, J.M., MacPherson, D., et al. (2019). Molecular subtypes of small cell lung cancer: a synthesis of human and mouse model data. Nat. Rev. Cancer *19*, 289–297.

Ruggiero, A., Trombatore, G., Triarico, S., Arena, R., Ferrara, P., Scalzone, M., Pierri, F., and Riccardi, R. (2013). Platinum compounds in children with cancer: Toxicity and clinical management. Anticancer. Drugs *24*, 1007–1019.

Safaei, R., Otani, S., Larson, B.J., Rasmussen, M.L., and Howell, S.B. (2008). Transport of cisplatin by the copper efflux transporter ATP7B. Mol. Pharmacol. *73*, 461–468.

Safaei, R., Adams, P.L., Maktabi, M.H., Mathews, R.A., and Howell, S.B. (2012). The CXXC motifs in the metal binding domains are required for ATP7B to mediate resistance to cisplatin. J. Inorg. Biochem. *110*, 8–17.

Schoch, S., Gajewski, S., Rothfuß, J., Hartwig, A., and Köberle, B. (2020). Comparative study of the mode of action of clinically approved platinum-based chemotherapeutics. Int. J. Mol. Sci. *21*, 1–20.

Schopf, F.H., Biebl, M.M., and Buchner, J. (2017). The HSP90 chaperone machinery. Nat. Rev. Mol. Cell Biol. *18*, 345–360.

Schulz-Heddergott, R., Stark, N., Edmunds, S.J., Li, J., Conradi, L.-C., Bohnenberger, H., Ceteci, F., Greten, F.R., Dobbelstein, M., and Moll, U.M. (2018). Therapeutic Ablation of Gain-of-Function Mutant p53 in Colorectal Cancer Inhibits Stat3-Mediated Tumor Growth and Invasion. Cancer Cell *34*, 298-314.e7.

Schulz, R., Marchenko, N.D., Holembowski, L., Fingerle-Rowson, G., Pesic, M., Zender, L., Dobbelstein, M., and Moll, U.M. (2012). Inhibiting the HSP90 chaperone destabilizes macrophage migration inhibitory factor and thereby inhibits breast tumor progression. J. Exp. Med. *209*, 275–289.

Senfter, D., Madlener, S., Krupitza, G., and Mader, R.M. (2016). The microRNA-200 family: Still much to discover. Biomol. Concepts *7*, 311–319.

Seo, Y.H. (2015). Small Molecule Inhibitors to Disrupt Protein-protein Interactions of Heat Shock Protein 90 Chaperone Machinery. J. Cancer Prev. *20*, 5–11.

Shi, Z., Lee, K., Yang, D., Amin, S., Verma, N., Li, Q. V., Zhu, Z., Soh, C., Kumar, R., Evans, T., et al. (2017). Genome Editing in hPSCs Reveals GATA6 Haploinsufficiency and a Genetic Interaction with GATA4 in Human Pancreatic Development. Cell Stem Cell *20*, 675-688.e6.

Shibbiru, T. (2016). Heat Shock Proteins : Their Role in Tumor Development and Their Therapeutic Heat Shock Proteins : Their Role in Tumor Development and Their Therapeutic Applications Against Cancer. 8–18.

Siddik, Z.H. (2003). Cisplatin: Mode of cytotoxic action and molecular basis of resistance. Oncogene *22*, 7265–7279.

Siegel, R.L., Miller, K.D., and Jemal, A. (2015). Cancer statistics, 2015. CA. Cancer J. Clin. *65*, 5–29.

Singh, M.P., Rai, S., Pandey, A., Singh, N.K., and Srivastava, S. (2021). Molecular subtypes of colorectal cancer: An emerging therapeutic opportunity for personalized medicine. Genes Dis. *8*, 133–145.

Sistonen, L., Sarge, K.D., and Morimoto, R.I. (1994). Human heat shock factors 1 and 2 are differentially activated and can synergistically induce hsp70 gene transcription. Mol. Cell. Biol. *14*, 2087–2099.

Smit, V.T.H.B.M., Boot, A.J.M., Smits, A.M.M., Fleuren, G.J., Cornelisse, C.J., and Bos, J.L. (1988). KRAS codon 12 mutations occur very frequently in pancreatic adenocarcinomas. Nucleic Acids Res. *16*, 7773–7782.

Solit, D.B., and Chiosis, G. (2008). Development and application of Hsp90 inhibitors. Drug Discov. Today *13*, 38–43.

Somerville, T.D.D., Xu, Y., Miyabayashi, K., Tiriac, H., Cleary, C.R., Maia-Silva, D., Milazzo, J.P., Tuveson, D.A., and Vakoc, C.R. (2018). TP63-Mediated Enhancer Reprogramming Drives the Squamous Subtype of Pancreatic Ductal Adenocarcinoma. Cell Rep. *25*, 1741-1755.e7.

Song, I.S., Savaraj, N., Siddik, Z.H., Liu, P., Wei, Y., Wu, C.J., and Kuo, M.T. (2004). Role of human copper transporter Ctr1 in the transport of platinum-based antitumor agents in cisplatin-sensitive and cisplatin-resistant cells. Mol. Cancer Ther. *3*, 1543–1549.

Spiegelberg, D., Abramenkovs, A., Mortensen, A.C.L., Lundsten, S., Nestor, M., and Stenerlöw, B. (2020). The HSP90 inhibitor Onalespib exerts synergistic anti-cancer effects when combined with radiotherapy: an in vitro and in vivo approach. Sci. Rep. *10*, 1–11.

Strimbu, K., and Tavel, J.A. (2010). What are biomarkers? Curr. Opin. HIV AIDS *5*, 463–466.

Sung, H., Ferlay, J., Siegel, R.L., Laversanne, M., Soerjomataram, I., Jemal, A., and Bray, F. (2021). Global Cancer Statistics 2020: GLOBOCAN Estimates of Incidence and Mortality Worldwide for 36 Cancers in 185 Countries. CA. Cancer J. Clin. *71*, 209–249.

Surowiak, P., Materna, V., Kaplenko, I., Spaczyński, M., Dietel, M., Lage, H., and Zabel, M. (2005). Augmented expression of metallothionein and glutathione S-transferase pi as unfavourable prognostic factors in cisplatin-treated ovarian cancer patients. Virchows Arch. *447*, 626–633.

Surowiak, P., Materna, V., Kaplenko, I., Spaczynski, M., Dolinska-Krajewska, B., Gebarowska, E., Dietel, M., Zabel, M., and Lage, H. (2006). ABCC2 (MRP2, cMOAT) can be localized in the nuclear membrane of ovarian carcinomas and correlates with resistance to cisplatin and clinical outcome. Clin. Cancer Res. *12*, 7149–7158.

Sy, S.M.H., Huen, M.S.Y., and Chen, J. (2009). PALB2 is an integral component of the BRCA complex required for homologous recombination repair. Proc. Natl. Acad. Sci. U. S. A. *106*, 7155–7160.

Tanaka, S., Hosokawa, M., Yonezawa, T., Hayashi, W., Ueda, K., and Iwakawa, S. (2015). Induction of epithelial-mesenchymal transition and down-regulation of MIR-200c and MIR-141 in oxaliplatin-resistant colorectal cancer cells. Biol. Pharm. Bull. *38*, 435–440.

Tavakkoli, A., Singal, A.G., Waljee, A.K., Elmunzer, B.J., Pruitt, S.L., McKey, T., Rubenstein, J.H., Scheiman, J.M., and Murphy, C.C. (2020). Racial Disparities and Trends in Pancreatic Cancer Incidence and Mortality in the United States. Clin. Gastroenterol. Hepatol. *18*, 171-178.e10.

Theodoraki, M.A., and Caplan, A.J. (2012). Quality control and fate determination of Hsp90 client proteins. Biochim. Biophys. Acta - Mol. Cell Res. *1823*, 683–688.

Tung, M.C., Lin, P.L., Wang, Y.C., He, T.Y., Lee, M.C., Yeh, S. Der, Chen, C.Y., and Lee, H. (2015). Mutant p53 confers chemoresistance in non-small cell lung cancer by upregulating Nrf2. Oncotarget *6*, 41692–41705.

Ushijima, R., Takayama, K., Izumi, M., Harada, T., Horiuchi, Y., Uchino, J., Hara, N., and Nakanishi, Y. (2007). Immunohistochemical expression of MRP2 and clinical resistance to platinum-based chemotherapy in small cell lung cancer. Anticancer Res. *27*, 4351–4358.

Vandewalle, C., Van Roy, F., and Berx, G. (2009). The role of the ZEB family of transcription factors in development and disease. Cell. Mol. Life Sci. *66*, 773–787.

Vesel, M., Rapp, J., Feller, D., Kiss, E., Jaromi, L., Meggyes, M., Miskei, G., Duga, B., Smuk, G., Laszlo, T., et al. (2017). ABCB1 and ABCG2 drug transporters are differentially expressed in non-small cell lung cancers (NSCLC) and expression is modified by cisplatin treatment via altered Wnt signaling. Respir. Res. *18*, 1–11.

Walden, H., and Deans, A.J. (2014). The fanconi anemia DNA repair pathway: Structural and functional insights into a complex disorder. Annu. Rev. Biophys. *43*, 257–278.

Wang, D., and Lippard, S.J. (2005). Cellular processing of platinum anticancer drugs. Nat. Rev. Drug Discov. *4*, 307–320.

Wang, H., Guo, M., Wei, H., and Chen, Y. (2021). Targeting MCL-1 in cancer: current status and perspectives. J. Hematol. Oncol. *14*, 1–18.

Wegele, H., Wandinger, S.K., Schmid, A.B., Reinstein, J., and Buchner, J. (2006). Substrate transfer from the chaperone Hsp70 to Hsp90. J. Mol. Biol. *356*, 802–811.

Whitesell, L., Shifrin, S.D., Schwab, G., and Neckers, L.M. (1992). Benzoquinonoid Ansamycins Possess Selective Tumoricidal Activity Unrelated to src Kinase Inhibition. Cancer Res. *52*, 1721–1728.

Winter, J., Jung, S., Keller, S., Gregory, R.I., and Diederichs, S. (2009). Many roads to maturity: MicroRNA biogenesis pathways and their regulation. Nat. Cell Biol. *11*, 228–234.

Woodhead, A.J., Angove, H., Carr, M.G., Chessari, G., Congreve, M., Coyle, J.E., Cosme, J., Graham, B., Day, P.J., Downham, R., et al. (2010). Discovery of (2,4-Dihydroxy-5-isopropylphenyl)-[5-(4-methylpiperazin-1- ylmethyl)-1,3-dihydroisoindol-2-yl]methanone (AT13387), a novel inhibitor of the molecular chaperone Hsp90 by fragment based drug design. J. Med. Chem. *53*, 5956–5969.

Woynarowski, J.M., Faivre, S., Herzig, M.C.S., Arnett, B., Chapman, W.G., Trevino, A. V., Raymond, E., Chaney, S.G., Vaisman, A., Varchenko, M., et al. (2000). Oxaliplatin-induced damage of cellular DNA. Mol. Pharmacol. *58*, 920–927.

Wu, S., Zhu, W., Thompson, P., and Hannun, Y.A. (2018). Evaluating intrinsic and non-intrinsic cancer risk factors. Nat. Commun. *9*.

Wynne, P., Newton, C., Ledermann, J.A., Olaitan, A., Mould, T.A., and Hartley, J.A. (2007). Enhanced repair of DNA interstrand crosslinking in ovarian cancer cells from patients following treatment with platinum-based chemotherapy. Br. J. Cancer *97*, 927–933.

Xu, Y., Liu, J., Nipper, M., and Wang, P. (2019). Ductal vs. acinar? Recent insights into identifying cell lineage of pancreatic ductal adenocarcinoma. Ann. Pancreat. Cancer *2*, 11–11.

Yamasaki, M., Makino, T., Masuzawa, T., Kurokawa, Y., Miyata, H., Takiguchi, S., Nakajima, K., Fujiwara, Y., Matsuura, N., Mori, M., et al. (2011). Role of multidrug resistance protein 2 (MRP2) in chemoresistance and clinical outcome in oesophageal squamous cell carcinoma. Br. J. Cancer *104*, 707–713.

Yamashita, T., Oda, T., and Sekimoto, T. (2007). Hsp90 and the Fanconi anemia pathway: A molecular link between protein quality control and the DNA damage response. Cell Cycle *6*, 2232–2235.

Yang, Q., Huang, J., Wu, Q., Cai, Y., Zhu, L., Lu, X., Chen, S., Chen, C., and Wang, Z. (2014). Acquisition of epithelial-mesenchymal transition is associated with Skp2 expression in paclitaxel-resistant breast cancer cells. Br. J. Cancer *110*, 1958–1967.

Yin, L., Yang, Y., Zhu, W., Xian, Y., Han, Z., Huang, H., Peng, L., Zhang, K., and Zhao, Y. (2021). Heat Shock Protein 90 Triggers Multi-Drug Resistance of Ovarian Cancer via AKT/GSK3β/β-Catenin Signaling. Front. Oncol. *11*, 1–16.

Ying, W., Du, Z., Sun, L., Foley, K.P., Proia, D.A., Blackman, R.K., Zhou, D., Inoue, T., Tatsuta, N., Sang, J., et al. (2012). Ganetespib, a unique triazolone-containing Hsp90 inhibitor, exhibits potent antitumor activity and a superior safety profile for cancer therapy. Mol. Cancer Ther. *11*, 475–484.

Yonezawa, A., Masuda, S., Yokoo, S., Katsura, T., and Inui, K.I. (2006). Cisplatin and oxaliplatin, but not carboplatin and nedaplatin, are substrates for human organic cation transporters (SLC22A1-3 and multidrug and toxin extrusion family). J. Pharmacol. Exp. Ther. *319*, 879–886.

Zhang, B., Pan, X., Cobb, G.P., and Anderson, T.A. (2007). microRNAs as oncogenes and tumor suppressors. Dev. Biol. *302*, 1–12.

Zhou, J., Kang, Y., Chen, L., Wang, H., Liu, J., Zeng, S., and Yu, L. (2020). The Drug-Resistance Mechanisms of Five Platinum-Based Antitumor Agents. Front. Pharmacol. *11*, 1–17.

6 Abbreviations

17-AAG	tanespymicin
3'-UTR	3' untranslated region
5-FU	5-Fluorouracil
ABC	ATP-binding cassette transporter
ADEX	aberrantly differentiated endocrine exocrine
ADP	adenosine diphosphate
AFU	arbitrary fluorescence units
AKT	Protein kinase B
ARID1A	AT-rich interactive domain-containing protein 1A
ATP	adenosine triphosphate
ATP7A/B	copper-transporting P-type ATPase ½
BCA	bicinchoninic acid
Bcl-2	B-cell lymphoma protein 2
Bcl-XL	B-cell lymphoma protein extra-large
BRCA1/2	breast cancer 1/2
BSA	Bovine serum albumin
CDK1	cyclin-dependent kinase 1
CDK4,6	cyclin-dependent kinase 4, 6
CDKN2A	cyclin-dependent kinase inhibitor 2
CHD1	E-cadherin
CI	combination index
Cisplatin	*cis*-diammine-dichloro-platinum
CO_2	Carbon dioxide
CTR1	copper transporter 1
DAPI	4′,6-Diamidin-2-phenylindol
DGCR8	Drosha- DiGeorge syndrome critical region 8
DIPH	Diphenhydramine
DMEM	Dulbecco's modified Eagle's medium

DMSO	Dimethyl sulfoxide
DNA	Deoxyribonucleic acid
DSB	double-strand break
E.coli	Escherichia coli
E-cadherin	epithelial cadherin
EDTA	Ethylenediaminetetraacetic acid
EMT	epithelial to mesenchymal transition
Epcam	epithelial cell adhesion molecule
ErbB2	receptor tyrosine-protein kinase erbB-2
ERCC-1	DNA excision repair protein
FA	Fanconi anemia
FBS	fetal bovine serum
FDA	Food and Drug Administration
FLT-3	fms like tyrosine kinase 3
GA	Geldanamycin
GAPDH	Glyceraldehyde 3-phosphate dehydrogenase
GATA6	GATA-binding protein 6
GSH	Glutathione
GSK	Glykogensynthase-Kinase 3
GTP	Guanosine triphosphate
GTPase	Guanosine triphosphatase
Her2	human epidermal growth factor receptor 2
HIF1α	Hypoxia-inducible factor 1-alpha
HR	homologous recombination
HRD	homologous recombination deficiency
HSF-1	heat shock factor 1
HSP40	heat shock protein 40
HSP70	heat shock protein 70
HSP90	heat shock protein 90
HSR	heat shock response pathway

IC_{50}	half maximal inhibitory concentration
ICL	inter-strand crosslinks
Jak2	Janus kinase 2
KPC	LSL-KrasG12D/+; LSL-Trp53R172H/+; Pdx-1-Cre
KRAS	Kirsten rat sarcoma
MAPK	mitogen-activated protein kinase
Mcl-1	myeloid cell leukemia-1
MEK	Dual specificity mitogen-activated protein kinase kinase 2
MET	tyrosine-protein kinase
MIF	Macrophage migration inhibitory factor
miRNA	microRNA
MMP2	matrix metalloproteinase-2
mRNA	messenger RNA
MRP2	multidrug resistance protein 2
MT	metallothionein
NaCl	sodium chloride
NaOH	sodium hydroxide
N-cadherin	neural cadherin
NER	nucleotide excision repair
NGS	normal goat serum
NRF2	nuclear factor erythroid 2-related factor 2
ns	not significant
PALB	partner and localizer of BRCA2
PanINs	pancreatic intraepithelial neoplasia
PARP1	Poly [ADP-ribose] polymerase 1
PB	phosphate buffer
PBS	phosphate buffer saline
PCR	polymerase chain reaction
PDAC	pancreatic ductal adenocarcinoma
phospho-H2AX	phosphorylated Histone 2AX

PI3K	phosphoinositide 3-kinases
pre-miRNA	precursor miRNA
pri-miRNA	primary miRNA
Pt-GpG	DNA platination product
QM	quasi-mesenchymal
qRT-PCR	real-time polymerase chain reaction
RD	radicol
RISC	RNA induced silencing complex
RNA	ribonucleic acid
RNA-seq	ribonucleic acid sequencing
RPMI	Roswell Park Memorial Institute 1640 Medium
RTK	receptor tyrosine kinases
RT-PCR	real-time polymerase chain reaction
S phase	Synthesis phase
SCL	solute carrier superfamily
SDS	sodium dodecyl sulfate
SMAD4	mothers against decapentaplegic homolog 4
snRNA	small nuclear ribonucleic acid
Src	proto-oncogene tyrosine-protein kinase
TCGA	The Cancer Genome Atlas
TGF-beta	Transforming Growth Factor beta
TP53	tumour protein p53
TRIS-HCl	Tris-(hydroxymethyl)-aminomethane-hydrochloride
TRP	tetratricopeptide repeat
VEGFA	vascular endothelial growth factor A
VIM	Vimentin
Zeb1/2	Zinc finger E-box-binding homeobox ½
zVad	carbobenzoxy-valyl-alanyl-aspartyl-[O-methyl]- fluoromethylketone